Dissecting the Role of c-Src in the Regulation of Adherens Junctions using Engineered Kinases

JENNIFER E. KLOMP

B.Sc., Grand Valley State University

M.Sc., Central Michigan University

THESIS

Submitted as partial fulfillment of the requirements for the degree of Doctor of Philosophy in Cellular and Molecular Pharmacology in the Graduate College of the University of Illinois at Chicago, 2017

Defense Committee:

Dr. Andrei V. Karginov, Chair and Advisor, Pharmacology

Dr. Yulia Komarova, Pharmacology

Dr. Dolly Mehta, Pharmacology

Dr. John P. O'Bryan, Pharmacology

Dr. Angela Tyner, Biochemistry and Molecular Genetics

This thesis is dedicated to my husband Dr. Jeffrey Klomp; my number one collaborator in life and science.

ACKNOWLEDGEMENTS

I would like to thank my advisor Dr. Andrei V. Karginov, who was a terrific mentor and colleague throughout my time in the GEMS Program. Dr. Karginov helped shape me into a better scientist and a more thoughtful researcher. He provided me with the perfect balance of guidance and freedom. I greatly appreciate his thoughtful mentorship. Furthermore, I would like to thank my committee members. Dr. Yulia Komarova and Dr. Dolly Mehta provided consistent mentorship during my time in the GEMS program. Dr. Karginov's laboratory had joint lab meetings with the laboratory of Dr. John O'Bryan. Dr. John O'Bryan provided helpful advice and suggestions for my research as well as my career development. I would like to thank Dr. Angela Tyner who also served on my preliminary exam committee and has watched this project evolve.

A special thank you for my amazing lab colleagues, both past and current: Vincent Huyot, Kerrie B. Collins, Dr. Anne-Marie Ray, Dr. Maulik Patel, Mark Shaaya, and Rima Rebiai. Vincent helped make my time in the Karginov laboratory enjoyable, educational, and productive. Kerrie and I began the GEMS program together and provided each other with inspiration and motivation throughout the process. All members of the Karginov laboratory have contributed to my work in various ways, either technically, through thoughtful discussions, or by providing a fun and productive work environment. I was lucky enough to work not only with wonderful colleagues but also good friends.

I would like to thank my family. My family has supported me personally and academically during my entire existence. I cannot express my gratitude for their unwavering love and constant motivation. We have and always will work as a team, celebrating our successes and mourning our losses together, and most of all having a lot of fun. You are the best.

Finally, a special thank you to my husband, Dr. Jeffrey Klomp, and mother, Dr. Rebecca Brinks. Thank you for motivating me to pursue my dream even when life had thrown so many hurdles at me and it seemed impossible.

Thank you to all of you.

Sincerely,

Jenny

CONTRIBUTION OF AUTHORS

Both the projects presented here are collaborative projects of which I was the primary author. The contributions of other authors are indicated in the respective figure legends.

TABLE OF CONTENTS

CONTENT **PAGE**

CHAPTER 1: LITERATURE REVIEW 1
1.1. The importance of endothelial cell barrier function 1
1.2. Adherens junctions serve a crucial role in endothelial cell barrier function 2
1.2.1. Structural components of adherens junction protein VE cadherin 2
1.2.2 Phosphorylation of VE cadherin 5
1.3. Regulation of endothelial cell barrier integrity via Src Family Kinases 7
1.3.1 The role of Src in regulating VE cadherin 9
1.3.2 Src-dependent regulation of Rho-GTPases 11
1.3.3 Effect of Src activation on other downstream signaling pathways 13
1.4. Approaches and challenges of studying kinases in living cells 15
1.5. Statement of Aims 21

CHAPTER 2: BARRIER ENHANCING FUNCTION OF SRC AND VE CADHERIN PHOSPHORYLATION IN ENDOTHELIAL CELLS REVEALED BY SYNTHETIC BIOLOGY APPROACH 23
2.1 Introduction 23
2.2 Materials and Methods 27
2.2.1 Antibodies and chemical reagents 27
2.2.2 Plasmids and Adenoviruses 28
2.2.3 Cell culture, transfection, and infection 29
2.2.4 Immunofluorescence staining 29
2.2.5 Immunoprecipitation 29
2.2.6 Protein expression comparisons 30
2.2.7 FITC-Avidin Assay 31
2.2.8 FITC-Dextran Assay 31
2.2.9 Trans-electrical Resistance 31
2.2.10 Image Collection 32
2.2.11 Image Analysis 33
2.3 Results 35
2.4 Discussion 66

CHAPTER 3: MIMICKING TRANSIENT ACTIVATION OF PROTEIN KINASES IN LIVING CELLS 72
3.1 Introduction 72
3.2 Materials and Methods 74
3.2.1 Antibodies and chemical reagents 74
3.2.2 DNA Constructs 75
3.2.3 Cell lines 77
3.2.4 Immunoprecipitation and kinase assay 77
3.2.5 Image collection 78
3.2.6 Image Analysis 78
3.3 Results 83
3.4 Discussion 115
3.5 Supplementary Index 117

CHAPTER 4: FUTURE DIRECTIONS 120
4.1 Summary of objectives 120

4.2 Src regulation of the endothelial barrier 121
4.3 Transient activation of kinases 127
4.4 Using RapR-Src-as2 to investigate Src mediated endothelial barrier changes 128
4.5 Conclusion 130
CHAPTER 5: CITED LITERATURE 131
CHAPTER 6: VITAE 151
CHAPTER 7: APPENDIX 154

LIST OF FIGURES

FIGURE **PAGE**

Figure 1.1: Adherens Junction complex 3
Figure 1.2: Activation of Src Family Kinases 8
Figure 1.3: VE cadherin phosphorylation by Src 10
Figure 1.4: Kinase inhibition using analog-sensitive alleles 17
Figure 1.5: Rapamycin-mediated regulation (RapR) of protein kinases 19
Figure 1.6: RapR targeted activation of pathways (RapRTAP) 20
Figure 2.1: Activation of Src Family Kinases by S1P treatment 37
Figure 2.2: Activation of Src Family kinases by thrombin treatment 38
Figure 2.3: Rapamycin efficiently activates RapR-Src and RapR-Lyn in HPAE cells 39
Figure 2.4: Activation of Src but not Lyn enhances endothelial cell barrier 41
Figure 2.5: Activation of Src but not Lyn enhances endothelial cell barrier recovery 42
Figure 2.6: Src mediated endothelial cell barrier enhancement in HUVE cells 43
Figure 2.7: Src activation causes transient endothelial cell barrier enhancement 44
Figure 2.8: Src activation causes an increase in VE cadherin at the adherens junctions 46
Figure 2.9: Live SIM shows broadening of adherens junctions via Src activation 47
Figure 2.10: Reticular adherens junctions are less leaky than linear adherens junctions 49
Figure 2.11: Src activation initiates changes in the actin-cytoskeleton 51
Figure 2.12: Src induces an increase in protrusive activity 52
Figure 2.13: Src activates Rac1 53
Figure 2.14: Src activation causes cortactin and F-actin bundling 54
Figure 2.15: F-actin forms a scaffold underneath rearranged VE cadherin 55
Figure 2.16: Paxillin and VE cadherin following Src activation 57
Figure 2.17: Src activation induces phosphorylation at VE cadherin 59
Figure 2.18: Cadherin and Catenin association after Src activation 61
Figure 2.19: P-Y731 and P-Y658 alter Src mediated VE cadherin localization changes 62
Figure 2.20: Y731F accumulates in the cytoplasm faster than WT VE cadherin 63
Figure 2.21: Src mediate enhancment requires P-731 on VE cadherin 64
Figure 2.22: VE cadherin Y731-P is required for S1P enhancement 65
Figure 3.1: Detecting Rac1 activity 81
Figure 3.2: Detecting PI3K activity 82
Figure 3.3: Transient activation of engineered Src kinase 85
Figure 3.4: Transient activation of engineered Src is improved by FRB modification 86
Figure 3.5: Activation of RapR-Src and RapR-Src-as2 with FRB versus iPEP-FRB 88
Figure 3.6: Characterization of RapR-Src-as2 in vitro 89
Figure 3.7: RapR-Src-as2 activation and inactivation in living cells 90
Figure 3.8: RapR-Src-as2 expression relative to endogenous Src expression 91
Figure 3.9: Inactivation of RapR-Src-as2 in HeLa cells 92
Figure 3.10: Transient activation with RapR-SrcCat-as2 94
Figure 3.11: Development and characterization of RapR-p38-as2 System in vitro 96
Figure 3.12: RapR-p38-as2 System in living cells 97
Figure 3.13: RapR-Src-as2 localization in HeLa cells 99
Figure 3.14: Effect of prolonged versus transient Src activity on cell morphodynamics 100

Figure 3.15: Regulation of Src mediated morphological changes 101
Figure 3.16: Regulation of Src mediated morphological changes 102
Figure 3.17: Regulation of Rac1 activity by RapR-Src-as2 104
Figure 3.18: Effect of Rac1 inhibition on Src induced morphological changes 105
Figure 3.19: Src and Rac1 mediated morphological changes 107
Figure 3.20: The role of Rac1 in the regulation of Src mediated morphological changes 108
Figure 3.21: PI3K remains active following Src inactivation 109
Figure 3.22: Regulation of PI3K signaling by RapR-Src-as2 111
Figure 3.23: Effect of PI3K inhibition on Src induced morphological changes 112
Figure 3.24: Src and PI3K mediated morphological changes 113
Figure 3.25: The role of PI3K in the regulation of Src mediated morphological changes 114
Figure 4.1: Lyn activation induces internalization of VE cadherin 122
Figure 4.2: Src does not activate RhoA 126

SUMMARY

The work described in this dissertation is the compilation of two independent projects, *Barrier enhancing function of Src and VE cadherin phosphorylation in endothelial cells revealed by a synthetic biology approach* and *Mimicking transient activation of protein kinases in living cells*. In the first project, *Barrier enhancing function of Src and VE cadherin phosphorylation in endothelial cells revealed by a synthetic biology approach*, we utilized a previously described inducible kinase system (RapR-kinase) to interrogate how the direct activation of the non-receptor tyrosine kinase c-Src (Src) alters the adherens junctions and subsequently the endothelial cell barrier. In the second project, *Mimicking transient activation of protein kinases in living cells*, we modified the RapR-kinase method to enable both efficient activation and inactivation of a kinase. Our modifications allowed us to activate a kinase for a finite amount of time and compare how transient and prolonged activation of a kinase alter down-stream signaling.

Barrier enhancing function of Src and VE cadherin phosphorylation in endothelial cells revealed by a synthetic biology approach

Permeability of the endothelial monolayer is regulated at the level of adherens junctions, multiprotein structures mediating cell-cell interactions. c-Src (Src) tyrosine kinase stimulates adherens junction disassembly, but its activity is also required for adherens junction formation, suggesting a dual function for Src in regulation of endothelial barrier. However, defining a barrier protective role for Src has been difficult due to limitations of current methods. To overcome existing limitations, we employed a novel protein engineering technology allowing for tight temporal regulation of Src kinase activity in living cells. This allowed us to identify a

previously undescribed role for Src in the regulation of endothelial barrier function. Src activation resulted in a distinct biphasic temporal effect on endothelial permeability.

Initially, Src induction led to strengthening of endothelial barrier and accumulation of VE cadherin at the adherens junctions. Only prolonged activation of Src increased barrier permeability. However, activation of fellow Src Family Kinase (SFK) member Lyn only promoted barrier permeability. Transient barrier strengthening via Src was accompanied by formation of morphologically distinct reticular adherens junctions. Reticular adherens junctions were found in areas of overlap between contiguous endothelial cells, and exhibited reduced localized permeability. Organization of reticular adherens junctions suggested that they form in membrane protrusions. In agreement with this hypothesis, we observed increased formation of lamellipodia concurrently with Src-mediated formation of reticular adherens junctions.

Interestingly, Src-induced barrier enhancement was also accompanied by robust phosphorylation of VE cadherin. However, VE cadherin phosphorylation did not affect its interaction with binding partners, p120- and β-catenin, and it did not disrupt VE cadherin localization to adherens junctions. Furthermore, VE cadherin phosphorylation at Tyr731 but not Tyr658 is required for Src-mediated barrier enhancement. Therefore, our results revealed an unexpected role for Src and VE cadherin phosphorylation in regulation of endothelial permeability. We found that activity of SFKs and VE cadherin phosphorylation on Tyr731 are both required for the barrier enhancing effect of S1P treatment. In addition, we found that Src but not Lyn activation enhanced the rate of recovery following disruption of the barrier by α-Thrombin. Our data indicate that Src, specifically, is an important regulator of the endothelial barrier via multiple physiological signaling pathways.

Mimicking transient activation of protein kinases in living cells

Under physiological conditions, kinases are activated for finite periods of time, and the duration of this activation is critical for specific biological outcomes. Mimicking transient biological activity of kinases is challenging due to the limitation of existing methods. We report a new strategy enabling transient kinase activation in living cells. The design combines two protein engineering methods that provide independent control of kinase activation and inactivation. Insertion of an allosteric switch, the iFKBP (insertable FKBP) domain, into the catalytic domain of a kinase enables specific and efficient activation of the engineered kinase by rapamycin. Shokat and colleagues demonstrated that specific inactivation of a kinase can be achieved by introducing a functionally silent mutation, making the kinase sensitive to allele-specific (AS) inhibitor, 1NA-PP1 (1-Napthyl-PP1). Using tyrosine kinase Src and serine/threonine kinase p38 as examples, we demonstrate that a rapamycin-regulated kinase bearing an inhibitor-sensitizing mutation (RapR-Src-as2 and RapR-p38-as2) can be efficiently activated by rapamycin and inactivated by 1NA-PP1.

We also show that by using this method we can transiently stimulate Src-induced phosphorylation of endogenous substrates, transiently regulate Src-mediated morphological changes, and control the duration of these morphological changes. Interestingly, transient activation of Src is followed by secondary Src-independent morphological processes: slow cell spreading and elevated protrusive activity. We found that the extent of these secondary morphodynamic changes depends on the duration of Src activation. This approach allowed us to dissect the different roles of PI3K and Rac1 signaling in regulation of morphological changes during Src activation and following Src inactivation. Inhibition of PI3K or Rac1 at the time of Src activation impedes Src-mediated cell spreading, while only PI3K inhibition alters Src

induced protrusive activity. However, once Src is activated for 15 min, neither PI3K nor Rac1 inhibition is sufficient to affect Src mediated cell spreading or protrusive activity. Following Src inactivation, secondary increase in cell area is PI3K dependent, while secondary stimulation of protrusive activity is Rac1 and PI3K dependent. Thus, this strategy enabled us to determine the role of Src-PI3K and Src-Rac1 sequential signaling. In conclusion, we present a novel broadly applicable strategy that provides new opportunities for dissecting kinase-mediated cellular pathways.

LIST OF ABBRIEVIATIONS

AP2	AP2 adaptor complex
AS	Analog Sensitive
ATF2	Activating Transcription Factor 2
BSA	Bovine Serum Albumin
CA	Constitutively Active
Cdc42	Cell division control protein 42 homolog
CRIB	Cdc42/Rac interactive binding
CSK	c-terminal Src kinase
DEP-1	Density-enhanced phosphatase-1
DMEM	Dulbecco's modified eagle medium
DMSO	Dimethyl sulfoxide
DN	Dominant negative
DNA	Deoxyribonucleic acid
Dock180	Dedicator of cytokinesis 180
EC	Extracellular
ECM	Extracellular matrix
ETOH	Ethanol
FAK	Focal adhesion kinase
FBS	Fetal Bovine Serum
FITC	Fluorescein isothiocynate
FKBP	FK506 binding protein
FRET	Foster resonance energy transfer

FRB	FKBP12-rapamycin-binding
FRG	Faciogenital dysplasia gene product-1 related Cdc42-GEF
GAP	GTPase accelerating protein
GEF	Guanine nucleotide exchange factor
GFP	Green Fluorescent Protein
GTP	Guanosine triphosphate
GDP	Guanosine diphosphate
GTPase	Guanosine triphosphate hydrolase
HPAE	Human Pulmonary Artery endothelial
H_2O_2	Hydrogen Peroxide
HUVE	Human Umbilical Vein Endothelial
ICAM	Intercellular adhesion molecule-1
iFKBP	insertion of a small FK506-binding protein
iPEP	FRB bearing the first 15 amino acids of FKBP12 at the N-terminus
LPS	Lipopolysaccharide
MLC	Myosin light chain
MLCK-1	Myosin light chain kinase-1
mTOR	Mechanistic target of rapamycin
mTORC	Mechanistic target of rapamycin complex
1NA-PP1	1-Naphthyl-PP1 CAS 221243-82-9
PAK	p21-activated kinase
PAR-1	Protease-activated receptor-1
PECAM-1	Platelet endothelial cell adhesion molecule 1

PDK	Phosphatidylinositide dependent kinase
PH	Pleckstrin homology
PI3K	Phosphatidylinositide 3 kinase
PtdIns	Phosphatidylinositide
PTP	Protein Tyrosine Phosphatase
PTP1B	Protein Tyrosine Phosphatase 1B
PTP-μ	Protein tyrosine phosphatase receptor type M
Pyk-2	Pyruvate kinase-2
Rac1	Ras-related C3 botulinum toxin substrate 1
RapR	Rapamycin Regulated
RapRTAP	Rapamycin-regulated targeted activation of pathways
RhoA	Rho homolog gene family member A
ROCK	Rho kinase
SH	Src homology
Shp2	Src homology-2 domain protein tyrosine phosphatase
SIM	Structured Illumination Microscopy
S1P	Sphingosine-1 phosphate
S1PR	Sphingosine-1 phosphate receptor-1
SFK	Src Family Kinase
Src	c-Src
TER	Trans Electrical Resistance
Tiam-1	T-Lymphoma invasion and metastasis inducing protein 1
TNFα	Tumor necrosis factor alpha

Vav2	Vav Guanine Nucleotide Exchange Factor 2
VEGF	Vascular endothelial growth factor
VE	Vascular endothelial
VE-PTP	VE-Protein Tyrosine Phosphatase
YFP	Yellow Fluorescent Protein

CHAPTER 1: LITERATURE REVIEW

1.1. The importance of endothelial cell barrier function

Endothelial cells line the vessel wall in a single monolayer, forming a semi-permeable barrier and restricting the interchange of protein-rich fluids from the underlying tissue. The endothelial cell barrier is paramount for the maintenance of physiological homeostasis by controlling the movement of cells, proteins, and fluid between interstitial and vascular spaces[1]. Numerous vascular pathologies are the result of altered permeability of the endothelial cell barrier. For example, compromising the endothelial cell barrier can lead to edema, which in turn alters the interstitial pressure[2]. Under conditions of acute vascular hyper-permeability there is a rapid increase in permeability after the microvasculature is exposed to factors such as histamine or vascular endothelial growth factor (VEGF)[3]. Typically edema is reversible and fluid balance is restored after the stimuli is removed[2]. In the case of chronic vascular hyper-permeability, as occurs under continuous exposure to VEGF (e.g. tumors, wound healing, and chronic inflammatory disease), the vasculature can undergo major structural changes that ultimately lead to pathological angiogenesis[3–6]. However, under basal conditions the vasculature needs to be both tightly regulated and remain permeable enough to allow for the exchange of small molecules and limited amounts of plasma protein in a controlled manner[3].

Permeability through the endothelial cell barrier occurs through two main routes- paracellular transport and transcellular transport. The paracellular route occurs via interendothelial junctions, which restrict transport of solutes larger than 3 nm in radius[7,8]. The interendothelial junctions are composed of adherens, tight, and gap junction complexes[1]. The adherens and tight junctions together maintain the endothelial cell barrier by establishing adhesion between cells in the endothelial monolayer[8]. Conversely, the gap junctions allow for the passage of water, ions, and

other small molecules by forming channels between neighboring cells and thus allowing signal transmission through the monolayer[1,8]. The movement of macromolecules through the transcellular route occurs via transcytosis, an energy-dependent mechanism that traffics macromolecules in vesicles across the endothelium[9]. Caveolae, cholesterol-rich pits that form on the cell surface, accumulate macromolecules using receptors on the luminal side and transport them across the endothelial monolayer where the macromolecules exit via exocytosis into the interstitium[8–10]. Both paracellular and transcellular routes of transport are essential for maintaining the semipermeable endothelial cell barrier.

1.2. Adherens junctions serve a crucial role in endothelial cell barrier function

1.2.1. Structural components of adherens junction protein VE cadherin

Endothelial cell permeability utilizing the paracellular route is tightly regulated via adherens junctions, multi-protein structures that mediate cell-cell interactions[11]. These adherens junctions are composed of the transmembrane protein vascular endothelial (VE) cadherin and the associated cytosolic catenins: p120-, β-, γ- (also called plakoglobin), and α-catenins (Figure 1.1)[12]. In the majority of the body, the predominant restrictive barrier of the endothelium is formed by VE cadherin-mediated adherens junctions[13]; enrichment of tight junctions is restricted to the blood-brain barrier[8]. In addition to regulating the endothelial cell barrier, VE cadherin is required for proper vasculature formation during embryonic development[14,15], maintenance of nascent vessels[16], endothelial cell maturation[14], and angiogenesis[17,18].

VE cadherin is a member of the cadherin superfamily belonging to the atypical class II cadherins; sharing about 23% amino acid sequence similarity to the classical type I cadherins (neural and epithelial cadherins)[19]. The adhesive interface that promotes VE cadherin dimerization is also larger than in the case of type I cadherins[20]. VE cadherin contains five

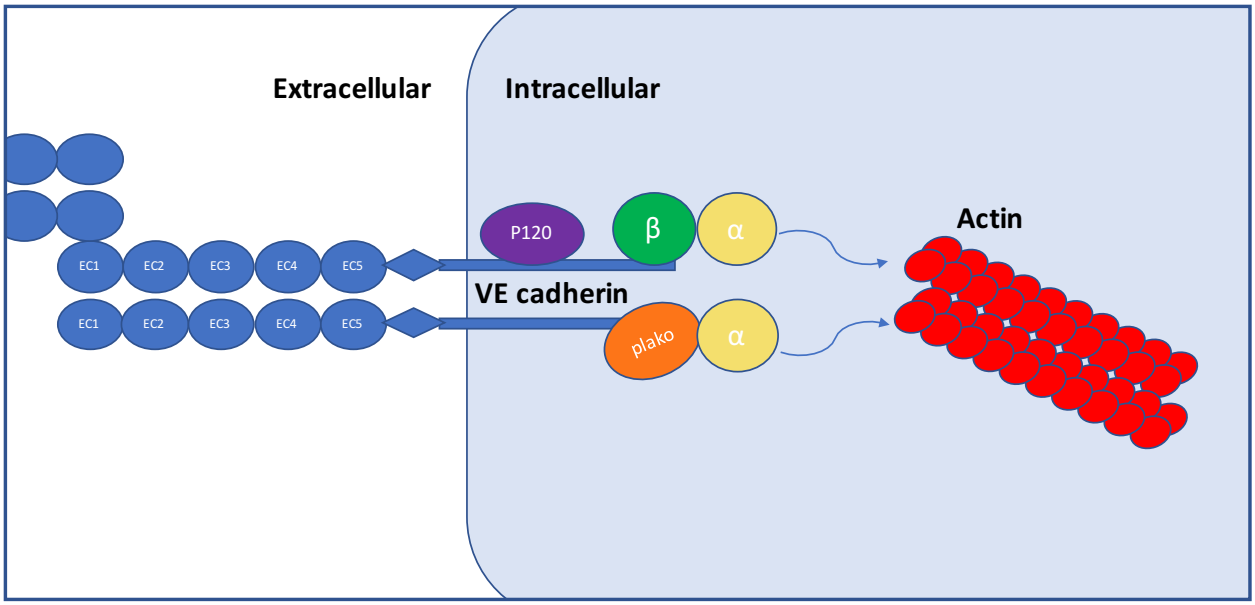

Figure 1.1: Adherens Junction complex
Adjacent cells are connected in a calcium-dependent manner through the extracellular domain of VE cadherin. The cytoplasmic domain of VE cadherin links it to the actin cytoskeleton through its associated catenin proteins P120-, β-, α-catenin, and plakoglobin. VE cadherin-mediated adhesions form the primary barrier of the endothelium.

extracellular (EC) repeats, a transmembrane domain, and a cytoplasmic tail[21]. The EC domains regulate homophilic cadherin adhesions in a calcium-dependent fashion in the form of *cis*- and *trans*- interactions, which occur on the same or adjacent cells, respectively[8,12]. The cytoplasmic tail of VE cadherin interacts with p120-catenin, β-catenin, and plakoglobin[22,23]. β-catenin and plakoglobin link VE cadherin to the actin cytoskeleton through α-catenin[22,24–26] (Figure 1.1). Adherens junctions are plastic structures, as evidenced by their functional variety that includes: linear, reticular, and focal adherens junctions[27]. Rearrangement from one of these functional types to another can occur either constitutively or via stimulation[28–30].

Filopodia containing VE cadherin form the initial cell-cell contacts via focal adherens junctions, linked to radial actin stress fibers. The junctions later expand laterally to form linear adherens junctions, which associate with bundled linear actin[27,29,31]. In a stable cell monolayer the adherens junctions typically arrange as continuous linear junctions[32]. Linear adherens junctions are stable cell-cell contacts and are closely associated with cortical actin (actomyosin located at the inner-face of the plasma membrane)[11]. Local activation of the GTPase Rac1 stabilizes the linear junctions and maintains a lower tension[33]. Conversely, activation of another GTPase, RhoA and subsequent contraction of the actin-cytoskeleton initiates an increase in tension on VE cadherin and causes the junctions to revert back to focal adherens junctions[29,34].

A third type of adherens junctions, reticular adherens junction, forms a 3-dimensional mesh-like network at the interface of two overlapping endothelial cells, with platelet endothelial cell adhesion molecule 1 (PECAM-1) interspaced between the cadherin-catenin complex[35]. It is hypothesized that reticular adherens junctions are a specialized type of adherens junction that facilitate specific endothelial cell barrier functions under distinct conditions[27]. They appear to be barrier-protective and may mediate leukocyte extravasation, as suggested by the presence of

PECAM-1[35]. There has been a growing interest in understanding the formation, morphology, and composition of the different types of adherens junctions[27].

1.2.2 Phosphorylation of VE cadherin

The phosphorylation status of the cadherin-catenin complex is an important regulator of the remodeling of adherens junctions, providing a mechanism for rapid alterations[8,36–38]. Sparsely plated endothelial cells have a high level of tyrosine (Y) phosphorylation at the cell-cell junctions, and as the cell confluency increases the phospho-Y level reduces and concurrently there is formation of mature cytoskeleton associated adherens junctions[39]. Phosphorylation of VE cadherin occurs following a variety of stimuli including: VEGF, TNFα, lipopolysaccharide (LPS), H_2O_2, histamine, and bradykinin[40–44]. VE cadherin Y phosphorylation has been described previously at: Y645[45], Y658[43,46,47], Y685[43,47,48], Y731[45–49], and Y733[45]. In addition to Y, phosphorylation of serine (S)665 occurs following VEGF treatment and leads to the internalization of VE cadherin[50]. Generally, the phosphorylation of VE cadherin is thought to be associated with the destabilization of the adherens junctions[41,45,46,50–53].

Although phosphorylation of VE cadherin may be necessary for destabilization of the adherens junctions, it does not appear to be sufficient for this process[43,47,48]. Furthermore, the kinetics of VE cadherin/catenin phosphorylation and the observed decrease in endothelial cell barrier function do not always correlate. Previous work demonstrates that two different factors, VEGF and the phosphatase inhibitor pervanadate, cause a rapid enhancement of the endothelial barrier, simultaneously with the tyrosine phosphorylation of VE-cadherin, P120- and β-catenins, and plakoglobin. Though adherens junction disruption did eventually occur, it was only after prolonged phosphorylation[54]. Therefore, although VE cadherin phosphorylation is correlated

with disruption of adherens junctions, it is still unclear how each of the different VE cadherin phosphorylation sites in addition to the duration of phosphorylation contribute to this disruption.

The phosphorylation status of VE cadherin is regulated by multiple phosphatases and kinases. For example, VE-Protein Tyrosine Phosphatase (VE-PTP) is key in stabilizing the cadherin-catenin complex[48,51]. VE-PTP de-phosphorylates residue Y685, which is known to induce vascular permeability when phosphorylated[48]. Src homology 2-domain phosphatase (Shp2) also stabilizes the adherens junction complex by de-phosphorylating β-catenin[55] and VE cadherin[56], allowing for re-establishment of the endothelial cell barrier following disruption by thrombin. Somewhat paradoxically, Shp2 de-phosphorylation of VE cadherin can also lead to its endocytosis, with de-phosphorylation of Y731 allowing for adaptin AP-2 binding and leukocyte extravasation[48]. Protein Tyrosine Phosphatase 1B (PTP1B)[57], density-enhanced phosphatase-1 (DEP-1)[58], and protein tyrosine phosphatase receptor type M (PTP-μ)[59] also appear to enhance endothelial barrier function by associating with VE cadherin either directly or indirectly to decrease its phosphorylation level[23].

Numerous kinases have been described to phosphorylate VE cadherin downstream of permeability promoting agents. Focal adhesion kinase (FAK) phosphorylates VE cadherin, mediating adherens junction disorganization and leading to increased permeability. *In vivo* VEGF activation results in FAK binding to VE cadherin, direct phosphorylation of β-catenin, and subsequent disassembly of adherens junctions[52]. FAK is additionally important for decreasing or increasing endothelial permeability when activated by sphingosine-1 phosphate receptor-1 (S1PR1) or protease-activated receptor-1 (PAR-1)[60], respectively. Moreover, VEGF is not able to induce endothelial permeability in the absence of FAK[52]. VEGF treatment also initiates the catalytic activity of p21-activated kinase (PAK), a serine/threonine (S/T) kinase,

which phosphorylates VE cadherin on S665 and leads to β-arrestin mediated endocytosis of VE cadherin[50]. Pyk2 and Src are both required for phosphorylation of VE cadherin to enable leukocyte trans-endothelial migration[49].

1.3. Regulation of endothelial cell barrier integrity via Src Family Kinases

The predominant kinases thought to be involved in the phosphorylation of VE cadherin are the Src Family Kinases (SFKs). Nine members make up the SFKs (Src, Yes, Fyn, Fgr, Lck, Hck, Blk, Lyn, and Frk), as based on conserved structural elements. Beginning at the N-terminus, these elements are: Src Homology domain 4 (SH4), which serves as a lipid modification site to target the protein to the cytoplasmic membrane; domain 3 (SH3) and domain 2 (SH2), which are important for protein-protein interactions; a linker sequence; and the tyrosine kinase domain (SH1)[61] (Figure 1.2).

SFKs are regulated predominantly by two phosphorylation sites. Phosphorylation of residue Y527 by c-terminal Src Kinase (CSK)[62] inactivates SFKs by inducing an intramolecular interaction between the phosphorylated residue and the SH2 domain. This interaction promotes the association of the SH3 domain and the linker domain and maintains the kinase in an inactive state. De-phosphorylation of Y527 allows SFKs to adopt an open conformation and autophosphorylate Y416, which enhances catalytic activity[63] (Figure 1.2). Activated SFKs are involved in the regulation of cellular proliferation, differentiation, survival, motility, and angiogenesis [61].

The SFK proteins: Src, Yes, Fyn, and Lyn are expressed in endothelial cells[41] and play critical roles in regulating vascular permeability via a variety of stimuli. Both Src and Yes are

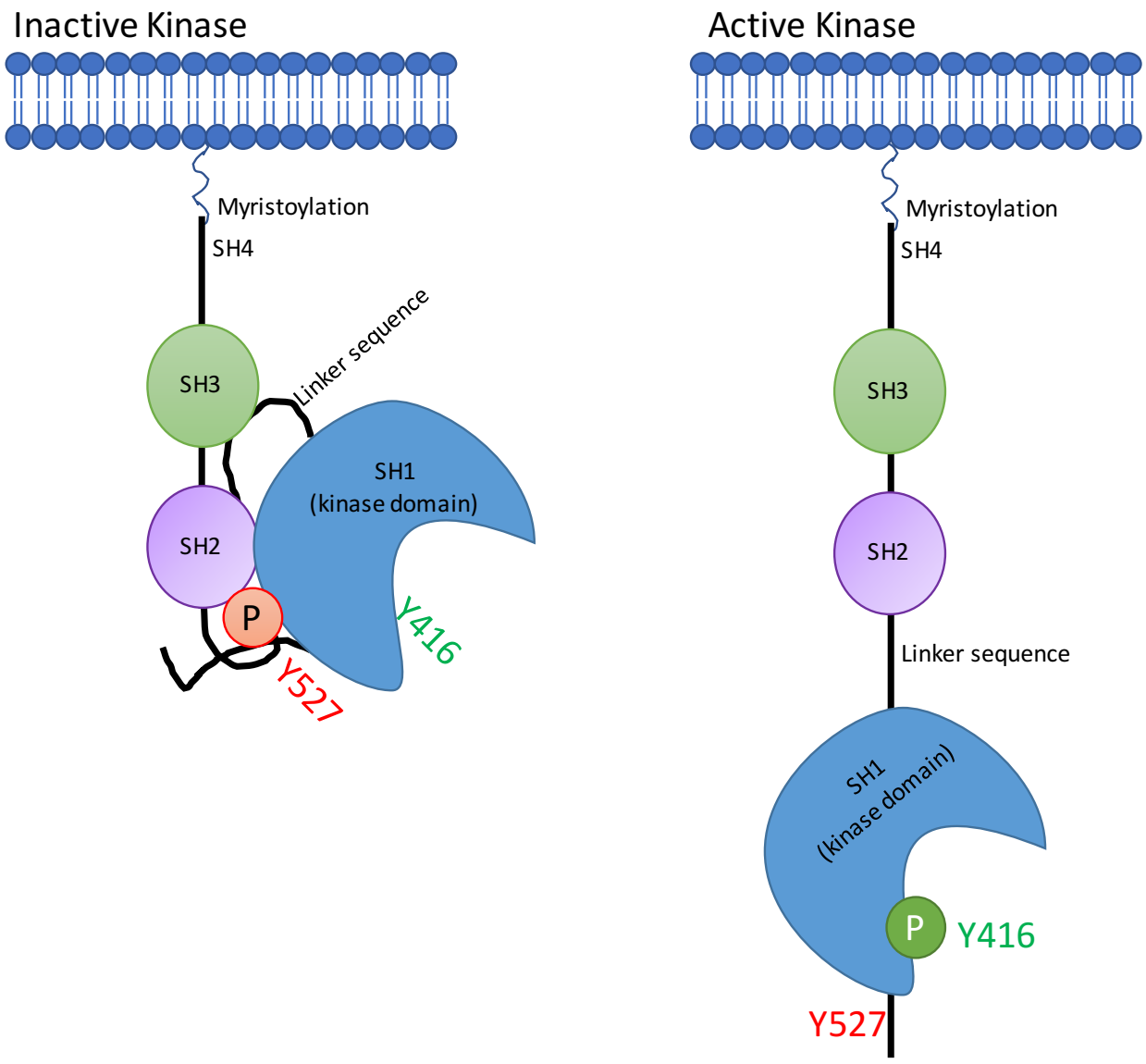

Figure 1.2: Activation of Src Family Kinases
Src Family Kinases (SFKs) are composed of 4 Src Homology (SH) domains. SH4 serves as a myristoylation site targeting the protein to the cytoplasmic membrane. The SH3 and SH2 domains regulate protein-protein interactions. These are followed by a linker sequence to the SH1 domain, which is the tyrosine kinase domain. Phosphorylation of Y527 inactivates the kinase by causing an intramolecular reaction between the SH2 domain and phosphorylation site. Conversely, phosphorylation of Y416 allows for complete activation of the kinase.

necessary *in vivo* for increasing vascular permeability following VEGF stimulation[64]. When cells are exposed to LPS, downstream activation of Src, Fyn, and Yes appear to impair barrier function[41]. In addition, thrombin-induced Src activation impairs barrier function, while conversely Fyn is essential in endothelial cell barrier recovery in response to thrombin[65]. Lyn activity may even inhibit permeability increase and stabilize the endothelial barrier in the presence of LPS and VEGF[66]. Src-dependent phosphorylation of the cadherin-catenin complex is thought to result in the dissociation and internalization of VE cadherin[8,11,38,43,67–69]. Depletion of CSK expression is sufficient to induce tyrosine phosphorylation via SFKs, but not internalization of VE cadherin[47]. Therefore SFK-mediated phosphorylation of VE cadherin is not sufficient for the disruption of the cadherin-catenin complex[47,48].

Previous studies demonstrate that not all SFKs regulate the endothelial barrier in the same manner, with activation of some resulting in barrier enhancement and others disruption. In cell culture, inhibition of SFKs through treatments such as PP2 or Dasatinib prevents the endothelial cell barrier from recovering after disruption[66,70]. However, such treatments inhibit all SFKs, which offers a possible explanation for the observed treatment-induced side effects of fluid retention and pleural effusion[71,72]. In addition, SFK activation is detected upon stimulation of the endothelial cell barrier enhancer S1P[73]. Therefore, SFKs are activated during both endothelial barrier enhancement as well as disruption, making it difficult to delineate their specific role in endothelial barrier function regulation.

1.3.1 The role of Src in regulating VE cadherin

Three of the five known tyrosine phosphorylation sites on VE-cadherin are phosphorylated in a Src-dependent manner (Y658, Y685 and Y731)[23,47,53] (Figure 1.3). Phosphorylation of Y658 is

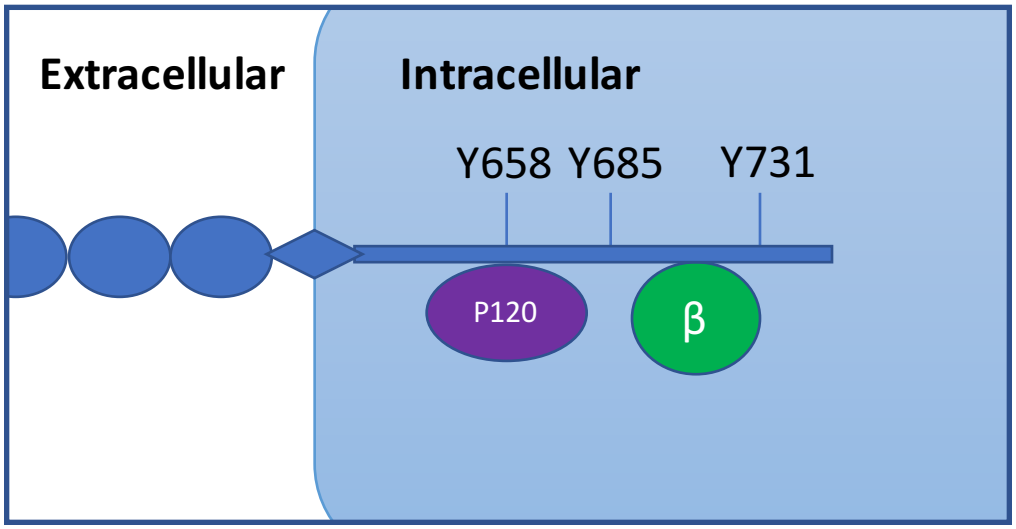

Figure 1.3: VE cadherin phosphorylation by Src
VE cadherin is phosphorylated at Y658, Y685, and Y731 in a Src Family Kinase-dependent manner. The canonical view is that phosphorylation of VE cadherin Y658 disrupts binding of VE cadherin with P120-catenin while phosphorylation of Y731 disrupts its binding with β-catenin. However, more recent studies have demonstrated that although phosphorylation of VE cadherin at these sites may be necessary for disruption of cadherin-catenin complex, it does not appear to be sufficient.

proposed to prevent interaction with p120-catenin, whereas phosphorylation of Y731 prevents interaction with β-catenin[46]. Thus, these two phosphorylation events are proposed to jointly stimulate adherens junction disassembly. Src-mediated phosphorylation of VE cadherin on these sites is not sufficient to cause disassembly of adherens junctions and disruption of the barrier[43,47]. VE cadherin mutations Y658F and Y685F have been shown to block VE cadherin internalization through permeability promoting agents; both of these residues have been found to be phosphorylated *in vivo* in veins but not arteries under basal conditions, noteworthy because in veinous Src is constitutively active due to continuously low shear stress[43]. In this same study it was concluded that phosphorylation of VE cadherin contributed to its dynamic state; however, phosphorylation of VE cadherin at Y658 and Y685 in the absence of an inflammatory agent is insufficient to induce its internalization[43]. Additional work has demonstrated that phosphorylation of Y685 is the main driver of permeability and that phosphorylation of Y731 is not required for increased endothelial permeability. De-phosphorylation of Y731 actually induces VE cadherin interaction with AP-2, leading to its endocytosis[48]. Thus, the phosphorylation of VE cadherin at specific sites appears to have different effects on VE cadherin internalization and its subsequent role in regulating the endothelial cell barrier.

1.3.2 Src-dependent regulation of Rho-GTPases

In addition to regulating the endothelial cell barrier function by directly altering the phosphorylation status of adherens junctions, Src also regulates the adherens junctions through activation of small Rho-GTPases leading to cytoskeletal rearrangement, and by the formation and regulation of focal adhesions[1,8]. Rho GTPases are important regulators of the endothelial cell barrier[74–76]. Rho GTPases are active when bound to guanosine-5'-triphosphate (GTP) while they are inactive when bound to guanosine 5'-diphosphate (GDP)[77]. Rho guanine nucleotide exchange

factors (GEFs) stimulate the exchange of GDP for GTP on Rho GTPases, thus leading to activation. Conversely, Rho GTPase activating proteins (GAPs) negatively regulate Rho GTPase activity by accelerating the hydrolysis of GTP[78,79].

Src signaling is important for the regulation of Rho GTPases, GEFs, and GAPs and their subsequent regulation of adherens junctions and the endothelial cell barrier function. For example, Vav2 is a Rac1 GEF that is phosphorylated following Src activation. This phosphorylation event leads to subsequent phosphorylation of VE cadherin on serine-665 via PAK, ultimately resulting in β-arrestin-mediated endocytosis of VE cadherin and an increase in barrier permeability[80]. Additionally, Src has been shown to target Tiam-1, a Rac1 GEF that is required for endothelial barrier maintenance, for destruction via phosphorylatoin[81]. Conversely, Src can also activate Rac1 through an alternative GEF called Dock180[82], making the overall regulation of Rac1 through Src complex.

The Cdc42 Rho GEF, faciogenital dysplasia gene product-1 related Cdc42-GEF (FRG), is also activated by Src[83]. Likewise, Src activates RhoA GAP, p190RhoGAP, resulting in the inhibition of RhoA and Rho kinase (ROCK) and the loss of stress fibers (contractile actin bundles)[84]. In general, Rac1 and Cdc42 are both thought to stabilize the endothelial cell barrier, while RhoA is thought to disrupt the barrier[76,85]. However, a basal level of RhoA promotes membrane localization of VE cadherin and maintains inter-endothelial junctions by increasing intracellular tension and decreasing cell spreading by the assembly of stress fibers and strengthening cortical actin[76,86,87]. On the other hand, sustained Rac1 activation results in endothelial dysfunction[88].

In summary, the regulation of RhoGTPases via Src is multi-faceted and exerts many different effects on the cell, likely due the fact that Src is activated for different amounts of time and to

various degrees by multiple stimuli. In addition, these stimuli also activate multiple kinases, which makes dissecting the specific role of Src difficult.

1.3.3 Effect of Src activation on other downstream signaling pathways

Following Src activation, cells undergo dramatic changes in their cytoskeleton that leads to rearrangement and cell contraction[89]. By phosphorylating myosin light chain kinase 1 (MLCK-1), Src activation causes actin-myosin contraction and subsequent changes in cell shape and interendothelial gap formation[68,89]. In addition to altering the cell morphology via RhoGTPases, Src is known to regulate focal adhesion formation and persistence through multiple pathways[90]. Focal adhesions are large macromolecular complexes that sense mechanical force and regulatory signals transmitted between the cell-extracellular matrix (ECM) adhesions[91]. Multiple Src substrates are components of focal adhesions; FAK and paxillin, two of these components, are regulated through phosphorylation by Src[92–94]. In addition, Src also phosphorylates integrins[95], leading to their activation and thus initiating tyrosine phosphorylation of the focal adhesion protiens[96]. Src-dependent phosphorylation of the integrins and the focal adhesion proteins is critical for establishing the focal adhesion attachment to actin stress fibers and thus focal adhesion formation[97]. The permeability of the endothelial cell barrier is not only regulated by the adhesions of the adherens junctions, but also through the focal adhesions[1], emphasizing the importance of this aspect of Src regulation.

Src regulates lamellipodia and adherens junction adhesion through the lipid kinase phosphatidylinositide 3 kinase (PI3K)[98]. PI3K phosphorylates the 3'-position hydroxyl of the D-myo-inositol head group generating phosphoinositide[99]. There are 3 classes of PI3K (I, II, and III). Class I signaling is activated by a variety of extracellular stimuli and has been implicated in a variety of cellular processes including: cell cycle, cell growth, cell motility, cell adhesion and

cell survival[100,101]. Class I PI3K (PI3K) phosphorylates PtdIns(4,5)P_2 producing PtdIns(3,4,5)P_3[102] which then can be subsequently converted to PtdIns(3,4)P_2 by inositol lipid phosphatases[100]. Both PtdIns(3,4,5)P_3 and PtdIns(3,4)P_2 bind to peckstrin homology (PH) domains of proteins, initiating the re-localization and altering the activity of PH containing proteins[103]. PI3Ks contain a p110 catalytic subunit, of which there are 4 isoforms (α, β, γ, and δ), and a regulatory adaptor subunit, encoded by 3 genes (p85α, p85β, and p55γ)[100,104]. The p85 and p110 subunits together initiate the re-localization and catalytic activity of PI3K.

Upon activation of a receptor tyrosine kinase (RTK) the SH2 domain of p85 interacts with the tyrosine phosphorylated cytoplasmic tail of the receptor[103,105]. The p85 subunit brings the catalytic subunit (p110) to the plasma membrane where it binds the SH2 of the RTK[106] allowing for it to generate PtdIns(3,4,5)P_3. PtdIns(3,4,5)P_3 binds to PH domain of AKT initiating its recruitment to the plasma membrane from the cytosol. Once at the plasma membrane AKT interaction with PtdIns(3,4,5)P_3 causes a conformational change in AKT, allowing it to be phosphorylated at threonine (T)308 and serine (S)473[107,108]. Phosphorylation of AKT at T308 by phosphoinositide dependent kinase 1 (PDK1)[109–111] partially activates AKT, however, for full activation AKT needs to be phosphorylated at S473 as well. A variety of kinases phosphorylate S473 including PDK2, mechanistic target of rapamycin complex (mTORC), and DNA-dependent protein kinase (DNA-PK)[112,113]. A decrease in PtdIns(3,4,5)P_3 causes the de-phosphorylation of AKT via S/T phosphatases leading to its inactivation[114]. Therefore, changes in the localization of AKT and its phosphorylation status at S473 and T308 are readouts for PI3K activity.

PI3K associates physically with multiple signaling proteins, including SFKs[115]. Upstream activation of Src initiates the binding of PI3K to E cadherin. Src dependent tyrosine

phosphorylation is necessary for PI3K coupling to E cadherin, lamellipodia formation, and initiation of cadherin-specific adhesive contact zones[98]. PI3K activity is an important mediator of lamellipodia formation. Constitutively active forms of PI3K are capable of activating RhoGTPases, including Rac-mediated membrane ruffles and focal complexes, as well as Rho-mediated stress fibers and focal adhesions[106]. However, PI3K is not able to activate all of the classical Rac/Rho-mediated cellular responses – instead, it appears that PI3K is only able to activates small pools of RhoGTPase effectors localized near the lipid products[100]. PtdIns(3,4,5)P_3 is enriched in protruding lamellipodia where it activates upstream actin polymerization signals, driving the formation of F-actin at the protrusion's leading edge[116–119]. PI3K, Rac1, and Src are all important components of lamellipodia formation and cell spreading; however, the temporal contribution of these 3 key regulators is not completely understood.

1.4. Approaches and challenges of studying kinases in living cells

Understanding the dual roles of SFKs in regulating the endothelial cell barrier function has been limited by the slow acting and non-specific tools previously employed to control kinase activity, including down-regulation of expression, overexpression of constitutively active (CA) mutants, and broadly acting stimuli. Genetic approaches of regulating kinase activity are often insufficient due to their slow effect and the adaptability of the signaling network. These methods do not allow for both specific and direct activation of a SFK with the ability to monitor cellular and biochemical changes over time.

Phosphorylation is involved in virtually every cellular process, providing cells with the ability to rapidly transduce signals through the cell in a reversible nature[120]. Kinase-mediated phosphorylation processes are multistep and contain complex networks of cross-talk, with both feed-forward and feed-back steps. Elucidation of how kinases regulate pathways is only

achievable by determining both how these networks connect spatiotemporally and how specific kinases contribute to individual steps of these networks[121]. The ability to study the temporal effects of kinase activity relies on strategies that allow for the specific activation and inactivation of kinases. It is crucial that these strategies are both rapid-acting and specific, so that individual dissection of kinase-mediated pathways is possible.

The use of protein inhibitors allows for the rapid blocking of the catalytic activity of a kinase; however, these inhibitors usually lack specificity and inhibit multiple kinases (e.g. PP1, Dasatinib). Shokat and colleagues have provided the ability to rapidly and specifically inhibit a variety of kinases via chemical-genetic inhibition of kinases[122–130]. Their approach is composed of two main components. First, there is a mutation of a conserved bulky residue in the catalytic domain of a kinase, designated the gate-keeper residue. By mutating a bulky side chain to a glycine or an alanine, the kinase pocket is enlarged. Second, bulky modifications are made to kinase inhibitors to form analog inhibitors that can no longer inhibit wild-type kinases. The increased steric hindrance of the derived analog inhibitor clashes with the bulky gatekeeper residues of wild-type kinases, restricting inhibition to only the engineered kinase (Figure 1.4). This method has addressed many of the concerns of inhibiting kinase activity using non-specific inhibitors or classical genetic approaches and allows for rapid and specific inhibition of kinases. However, this approach limits the studies of kinases to a loss-of-function approach. Therefore, methods that allow for the induction or activation of a specific kinase are also needed.

Karginov and Hahn developed an inducible kinase method allowing for specific activation of engineered kinases[90,131]. This method works through the insertion of a small FK506-binding protein (iFKBP) into the kinase, rendering it catalytically inactive. The iFKBP serves as an

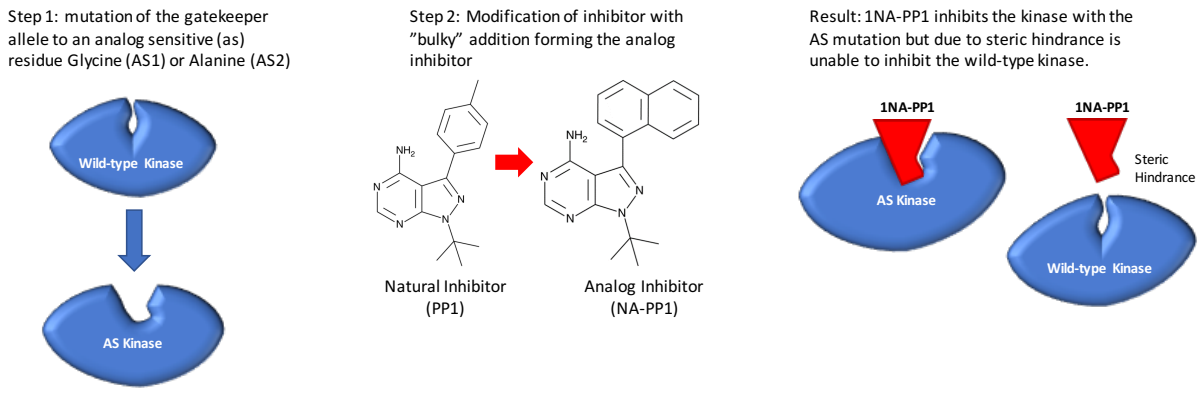

Figure 1.4: Kinase inhibition using analog-sensitive alleles
Schematic depicting the steps required to engineer specific kinase inhibition using analog-sensitive (AS) alleles. This approach requires mutation of a conserved bulky hydrophobic residue in the kinase active site (designated the gatekeeper residue) to a smaller residue such as glycine or alanine. This modified kinase can be specifically targeted using modified natural kinase inhibitors. These modified natural kinase inhibitors contain a bulky group, and the analogue is sterically confined to the engineered kinase (AS kinase) Meanwhile the unmodified kinases (wild-type) are not inhibited due to their smaller kinase active sites.

allosteric switch that allows for induction of catalytic activity only in the presence of the FKBP12-rapamycin-binding (FRB) domain of mTOR and rapamycin. When treated with rapamycin (or a non-immunosuppressive rapamycin analog), the FRB heterodimerizes with the iFKBP. This heterodimerization stabilizes the catalytic domain and reactivates catalytic activity. The FRB can either be co-transfected/infected with the rapamycin-regulated kinase (RapR-kinase) (Figure 1.5).

A modified version of the RapR-kinase method can also be used to dissect specific pathways downstream of the kinase. Rapamycin-regulated targeted activation of pathways (RapRTAP) allows for the coupling of a specific kinase to a protein complex or subcellular region (Figure 1.6)[90]. This is achieved by fusing FRB to a protein of interest or directing its localization to a specific subcellular region. The RapRTAP method has been previously used to dissect Src signaling through two of its known substrates, p130Cas and FAK. To restrict Src interaction with endogenous proteins, Src amino acid 175 was mutated from an arginine (R) to a leucine (L) (R175L). The Src R175L mutation blocks the ability of Src to bind through its SH2 domain while not altering its catalytic activity[90]. The RapRTAP method expands the ability of the RapR-kinase system by allowing for a more precise dissection of kinase mediated pathways than global activation of a kinase.

However, one limitation of the RapR-kinase methodology is that it only allows for activation of a kinase and not its subsequent inactivation. Due to the dynamic nature of phosphorylation, having a system that allows for both specific and rapid activation and subsequent inactivation is needed to more accurately recapitulate kinase activity in signaling pathways of interest. The ability to control activity of a kinase for a finite period of time would allow for dissecting how the length of kinase activity alters downstream signaling.

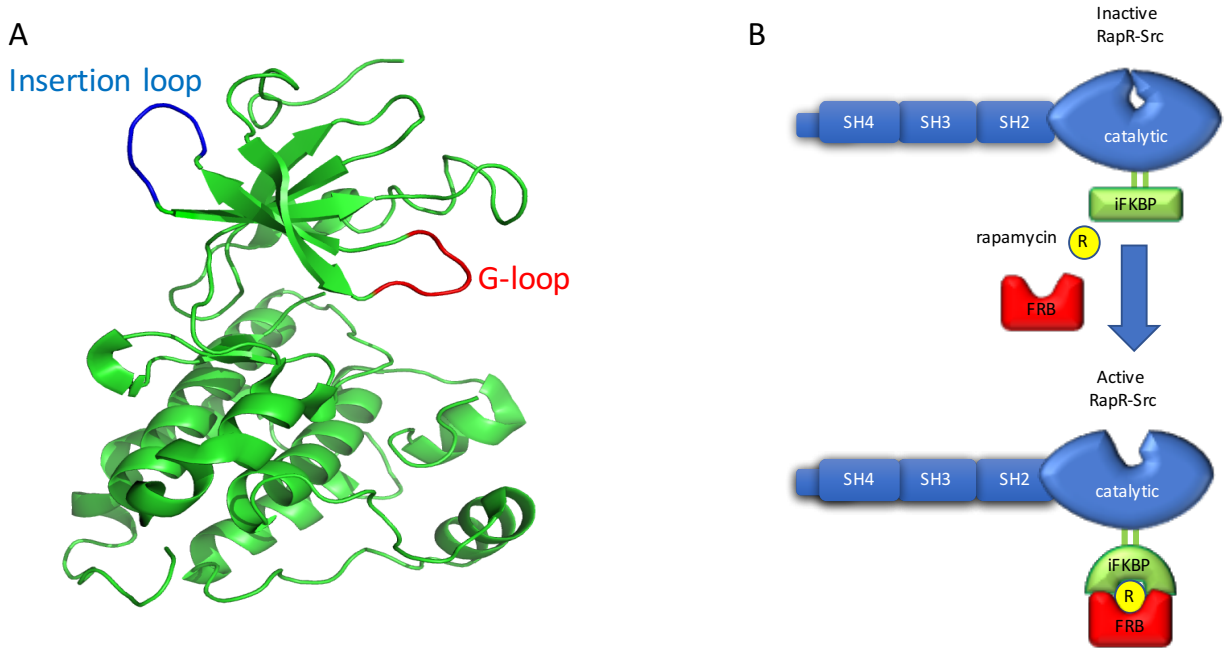

Figure 1.5: Rapamycin-mediated regulation (RapR) of protein kinases
(A) iFKBP, a small protein derived from human FKBP12, is inserted into c-Src in the area designated as the insertion loop (blue) across form the G-loop (red). (B) In the absence of rapamycin, the RapR-kinase is rendered catalytically inactive; however, in the presence of rapamycin, iFKBP forms a tight complex with another small protein domain – FRB. Rapamycin and FRB binding dramatically reduce the structural dynamics of iFKBP, thus restoring the catalytic activity of the kinase.

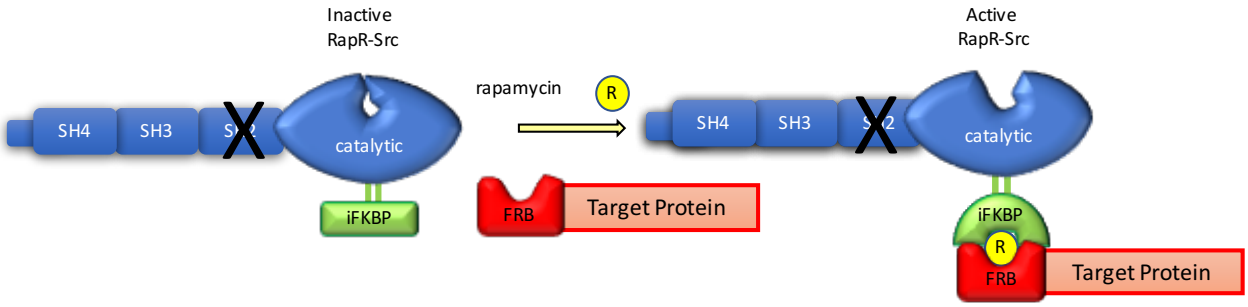

Figure 1.6: RapR targeted activation of pathways (RapRTAP)
RapRTAP technology allows for the activation of a specific kinase in a specific protein complex by fusing FRB to a known binding partner of the kinase. Mutating Src at R175L blocks the ability of Src to bind to endogenous proteins through its SH2 domain without affecting its catalytic activity.

1.5. Statement of Aims

Aim 1. Determine how Src regulates endothelial cell barrier function through adherens junctions. Using engineered Src (RapR-Src), we specifically activated Src and monitored the temporal effects on the endothelial cell barrier function using trans-electrical resistance as well as fluorescent-based assays that allowed for evaluating changes in total and localized permeability. Using a combination of biochemical techniques and variety of microscopy strategies, including classical approaches such as confocal and wide-field, as well as more advanced techniques such as live cell imaging and structured illumination microscopy, we evaluated the localization and rearrangement of VE cadherin, VE cadherin's association with P120- and β-catenin, and its phosphorylation status. In addition, we evaluated the effect of mutating key tyrosine phosphorylation residues (Y658 and Y731) of VE cadherin to phenylalanines to determine their role in Src-dependent changes on the endothelial cell barrier.

Aim 2. Engineering RapR-kinases with on/off capabilities to dissect molecular pathways. We combined the RapR-kinase method with the previously described chemical-genetic inhibition technique developed by Shokat and colleagues[122–130]. By inserting the gatekeeper mutation into RapR-kinases and modifying the FRB protein, we engineered kinases with on/off capabilities. We biochemically evaluated our ability to turn engineered kinase, Src (RapR-Src-as2), on and off. Using live cell imaging and biosensors, we analyzed how the length of Src activation altered cell signaling and morphology through the RhoGTPase Rac1 and the lipid kinase PI3K. Furthermore, we used biochemical assays to analyze the ability to transiently activate kinases with targeted substrates using a modified version of the RapR-TAP approach.

Finally, we evaluated whether both the RapR-kinase and RapR-TAP approach could be utilized with other kinases by engineering the serine/threonine kinase p38.

CHAPTER 2: BARRIER ENHANCING FUNCTION OF SRC AND VE CADHERIN PHOSPHORYLATION IN ENDOTHELIAL CELLS REVEALED BY SYNTHETIC BIOLOGY APPROACH

**This project was a collaborative project; figures produced by other researchers are indicated in legends.*

2.1 Introduction

The endothelium is composed of a single layer of cells which line the vessel wall and form a semi-permeable barrier that regulates the interchange of cells, proteins, and fluid between the interstitial and vascular space[1]. Regulation of the endothelial cell barrier is crucial for maintaining proper fluid balance and interstitial pressure. Permeability-increasing agents or inflammatory cytokines can disrupt the endothelial cell barrier; causing gaps in the cell-cell contacts and allowing the passage of solutes and cells[8,11,132,133]. The endothelial cell barrier is maintained by a combination of cell-cell adhesions and cell-extracellular matrix (ECM) adhesions. The cell-cell adhesions are regulated by interendothelial junctions composed of adherens, tight, and gap junction complexes[1,8]. The adherens and tight junctions form the cell-cell contacts while the gap junctions allow the passage of water, ions, and other small molecules from cell to cell. In the majority of the endothelium tissues adherens junctions are the predominant regulators of the cell-cell adhesions, because for the most part, tight junctions are only abundant in the brain endothelium[8]. Endothelial adherens junctions are predominantly mediated by the transmembrane protein vascular endothelial (VE) cadherin. VE cadherin contains five extracellular repeats, a transmembrane domain, and a cytoplasmic tail[21]. The extracellular repeats control the cell-cell contacts in a calcium dependent manner. Through the cytoplasmic tail, VE cadherin interacts with catenins (p120-, β-, γ- (also called plakoglobin), and α-catenins) (Figure 1.1)[12].

Phosphorylation of the cadherin-catenin complex is key for the regulation of the adherens junctions, providing a mechanism for rapid alterations of their composition and arrangement[8,36–38]. The phosphorylation of VE cadherin is thought to result in the destabilization of the adherens junctions disrupting the cadherin-catenin complex[41,45,46,50–53]. However, phosphorylation of VE cadherin does not appear to be sufficient for the disruption of the adherens junctions[43,47,48]. For example, the kinetics of VE cadherin/catenin phosphorylation and the subsequent increase in endothelial cell permeability do not always correlate with one another. Phosphorylation of VE cadherin via treatment with VEGF or the phosphatase inhibitor pervanadate both result in a rapid enhancement of the endothelial cell barrier; occurring simultaneously with the tyrosine phosphorylation of the cadherin-catenin complex. The subsequent disruption of the adherens junction and increase in permeability only occur following prolonged cadherin-catenin phosphorylation[54]. Therefore, the disruption of the barrier following VE cadherin phosphorylation is neither sufficient nor does it always temporally correspond to enhanced permeability of the endothelium.

Src Family Kinase (SFK) member c-Src (Src), a non-receptor tyrosine kinase, phosphorylates VE cadherin on Y658, Y685 and Y731 downstream of multiple permeability promoting agents and cytokines[8,11,23,38,43,67–69]. Like all SFKs, Src activity is regulated by two phosphorylation sites. Phosphorylation of residue Y527 by c-terminal Src Kinase (CSK)[62] inactivates Src by creating an intramolecular interaction between the phosphorylated residue and the SH2 domain. Dephosphorylation of Y527 allows Src to adopt an open conformation and autophosphorylate itself at Y416, initiating full catalytic activity[63] (Figure 1.3). Phosphorylation of Y658 and Y731 via Src are thought to disrupt the cadherin interaction with p120-catenin and β-catenin respectively[46]. However, Src-mediated phosphorylation of VE cadherin on these sites is not

sufficient to cause disassembly of adherens junctions nor endothelial cell barrier disruption[47]. Mutations of VE cadherin at Y658 or Y685 to a phenylalanine block VE cadherin internalization by inflammatory agents, however, phosphorylation of these sites in the absence of an inflammatory agent is insufficient to induce VE cadherin internalization[43,47]. Alternatively, de-phosphorylation of Y731 by Src homology 2-domain phosphatase (Shp2) induces VE cadherin interaction with AP-2, leading to its endocytosis[48]. Thus, the phosphorylation of VE cadherin at specific sites appear to have different effects on VE cadherin internalization and its role in regulating the endothelial cell barrier.

Activation of Src and other SFKs is generally thought to be endothelial cell barrier disruptive[43,73,134–136]. However, in addition to being activated during disruption of the endothelial cell barrier, SFKs are activated upon stimulation with the endothelial cell barrier enhancer sphingosine-1-phosphate (S1P)[73]. Furthermore, inhibition of SFKs through treatments such as PP2 or Dasatinib prevents the endothelial cell barrier from recovering following disruption[66,70]. Understanding the role of Src and other SFKs in regulation of the endothelial cell barrier has been unclear partially because of the limitation in tools used to study specific kinases in live cells. Previous evaluations have relied on slow acting and non-specific techniques to control kinase activity, including down-regulation of *Src* expression, overexpression of constitutive active (CA) *Src* mutants, and broadly acting stimuli. These methods do not allow for both the specific and direct activation of Src with the added ability to monitor cellular and biochemical changes over time. Rather, an inducible kinase activation system is required to temporally dissect the effects of activating a specific kinase.

To circumvent the difficulties associated with inhibition and genetic approaches of studying a kinase, we employed an inducible kinase system, the rapamycin-regulated (RapR)-kinase

system[90,137,138]. The RapR-kinase system allows for the direct activation of a specific kinase. Furthermore, it allows for the ability to monitor the temporal effects of activating the kinase. In brief this method works by inserting a portion of the FK506 binding protein-12 (iFKBP) into the kinase of interest, rendering it catalytically inactive. The iFKBP domain then serves as an allosteric switch that allows for induction of catalytic activity only in the presence of the FKBP12-rapamycin-binding (FRB) domain and rapamycin. Previous work has verified that insertion of the iFKBP only regulates catalytic activity and does not affect protein-protein interactions, intramolecular interactions, or localization of RapR-kinases, and extensive characterization of RapR-Src shows that it functions the same as endogenous Src[90,137]. RapR-Src allowed for interrogation of how Src activity temporally regulates the endothelial cell barrier.

By activating Src with the RapR-kinase method we observed that Src activation resulted in a transient increase in endothelial cell barrier enhancement followed by a subsequent decrease. In addition, we only observed VE cadherin gap formation and internalization following prolonged Src activation. Furthermore, we found that Src activation enhanced the rate of barrier recovery following disruption of the endothelial cell barrier. Conversely, activation of fellow SFK member Lyn only promoted endothelial cell barrier disruption and did not change the rate of recovery following disruption. Src mediated endothelial barrier enhancement occurred concurrently to rearrangement of the adherens junctions and actin, as well as the production of lamellipodia. In addition, phosphorylation of VE cadherin at Y731 was found to be required for retention of VE cadherin at the cell periphery and endothelial cell barrier enhancement following Src activation. Furthermore, blocking the Y731 phosphorylation site with a phenylalanine mutation blunted endothelial barrier enhancement via the physiological stimuli S1P. In conclusion, we found that Src activation not only resulted in a transient enhancement of the

endothelial cell barrier but that Y731 phosphorylation is required for both Src and S1P mediated enhancement.

2.2 Materials and Methods

2.2.1 Antibodies and chemical reagents

The following antibodies were used: anti-GAPDH (Ambion, cat. no. AM4300), anti-mCherry (Biovision, cat. no. 5993-100), anti-GFP (Clontech, cat. no. 632381), anti-paxillin (Fisher Scientific, cat. no. BDB612405), anti-phospho-paxillin (Y118) (Invitrogen, cat. no. 44-722G), anti-c-Src (Santa Cruz, cat. no. sc-8056), anti-phosphotyrosine (4G10) (Millipore, cat. no 05-321), anti-VE-cadherin (Santa Cruz, cat. no. sc-6458), anti-phospho-VE-cadherin (Y658) (Thermo Fisher, cat. no. 44-1144G), anti-phospho-VE-cadherin (Y731) (Thermo Fisher, cat. no. 44-1145G), anti-phospho-VE-cadherin (Y685) was a gift from the laboratory of Dr. Elisabetta Dejana (IFOM), anti-β-catenin (Santa Cruz, cat. no. 1496), anti-myosin light chain 2 (Cell Signaling, cat. no. 3672), anti-phospho-myosin light chain 2 (S19) (Cell Signaling, cat. no. 3671), anti-Src (Santa Cruz, cat. no. 8056), anti-Src (Cell Signaling cat. no. 2108), anti-phospho-Src family (Y416) (Cell Signaling cat. no. D49G4), anti-P120-catenin (Santa Cruz, cat. no. sc-1101), anti-cortactin (BD Sciences, cat. no. 610049), anti-Rac1 (Fisher Scientific, cat. no. BDB 610650), phalloidin Alexa Fluor™ 647 (Thermo Fisher, cat. no. A22287), Cy™5 anti-rabbit (Jackson ImmunoResearch Laboratories, cat. no. 711-175-152), Alexa Fluor® 488 anti-goat rabbit (Jackson ImmunoResearch Laboratories, cat. no. 705-545-003), Alexa Fluor® 647 anti-goat rabbit (Jackson ImmunoResearch Laboratories, cat. n.o 705-607-003), Fluorescein isothiocynate (FITC) (Jackson Immuno Research Laboratories, cat. no. 715-096-151). The following reagents were used: IgG-coupled agarose beads (Millipore, cat. no. IP04-1.5ML), Rapamycin (LC Laboratories, cat. no. R5000) Leupeptin hemisulfate (Gold Biotechnology, cat.

no. L-010-5), and Aprotinin (Gold Biotechnology, cat. no. A-655-25), Fluorescein isothiocyanate-dextra (Sigma-Aldrich cat. no. 46944), D-*erythro*-sphingosine-1-phosphate (Avanti Polar Lipids, cat. no. 860492), Human Alpha Thrombin (Factor IIa) (Enzyme Research Laboratories, cat. no. HT1002a), Avidin-FITC (Invitrogen, cat. no. 43-4411), biotinylated gelatin (Sigma cat. no. G2500), Saracatinib (Santa Cruz, cat. no. sc-364607), Rac1 pull-down activation assay biochem kit (Cytoskeleton, Inc. cat. no. BK035), and donkey serum (Jackson ImmunoResearch, cat. no. 017-000-121)

2.2.2 Plasmids and Adenoviruses

Stargazin-mVenus construct (previously described[138]) was used for transient transfection. Adenoviral VE cadherin constructs were a gift from Dr. William Mueller (Northwestern University). RapR-Lyn-cerulean-myc was produced from RapR-Lyn-GFP-myc[139] by site-directed mutagenesis as described by[131,140]. The principles of site-directed mutagenesis have been previously described in greater detail [131,137]. In brief this method works via the generation of a "mega primer" which is used to insert desired DNA fragments into plasmids. The "mega primer" contains the desired insertion sequence flanked by two target sequences which anneal to the plasmid on either side of the insertion sequence. To generate adenoviruses RapR-Src-cerulean-myc[90], RapR-Src-as2-mCherry-myc[138], RapR-Src-as2-cerulean-myc[138], RapR-Src-R175L-cerulean-myc, RapR-Src-Lyn-cerulean-myc, and mCherry-FRB[140] were moved into a pShuttle construct. The RapR-Src-as2 constructs contain Threonine 338 to Alanine mutation making them sensitive to the allele specific inhibitor 1NA-PP1 (1-Naphthyl-PP1). To move mCherry-FRB and Y66S-GFP-FRB (colorless) into pShuttle, mCherry-FRB and Y66S-GFP-FRB[138] were amplified using primers flanked with the restriction sites Not1 and EcoRV. The pShuttle vector was also cut with Not1 and EcoRV. The insert and vector were gel purified and the insert was ligated into

the construct. RapR-constructs and the pShuttle vector were all digested XhoI and HindIII restriction sites. The inserts and vector were gel purified and ligated together. Adenovirus production and amplification was done in collaboration with Dr. Jody Martin (Vector Core Facility at University of Illinois – Chicago).

2.2.3 Cell culture, transfection, and infection

HPAEC-Human Pulmonary Artery Endothelial Cells (Lonza, cat. no. CC-2530) and HUVEC-Human Umbilical Vein Endothelial cells (Lonza, cat. no. C2517A) were grown in EGM™-2 BulletKit™ (Lonza, cat. no. CC-2162) with 10-% FBS at 37°C and 5% CO_2. Low passage cells were purchased from Lonza, amplified and frozen at passage 5, and subsequently used for experimentation between passages 6 and 8. Cells were grown on surfaces coated with 0.2% gelatin (plastic dishes and electrodes) or 0.2% gelatin and fibronectin (5 mg/L) when plated on glass coverslips. Transfections were done on cells at 70-80% confluency using Fugene 6 reagent (Promega Corporation) according to manufacturer's protocol; experiments were performed 24 hours after transfection. For adenoviral infections, cells were exposed to the virus for 24 hours prior to use.

2.2.4 Immunofluorescence staining

Cells were fixed with 4% paraformaldehyde, permeabilized with 0.5% Triton X-100, blocked in 20% donkey serum and 2% Bovine Serum Albumin (BSA). Samples were incubated with the designated primary antibodies (1:100) in 10% donkey serum and 1% BSA for 1 hour at room temperature or overnight at 4°C and then in secondary antibodies (1:200) in 0.5% BSA for 45 minutes. Prepared coverslips were mounted on slides using Fluoromount-G™.

2.2.5 Immunoprecipitation

RapR-Src constructs were activated by treating cells with either rapamycin or equivalent volumes of ethanol (solvent control) for the indicated amount of time. After treatment, cells were lysed with lysis buffer (20 mM HEPES-KOH, pH 7.8, 50 mM KCl, 100 mM NaCl, 1 mM EGTA, 1% NP40, 1 mM NaF, 0.1 mM Na_3VO_4, 0.033% ethanol, aprotinin 16 μg/ml, and Leupeptin hemisulfate 3.2 μg/mL), and centrifuged at 4,000 rpm, 4°C, for 10 minutes. Cleared cell lysates were immunoprecipitated with the indicated antibody for 1.5 hours at 4°C. Beads were washed (20 mM Tris-HCl, 1 mM DTT, 40 mM NaCl, 30 mM $MgCl_2$, 1 mM NaF, 0.1 mM Na_3VO_4, 0.033% ethanol, aprotinin 16 μg/ml, and Leupeptin hemisulfate 3.2 μg/mL) and then re-suspended in 2X Sample Buffer + 2% 2-Mercaptoethanol.

2.2.6 Protein expression comparisons

Western blot band intensities were analyzed using ImageJ. The percent phosphorylation relative to time 0 values for S1P and thrombin treatments were determined by dividing the Y416 level by the total Src level. All time points were then standardized to time 0. The average and standard deviation for each time point was calculated for 4 independent experiments. A two-sample t-test was used to compare the averages for each time point to time 0. Myosin light chain-2 phosphorylation levels after rapamycin was calculated using the same approach. Since the basal level of VE cadherin phosphorylation was so low instead of dividing by time 0, we instead divided by the time point with the maximum phosphorylation level for each experiment. An average of 5-6 independent experiments was calculated and a two-sample t-test was used to compare the averages of each time point to time 0. Co-immunoprecipitation (percent) of the catenins was determined by dividing the amount of each catenin in the immunoprecipitation sample by the amount of VE cadherin in the immunoprecipitation sample for the corresponding time point. All time points for each experiment were then standardized to time 0. The average

and standard deviation of 4 independent experiments was determined and a two-sample t-test was used to compare each time point to time 0.

2.2.7 FITC-Avidin Assay

The FITC-Avidin assay was performed as previously described[141]. In brief, HPAE cells were plated on sterilized glass coverslips coated with biotinylated gelatin for 48 hours until a monolayer had formed. Cells were treated with FITC-avidin (1:200) for 2 minutes. Coverslips were quickly washed with pre-warmed 4% formaldehyde and immunofluorescence stained (see above) for VE cadherin-Alexa647.

2.2.8 FITC-Dextran Assay

HPAE cells were plated on transwells (Corning Inc, cat. no. 353495) for 48 hours. To be able to visualize cells and test for construct(s) expression, an equal number of cells/cm^2 were plated on a non-transwell plate, from which cell lysates were collected and analyzed by Western Blot. Cells were infected with RapR-Src-as2-cerulean-myc and mCherry-FRB or mCherry-FRB alone for 24 hours. Cells on the transwell plate were treated with rapamycin (500 nM) for the designated amount of time and 15 minutes prior to collection, Dextran (40 kDa) labeled with FITC was added to the top chamber. Aliquots from both the top chamber and bottom chamber were removed and the amount of FITC-fluorescence was measured in duplicate. The amount of fluorescence from the lower chamber was divided by the amount in the upper chamber. Values for each condition were standardized to their respective time 0. The average and standard deviation from 3 independent experiments were calculated. A two-sample t-test was used to compare each time point to time 0.

2.2.9 Trans-electrical Resistance

Cells were plated on gelatin-coated 8W10E+ electrodes (Applied Biophysics). Changes in electrical resistance were measured at an impedance of 4000Hz and a constant voltage using an Electric Cell Substrate Impedance Sensing system (Applied Biophysics). Cell lysates were prepared in parallel for all construct expressing cells to verify expression and activation via rapamycin when appropriate.

2.2.10 Image Collection

Fixed sample Imaging**:**

Samples were imaged using wide-field, confocal, or via Structured Illumination Microscopy (SIM), figure legends designate what type of microscopy was used. Wide-field images were collected on an Olympus IX-83 microscope with a PlanApo N 60x TIRFM objective (oil, NA 1.45) or UPlanSAPO 40X (oil, NA 1.25) objective. Confocal images were collected on a Zeiss 880 equipped with a PlanApo 63X (oil, NA 1.4) objective. SIM images were collected on a Nikon N-SIM microscope with a CFI Apochromat TIRF (oil, NA 1.49). 3D renderings were generated using IMARIS software.

Live cell Imaging:

HPAE coverslips were placed into an Attufluor Cell Chamber (Invitrogen, cat. no. A78-16) with Leibovitz (L-15) medium (Sigma Aldrich, cat. no. L1518-500mL) supplemented with 5% FBS. Samples were imaged either via wide-field or 3D-SIM. Wide-field imaging was done using an Olympus IX-83 microscope controlled by Metamorph software and equipped with a heated stage (Warner Instruments), PlanApo N 60x TIRFM objective (oil, NA 1.45), Xcite 120 LED (Lumen Dynamics) light source, and Image EMX2 CCD (Hamamatsu) camera. Live cell 3D-SIM imaging was performed as previously described[142] at Janelia Research Center with the assistance of the Advanced Imaging Center. Samples were maintained at 37 °C and 5%

CO_2 using a stage-top incubator (H301, Okolabs, Naples, Italy). Excitation patterns were produced using a phase-only spatial light modulator (Bolder Vision Optik, BVO AHWP3). A mask system was employed to select the 0 and ±1 diffraction orders, which were then focused onto the back focal plane of a Zeiss Plan-Apochromat × 100 1.46NA objective. Optimal interference contrast was achieved in the sample, by rotation of the polarity of the light to match the angle of the pattern using a liquid crystal variable retarder (LC, Meadowlark, SWIFT) and wave plates. Interference filters were used to collect the emissions and a pair of sCMOS cameras (Hamamatsu, Orca Flash 4.0 v2 sCMOS) were used to collect images. Raw image sets were reconstructed as described previously[143].

2.2.11 Image Analysis

FITC-Avidin:

Images of VE cadherin-Alexa647 and FITC-Avidin were collected on a wide-field microscope at 60X and analyzed using Metamorph. Specifically, the VE cadherin channel was used to designate reticular adherens junctions (>4.5 μm wide) and linear (<2.5 μm wide) adherens junctions. The total integrated intensity of the FITC-Avidin was measured directly underneath the two types of junctions manually. The average total integrated intensity and standard deviation for each type of junction was calculated. For each adherens junction type 30 junctions from 3 independent experiments were measured. An equal number of reticular and linear junctions were imaged from each sample preparation. A blocked-Anova test was used to compare the two types of junctions across experiments.

VE cadherin Average Intensity and Area:

HPAE cells infected with RapR-Src-as2-cerulean-myc and mCherry-FRB or mCherry-FRB. Cells were treated with Rapamycin for 0 or 30 minutes, fixed, and stained with DAPI and

VE cadherin-Alexa488. Images were analyzed using Metamorph as follows. A mask of the nucleus was made and dilated by 6.7 μm. This was then subtracted from the VE cadherin image to remove the perinuclear accumulation of VE cadherin. A mask of the adherens junctions as designated by VE cadherin was generated and the average relative intensity inside of the adherens junctions was measured. The average intensity of the VE cadherin at the adherens junctions was then divided by the average intensity of the raw VE cadherin image to determine the relative average intensity of VE cadherin in the adherens junctions. A binary mask was generated of the VE cadherin in the adherens junctions and the total integrated intensity was measured to determine the area of VE cadherin in the adherens junctions. For each condition the average and standard deviation of the relative average intensity was determined. Between 60-70 frames from 3-4 independent experiments were analyzed. A blocked-Anova test was used to compare 0 and 30 minute samples for each condition.

Protrusive Activity Analysis:

Changes in protrusive activity were calculated following the previously described method[90]. In brief, Stargazin-mVenus construct was used to label the cell plasma membrane. Cells expressing Stargazin-mVenus and the adenovirus constructs (RapR-Src-cerulean-myc and mCherry-FRB) were selected using epifluorescence imaging. Cells were only imaged if they were in a monolayer. Time-lapse movies (N= 30 cells) were generated by collecting images in 2 minute intervals and analysis was performed using Metamorph and CellGeo software[144]. Stargazin-mVenus images were used to create a binary mask of a cell via MovThresh software[144]. Protrusive activity (the sum of areas which undergo local extensions between consecutive movie frames) was analyzed using ProActive software[144]. To determine the change in protrusive activity the protrusive activity at a given time point was divide by the average

protrusive activity prior to rapamycin treatment. The average and 90% confidence interval for each time point of all cells treated in the same conditions was calculated, these values were then standardized to the initial time point.

VE cadherin Cytoplasm Accumulation Analysis:

Monolayers of HPAE cells expressing the appropriate adenoviruses at nearly 100% efficiency (VE cadherin-gfp constructs, RapR-Src-as2-cerulean-myc and mCherry-FRB) were imaged live every 2 minutes in YFP, CFP, and mCherry. VE cadherin constructs were imaged using the YFP filter to separate from cerulean tagged RapR-Src-as2. Metamorph was used to create a binary mask of the cytoplasm using mCherry-FRB, which localizes to the cell cytoplasm, for each time point. The cytoplasm binary was then multiplied by the VE cadherin YFP image for the corresponding time point. The resulting image was used to calculate the average intensity of VE cadherin in the cytoplasm. This value was divided by the average intensity of the raw VE cadherin image, producing the relative average intensity for each time point. The relative average intensity for each time point was divided by the average of the relative average intensity for the frames prior to rapamycin treatment, calculating the standardized relative average intensity. For each VE cadherin construct the standardized relative average intensity for all frames at each time point was averaged and the 90% confidence interval was calculated. A two-sample t-test was used to test for significance every 30 minutes between the two mutant VE cadherin and wild-type VE cadherin expressing cells. The following number of fields were imaged for each VE cadherin construct: Wild-Type N=15, Y658F N=21, and Y731F N=28.

2.3 Results

SFKs are activated during both endothelial cell barrier enhancement and disruption

S1P and thrombin both activate Src family kinases (SFKs) and exert differing effects on the endothelial cell barrier[70,145]. We confirmed these previous observations in human pulmonary arterial endothelial (HPAE) cells. S1P activation caused a significant increase in SFK activation, as measured by Y416 phosphorylation as early as 1 minute post-treatment (Figures 2.1a-b). Furthermore, co-treatment with S1P and the SFK inhibitor Saracatinib drastically reduced S1P mediated endothelial cell barrier enhancement as measured by trans electrical resistance (TER) (Figures 2.1c-d). In addition, we observed that treatment with α-thrombin caused activation of SFKs both during the endothelial cell barrier disruption (1 minute) and recovery phases (30 minutes and 2 hours) (Figures 2.2a-b). Inhibition of SFKs at 15 minutes, post-α-thrombin treatment significantly diminished recovery of the endothelial cell barrier as measured by TER (Figures 2.2c-d). Therefore, SFK activation occurs both in endothelial cell barrier enhancement as well as disruption scenarios.

Src but not Lyn activation enhances the endothelial cell barrier

To further investigate how SFKs regulate the endothelial cell barrier we employed the RapR-kinase system[90,137,138]. This approach allowed us to directly activate c-Src (Src) and LynA (Lyn) in HPAE cells. To do this we generated adenoviruses of: RapR-Src, RapR-Src-as2 (a reversible form of RapR-Src), RapR-Lyn, and FRB constructs tagged with fluorescent proteins. The constructs efficiently infected HPAE cells and both RapR-Src and RapR-Lyn were potently activated via rapamycin treatment as demonstrated by their ability to phosphorylate the SFK substrate paxillin (Figures 2.3a-c). Furthermore, RapR-Src and RapR-Src-as2 both phosphorylated paxillin equivalently, meaning that the two constructs behaved the same in HPAE cells and were interchangeable; subsequent experiments indicate which construct was used (Figures 2.3a-b). Rapamycin treatment with FRB alone had no effect on paxillin

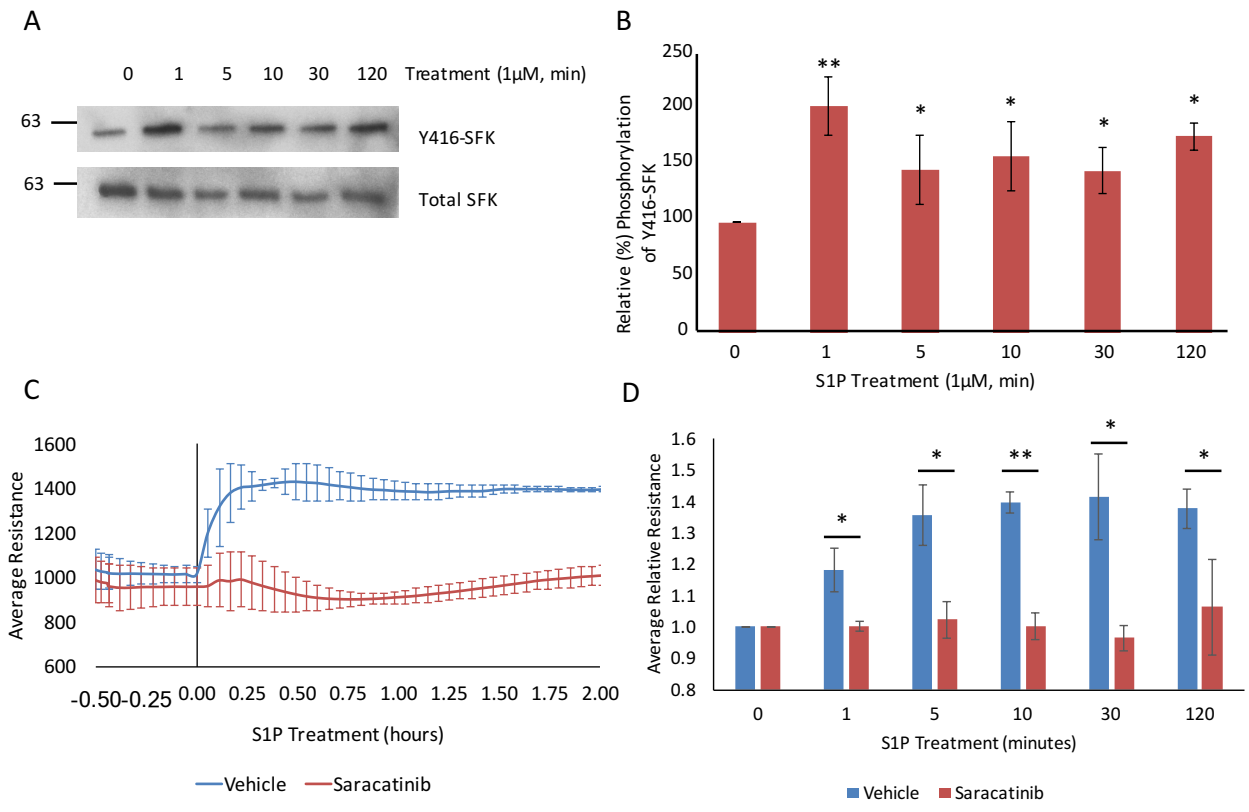

Figure 2.1: Activation of Src Family Kinases by S1P treatment
(A-B) HPAE cells were serum starved for 1 hour and then treated with 1 μM S1P, cell lysates were collected at the indicated time points and Western Blotted for: Y416-SFK, Total SFK, and GAPDH. (B) The average of 4 independent experiments was calculated and standardized to time 0. A two-sample t-test for each time point compared to 0 was used to determine significance. (C-D) HPAE cells were serum starved for 1 hour and then analyzed via TER at a constant voltage; 1 μM S1P and 100 nM Saracatinib or vehicle (DMSO) were added at time point 0. (C) The graph is from 3 experiments depicting the average resistance and 90% confidence interval for each treatment. (D) Average relative resistance was calculated and analyzed at the designated time points. A two sample t-test was used to compare vehicle to Saracatinib treated at each of the indicated time points. **$p<0.001$, *$p<0.05$.

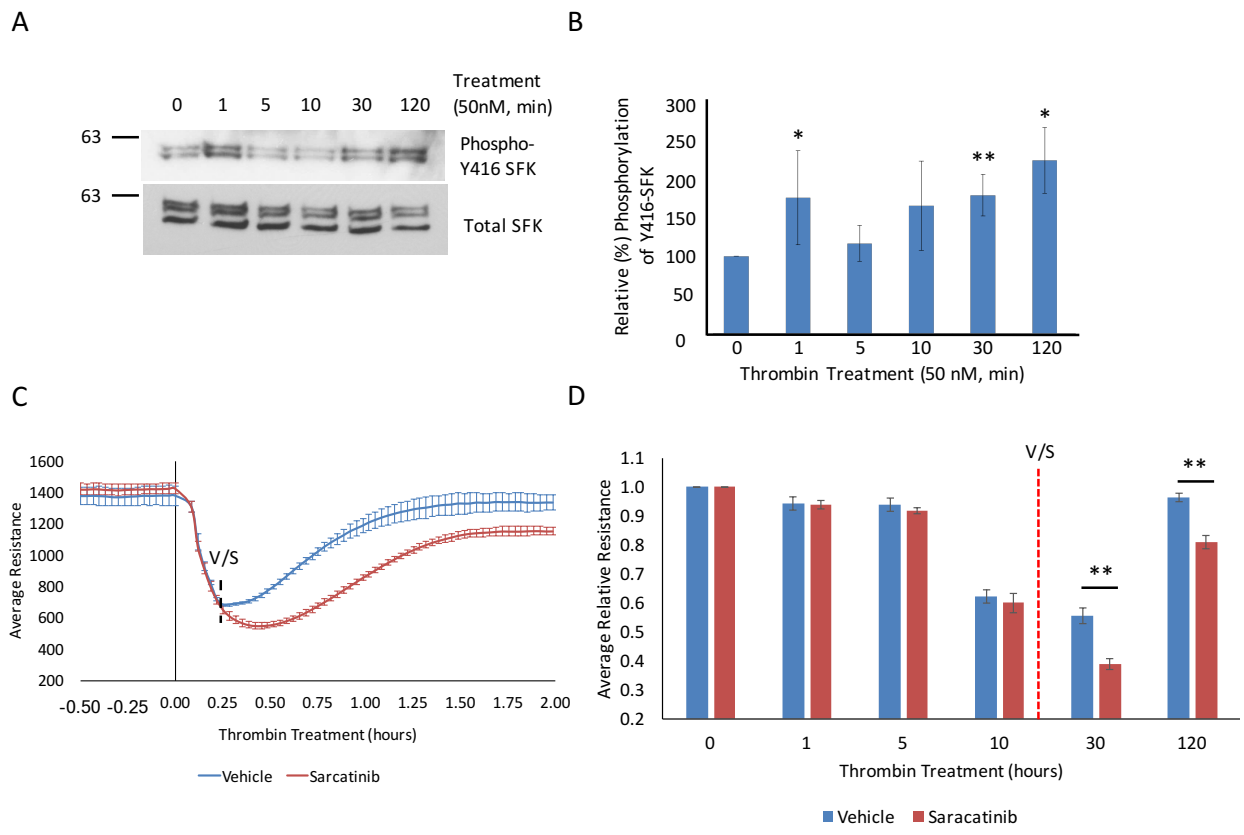

Figure 2.2: Activation of Src Family kinases by α-thrombin treatment
(A and B) HPAE cells were serum starved for 1 hour and then treated with 50 nM of Thrombin, cell lysates were collected at the indicated time points and Western Blotted for: Y416-SFK, Total SFK, and GAPDH. (B) The average of 4 independent experiments was calculated and standardized to time 0. A two-sample t-test for each time point compared to 0 was used to determine significance. (C) Inhibition of SFKs blocks endothelial cell barrier recovery following thrombin treatment. HPAE cells were serum starved for 1 hour and then analyzed using TER at a constant voltage. Thrombin (50 nM) (TH) was added at time point 0 and Saracatinib (100 nM) (S) or vehicle (ethanol) was added 15 minutes later (V). (C) The graph is from 4 experiments depicting the average resistance and 90% confidence interval for each treatment. (D) Average relative resistance was calculated and analyzed at the designated time points. A two sample t-test was used to compare vehicle to Saracatinib treated at each of the indicated time points. **$p<0.001$, *$p<0.05$.

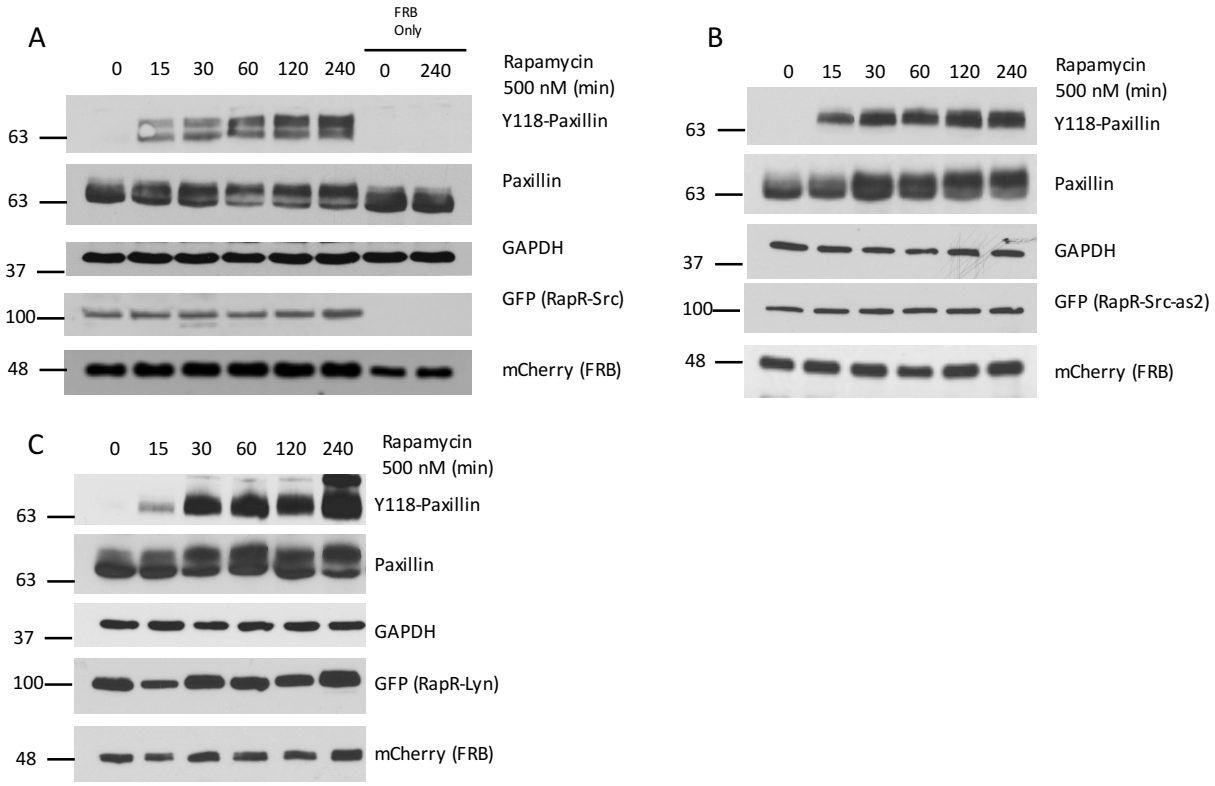

Figure 2.3: Rapamycin efficiently activates RapR-Src and RapR-Lyn in HPAE cells
HPAE cells were infected with: RapR-Src-cerulean-myc (A), RapR-Src-as2-cerulean-myc (B) or RapR-Lyn-cerulean-myc (B) and mCherry-FRB or mCherry-FRB only (A). Cells were activated with rapamycin (500 nM) for the specified amount of time. Cell lysates were collected and immunoblotted for the designated proteins.

phosphorylation (Figure 2.3a), verifying the observed phosphorylation was due to kinase activation and not rapamycin treatment. To investigate how each of these kinases independently affected the endothelial cell barrier we temporally monitored how their activation altered the endothelial cell barrier using TER. Src activation resulted in a dynamic biphasic change in endothelial cell barrier function, initially causing a transient increase in endothelial cell barrier resistance, followed by drop at later time points. Conversely, Lyn activation only initiated an increase in endothelial cell permeability (Figures 2.4a-c). Interestingly, the R175L mutation in Src, which prohibits the binding of Src to other proteins through its SH2 domain, blocked Src mediated enhancement of the endothelial cell barrier (Figures 2.4a-c). Furthermore, Src (Figure 2.5a) but not Lyn (Figure 2.5b) activation following α-thrombin treatment enhanced the rate of endothelial cell barrier recovery. Treatment of cells expressing FRB alone with rapamycin verified that the observed changes in endothelial cell barrier were dependent on the activation of the kinases (Src and Lyn) not rapamycin (Figures 2.4a-b and 2.5d). Since Src but not Lyn seemed to induce endothelial cell barrier enhancement, we opted to focus on the role of Src in regulating the endothelial cell barrier. To verify that the observed transient increase in endothelial cell barrier induced by Src was not specific to HPAE cells, we also tested Src activation in Human Umbilical Vein Endothelial (HUVE) cells. Src activation effects on the endothelial cell barrier in HUVE cells mirrored HPAE cells (Figure 2.6). To further confirm the role of Src activation on the endothelial cell barrier we used an alternative method to detect changes in permeability. A FITC-Dextran transwell assay done on HPAE cells showed an even more dramatic enhancement of the endothelial cell barrier following Src activation as well as a subsequent decrease following prolonged activation. However, rapamycin treatment of cells

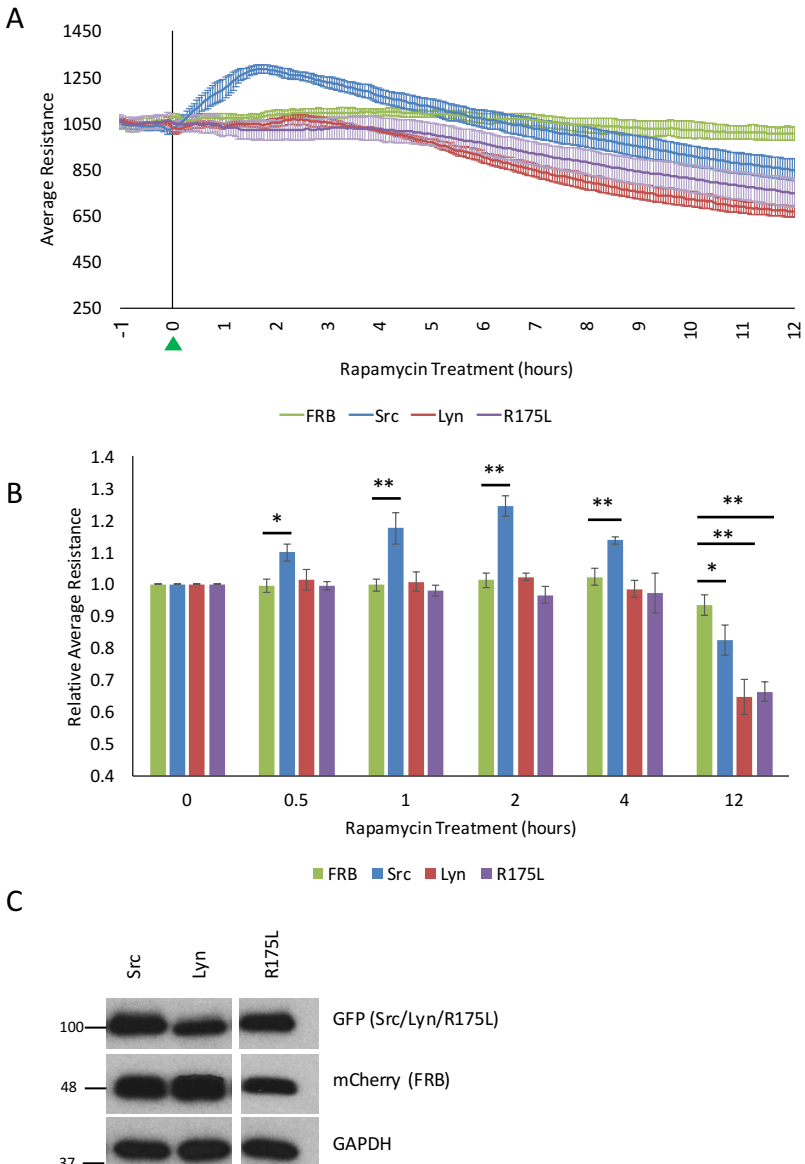

Figure 2.4: Activation of Src but not Lyn enhances endothelial cell barrier
HPAE cells cells infected with RapR-Src-as2-cerulean-myc (Src) and mCherry-FRB, RapR-Lyn-cerulean-myc (Lyn) and mCherry-FRB, RapR-Src-R175L-cerulean-myc (R175L) and mCherry-FRB or mCherry-FRB alone (FRB). (A) Cells were analyzed using TER at a constant voltage. Rapamycin (500 nM) was added at time point 0 (green triangle). The graphs are representative of 3 independent experiments depicting the average resistance and 90% confidence interval for each treatment. (B) The average relative resistance at the indicated time points for: Src, Lyn, and R175L and compared to FRB only using two sample t-test; graphs depict average and standard deviation. *$p<0.05$, **$p<0.001$. (C) Western blot comparing RapR-Src, RapR-Lyn, and R175L expression in cells infected in parallel to TER assay.

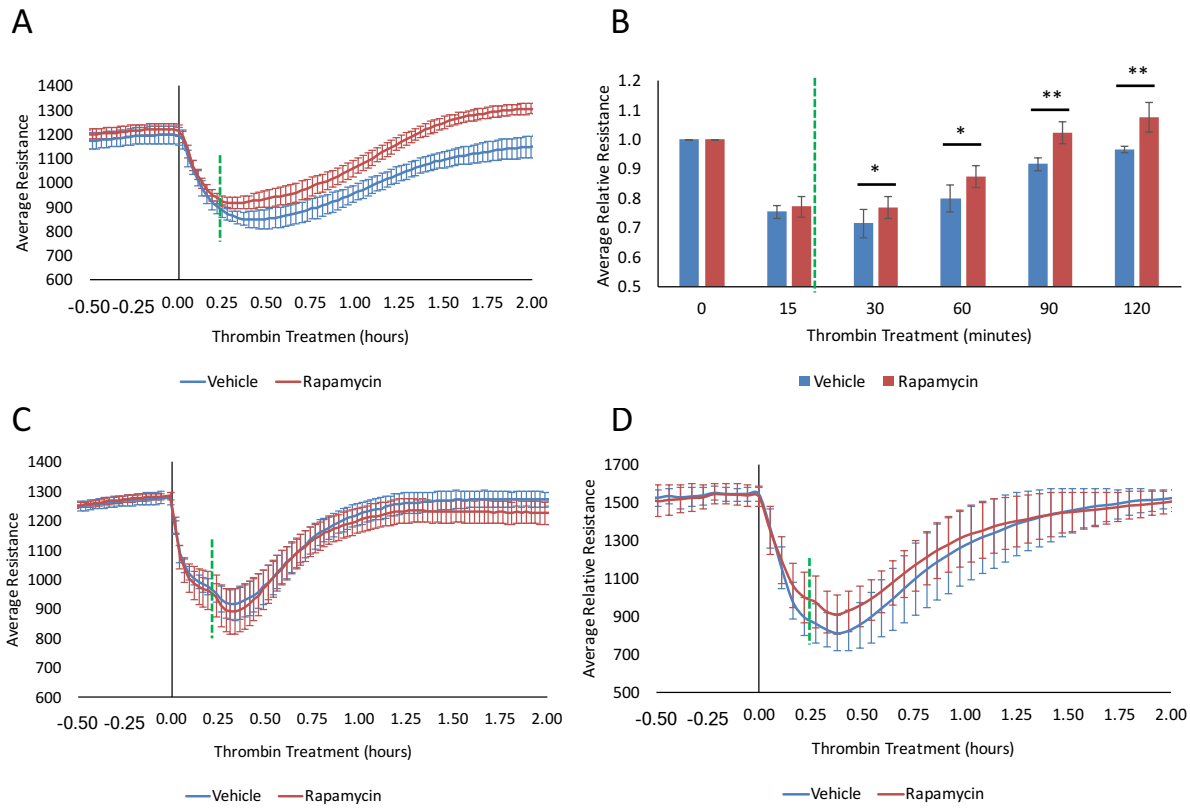

Figure 2.5: Activation of Src but not Lyn enhances endothelial cell barrier recovery
HPAE cells infected with: (A-B) RapR-Src-cerulean-myc and mCherry-FRB, (C) RapR-Lyn-cerulean-myc and mCherry-FRB, (D) or mCherry-FRB alone. (A, C, and D) Cells were analyzed using TER at a constant voltage with readings taken every 30 seconds. α-thrombin (50 nM) was added at time point 0 (dashed line –TH) and rapamycin (500 nM) or vehicle (ethanol) (green triangle) was added 15 minutes later. The graphs are an average of 3 experiments and the error bars depict the 90% confidence intervals. (B) Average relative resistance was calculated and analyzed at the designated time points. A two sample t-test was used to compare vehicle to rapamycin treated at each of the indicated time points. *$p<0.05$, **$p<0.001$.

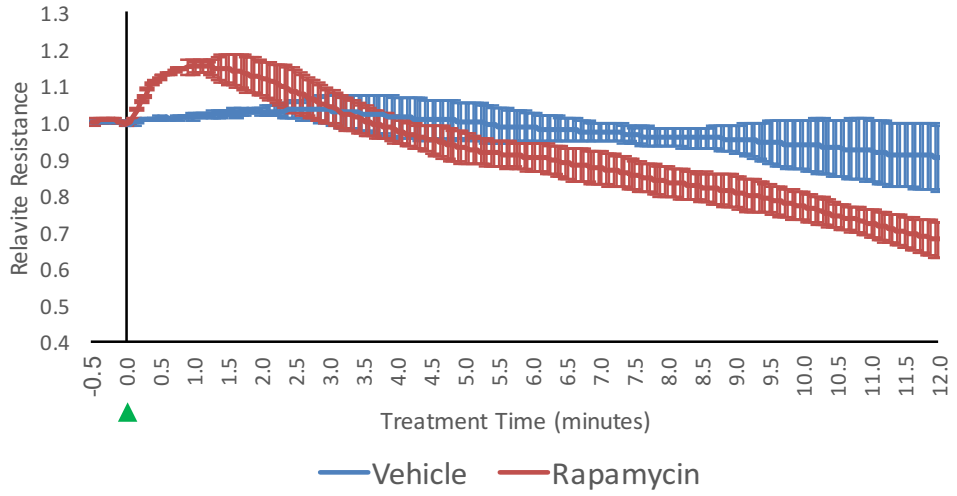

Figure 2.6: Src mediated endothelial cell barrier enhancement in HUVE cells
HUVE cells were infected with RapR-Src-cerulean-myc and mCherry-FRB and were analyzed using TER at a constant voltage. Rapamycin (500 nM) or vehicle (ethanol) was added at time point 0 (green triangle). All wells were standardized to their average prior to treatment at time point 0. The average for 4 wells for each treatment was determined and graphed over time, error bars represent standard error of the mean for each treatment.

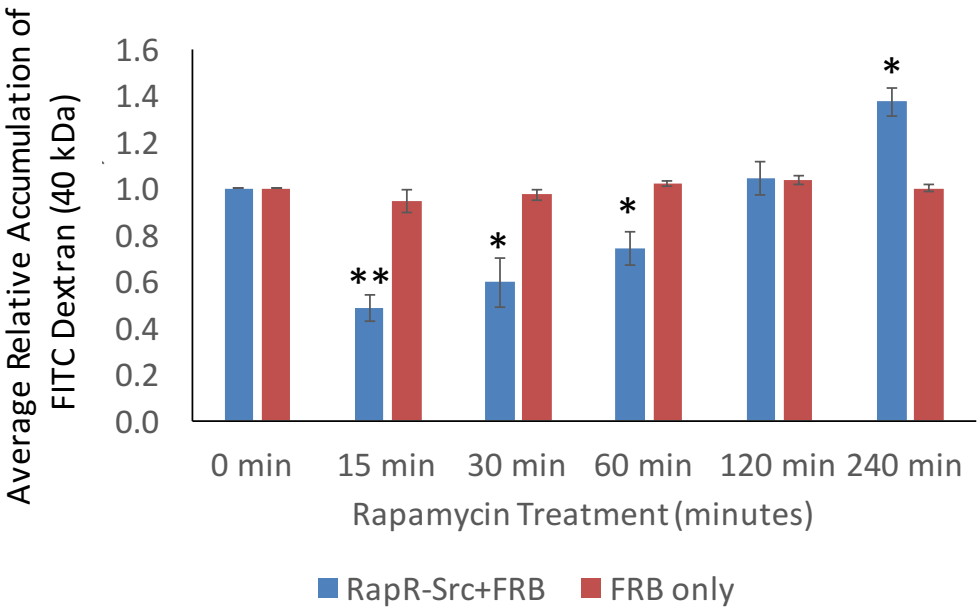

Figure 2.7: Src activation causes transient endothelial cell barrier enhancement
HPAE cells were infected with RapR-Src-as2-cerulean-myc and mCherry-FRB or mCherry-FRB only and activated with rapamycin. FITC-Dextran was added to the cell media for the last 15 minutes of designated amount of time following rapamycin addition. The fluorescence intensity was measured in media collected from both the top and bottom well in duplicate. The average relative intensity of FITC from the bottom of the transwell compared to the average from the top was calculated for each well. Each well was then standardized to time 0. The averages and standard deviations are from 4 independent experiments. A two-sample t-test was used to compare each treatments time point 0, p**<0.001, *p<0.05.

expressing FRB alone had no effect at any time point (Figure 2.7). Therefore, different SFKs affect the endothelial cell barrier differently; with Src but not Lyn exerting a transient enhancement of the barrier as well as increasing the rate of barrier recovery.

Src activation increases VE cadherin at the adherens junctions

To determine how direct Src activation affects adherens junction components localization and structure, we stained endogenous VE cadherin and P120-catenin in confluent HPAE cells both during the barrier enhancement (30 minutes) and disruption (4 hours) phases. The enhancement and disruption phases were defined by TER and the FITC-Dextran assay (Figures 2.4 and 2.7). VE cadherin and P120-catenin were both localized at the adherens junctions at 30 minutes post Src activation. Gaps in the monolayer and re-localization of the adherens junctions were observed at 4 hours post-activation (Figure 2.8a) corresponding with the changes observed in permeability (Figures 2.4 and 2.7). Wide-field imaging suggested a broadening and increased intensity of VE cadherin at the 30 minute time point (Figures 2.8a-b). To quantify this observation, we measured the relative amount of VE cadherin at the adherens junctions at 0 minutes and 30 minutes after Src activation. At 30 minutes, we observed a significant increase in intensity of VE cadherin at the adherens junctions and treatment of cells expressing FRB alone showed no accumulation of VE cadherin at 30 minutes (Figure 2.8c). We also quantified the area of VE cadherin in the adherens junctions at 0 and 30 minutes following Src activation. Activation of Src initiated a significant increase in the area of VE cadherin in the junctions, conversely, rapamycin treatment of cells expressing FRB alone had no effect on the area of VE cadherin (Figure 2.8d).

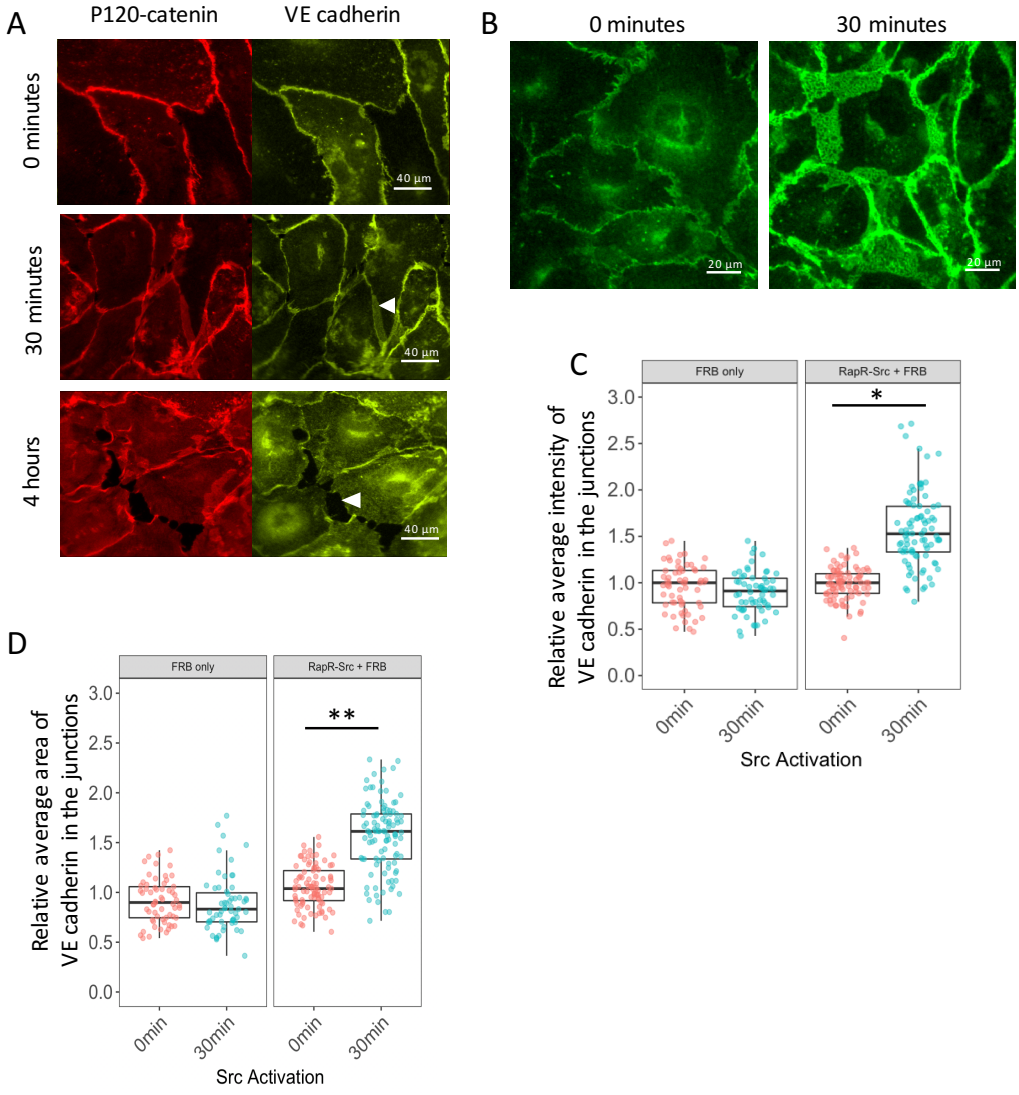

Figure 2.8: Src activation causes an increase in VE cadherin at the adherens junctions
(A-C) HPAE cells infected with RapR-Src-cerulean-myc and mCherry-FRB or (C and D) mCherry FRB alone were activated with rapamycin (500 nM) for the designated amount of time. Cells were fixed and stained for P120-catenin with Alexa647 secondary (A) and/or VE cadherin with Alexa488 secondary (A-D) and imaged (wide-field) on an Olympus IX-83 at 40x (A) or 60x (B and C) magnification. (A) The arrows at 30 minutes indicate broader adherens junctions and at 4 hours gaps in the monolayer. (C-D) The relative average intensity (C) and area (D) of VE cadherin at the cell edge was quantified for RapR-Src and FRB expressing cells, 85 fields from 4 independent experiments for each time point, and FRB only expressing cells, 62 fields from 3 independent experiments for each time point. The values are standardized to the median value for 0 minutes and analyzed using a blocked Anova, **p<0.001, *p<0.05 to compare across experiments.
**(C-D) Rima Rebiai (Karginov laboratory) and Jennifer Klomp both performed sample preparation and imaging; Jennifer Klomp performed image analysis.*

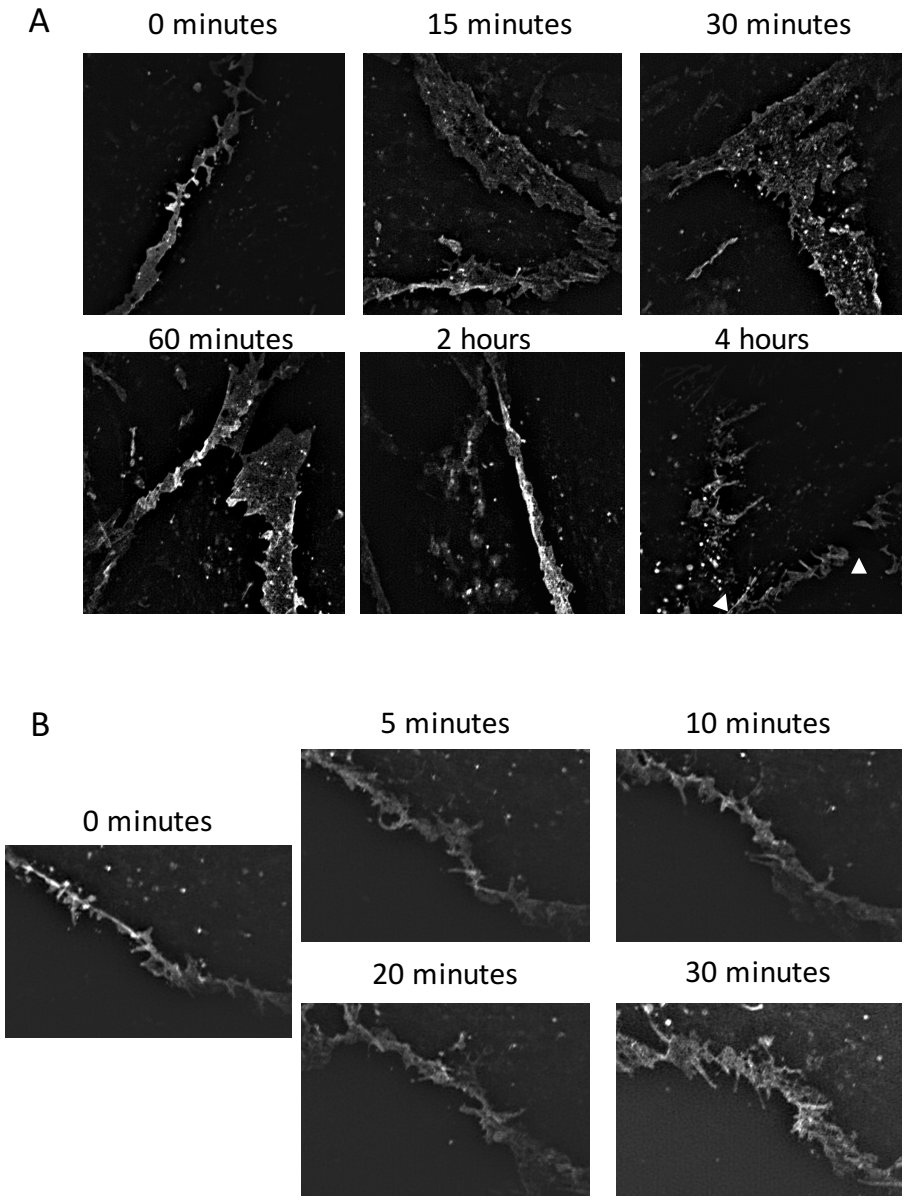

Figure 2.9: Live SIM shows broadening of adherens junctions via Src activation
(A and B) HPAE cells infected with RapR-Src-as2-cerulean-myc, mCherry-FRB, and VE cadherin-GFP were imaged in GFP live on a 3D-SIM microscope. (A) Images from different areas of a confluent endothelial cell monolayer collected at the designated time points following rapamycin (500 nM) treatment. White triangles indicate gaps in VE cadherin. (B) The same area was imaged at the designated time points following rapamycin treatment (500 nM).

Src activation induces the formation of reticular adherens junctions

To further evaluate the broadening of the adherens junctions we used live Structured Illumination Microscopy (SIM). We expressed VE cadherin GFP in cells with RapR-Src and FRB, activated with rapamycin and imaged adherens junctions at different cellular locations for 4 hours. As before, we observed an initial broadening of the adherens junctions during the Src mediated endothelial cell barrier enhancement period (Figure 2.9a). Live imaging of the same adherens junction during the first 30 minutes following Src activation also demonstrated widening of the adherens junctions (Figure 2.9b). Wide-field and confocal images of fixed cells revealed that the VE cadherin in the broader regions appeared to be rearranging into distinct structures, previously described as overlapping or reticular adherens junctions[35,146,147] (Figures 2.8b and 2.10a). Furthermore, we observed reticular adherens junctions in live cells expressing VE cadherin-GFP, RapR-Src, and FRB at 30 minutes using live SIM as well, verifying that they were not an artifact of the staining process (Figure 2.10b). Next, we investigated whether the broader reticular adherens junctions were less leaky than linear adherens junctions in basal HPAE cells. To do this we utilized a FITC-avidin assay and subsequent staining for endogenous VE cadherin[141]. The FITC- avidin assay demonstrated that FITC accumulated in significantly higher intensities under linear junctions than reticular junctions, thus demonstrating that linear junctions are leakier than reticular junctions (Figures 2.10c and 2.10d). The observation that reticular adherens junctions are less leaky confirms previous hypotheses[35,147] which suggested that reticular adherens junctions contribute to enhancement of the endothelial cell barrier. Therefore, Src activation induces VE cadherin accumulation and broadening in the adherens junctions as well as the rearrangement of the adherens junctions into reticular junctions.

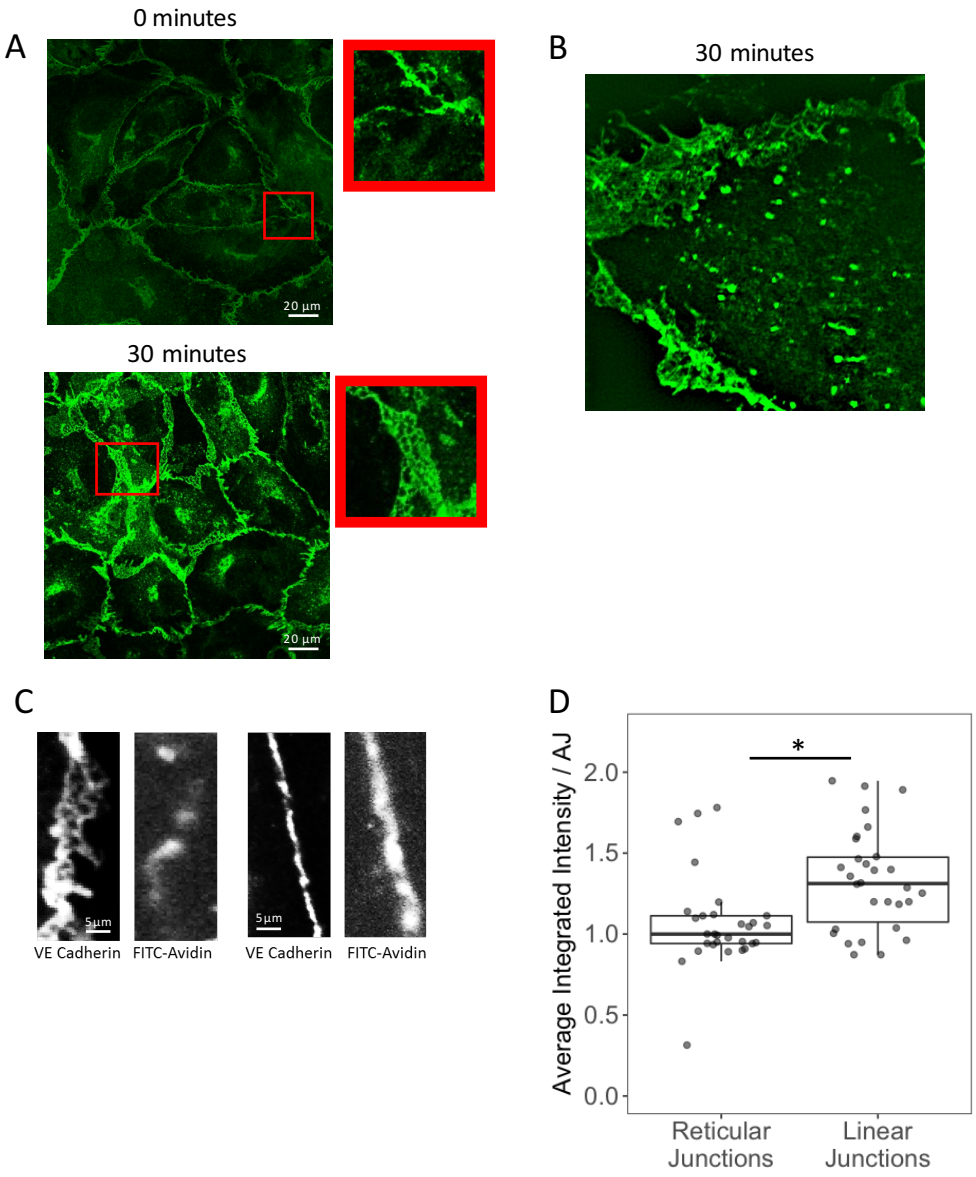

Figure 2.10: Reticular adherens junctions are less leaky than linear adherens junctions
(A) HPAE cells were infected with RapR-Src-as2-cerulean-myc and mCherry-FRB. Cells were activated for 0 or 30 minutes and stained for endogenous VE cadherin with Alexa488 secondary. Confocal images were taken on a Zeiss LSM 880 microscope. (B) HPAE cells infected with RapR-Src-as2-cerulean-myc and mCherry-FRB, and VE cadherin-GFP were imaged live on a 3D-SIM microscope at 30 minutes, post-rapamycin treatment (500 nM). (C and D) HPAE cells under basal conditions were analyzed using a FITC-avidin assay. FITC-avidin was added to cell media for 2 minutes, cells were then washed, fixed, and stained for VE cadherin with Alexa647 secondary. (D) The average integrated intensity of FITC-Avidin was measured under 30 reticular (>4.5 µm wide) and 30 linear (<2.5 µm wide) adherens junctions, designated by VE cadherin staining, from 3 independent experiments, a blocked Anova test was used to compare the two types of junctions. *p=0.001.

Furthermore, reticular junctions exhibit lower permeability and their formation correlates temporally with Src-mediated endothelial cell barrier enhancement.

Src activation causes changes in the actin-cytoskeleton and an increase in lamellipodia

In addition to rearranging the adherens junctions, we hypothesized that Src activation was causing changes in the actin-cytoskeleton. Previous work using a constitutively active (CA-)Src in endothelial cells had demonstrated that there was drastic rearrangement of F-actin following CA-Src expression[47]. Therefore, we assessed the organization of F-actin in HPAE cells and the phosphorylation of myosin-light chain (MLC-P), an indicator of myosin activation following Src activation. Src activation demonstrated an increase in F-actin. F-actin formed actin foci during endothelial cell barrier enhancement (30 minutes) and during the disruption phase (4 hours). F-actin arranged into contractile actin rings (Figure 2.11a), the same phenotype previously described by others using CA-Src expression[47]. Furthermore, MLC-P was significantly elevated at 30 minutes and stayed elevated through 4 hours (Figure 2.11b). Previous work with Src activation using the RapR-kinase method had revealed a transient increase in protrusions following Src activation[90,137,138]. We therefore hypothesized that Src activation in HPAE cells may also increase protrusions and that protrusions may be driving the rearrangement of adherens junctions, actin, and focal adhesions leading to the formation of the broader reticular adherens junctions. Activation of Src in confluent HPAE cells showed a sustained increase of protrusive activity with the highest activity coinciding with endothelial cell barrier enhancement (Figure 2.12). There was also a significant increase in Rac1 activity following Src activation during both the endothelial cell barrier enhancement and disruption phases (Figure 2.13). Furthermore, Src activation resulted in the targeting of actin and cortactin to membrane ruffles (Figure 2.14), both of which are important components of lamellipodia formation and stability[148,149]. To examine in

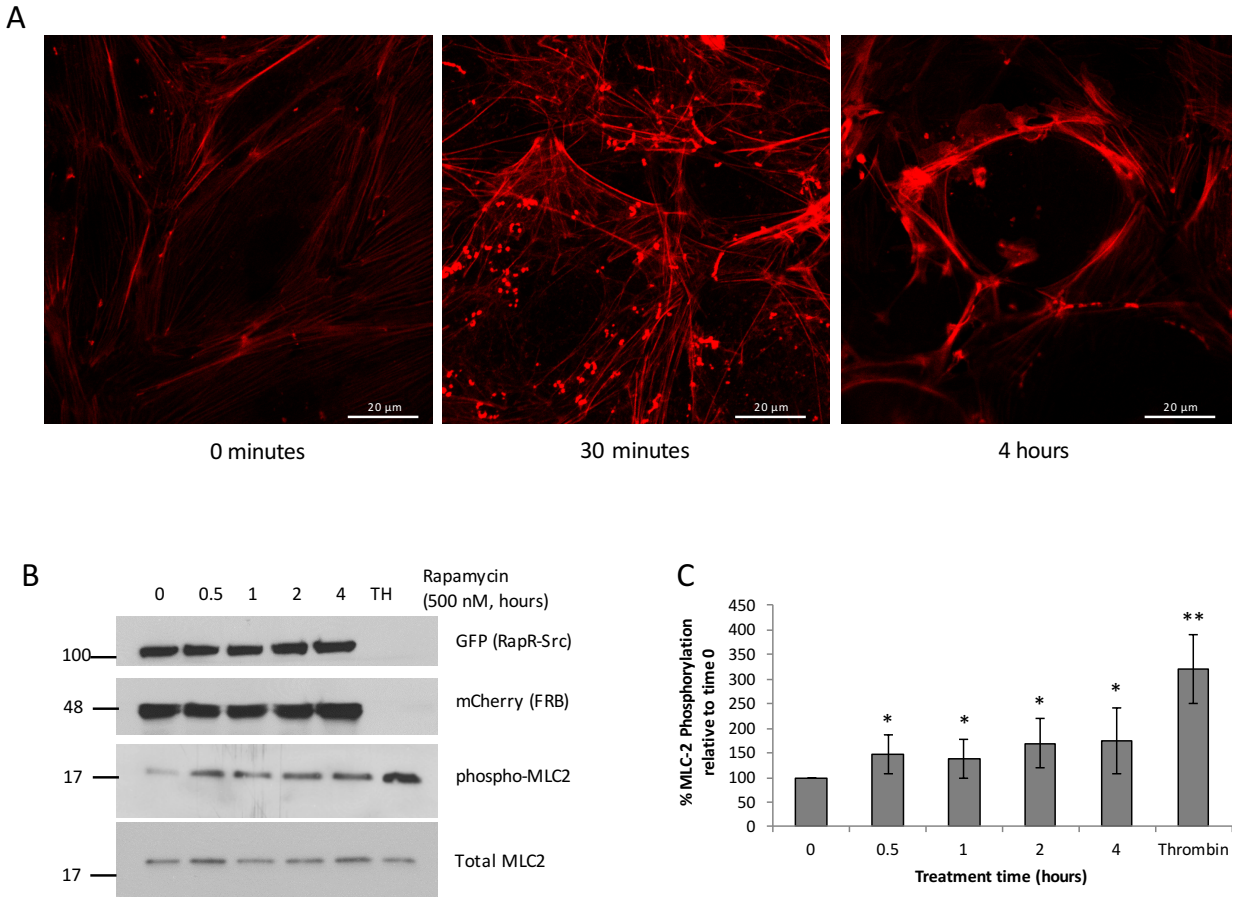

Figure 2.11: Src activation initiates changes in the actin-cytoskeleton
HPAE cells were infected with adenoviruses expressing RapR-Src-cerulean and mCherry-FRB. Cells were activated with rapamycin (500 nM) for the specified amount of time. (A) Cells were fixed and stained for Phalloidin-Alexa647. Images were taken on a Zeiss LSM 880 confocal microscope. (B and C) Cell lysates were collected and probed for activation of myosin light chain via Western blot for Phospho-MLC and total MLC and then the relative amount of P-MLC was determined. As a positive control HPAE cells were treated with 50 nM α-thrombin for 5 minutes. (C) The averages for each time point were normalized to time 0 and then the 6 independent experiments were averaged and graphed. Error bars represent the standard deviation between the 6 experiments. A two-sample t-test between time 0 and each of the treatment samples was used to access significance. *$p<0.05$, **$p<0.01$.

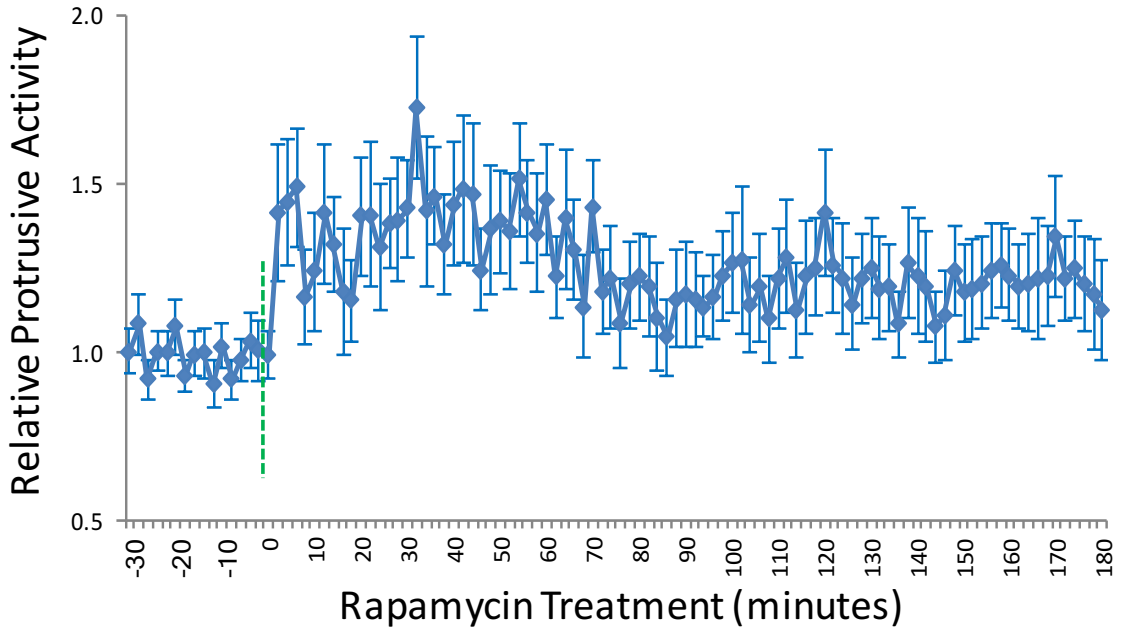

Figure 2.12: Src induces an increase in protrusive activity
HPAE cells were infected with adenoviruses expressing RapR-Src-cerulean and mCherry-FRB and transfected with the membrane marker Stargazin-mVenus. Cells were imaged live every 2 minutes, 500 nM rapamycin was added a time point 0 (green line). Protrusive activity (N=30 cells) was calculated and standardized to the average activity for each cell prior to rapamycin treatment. Error bars represent the 90% confidence interval for each time point.

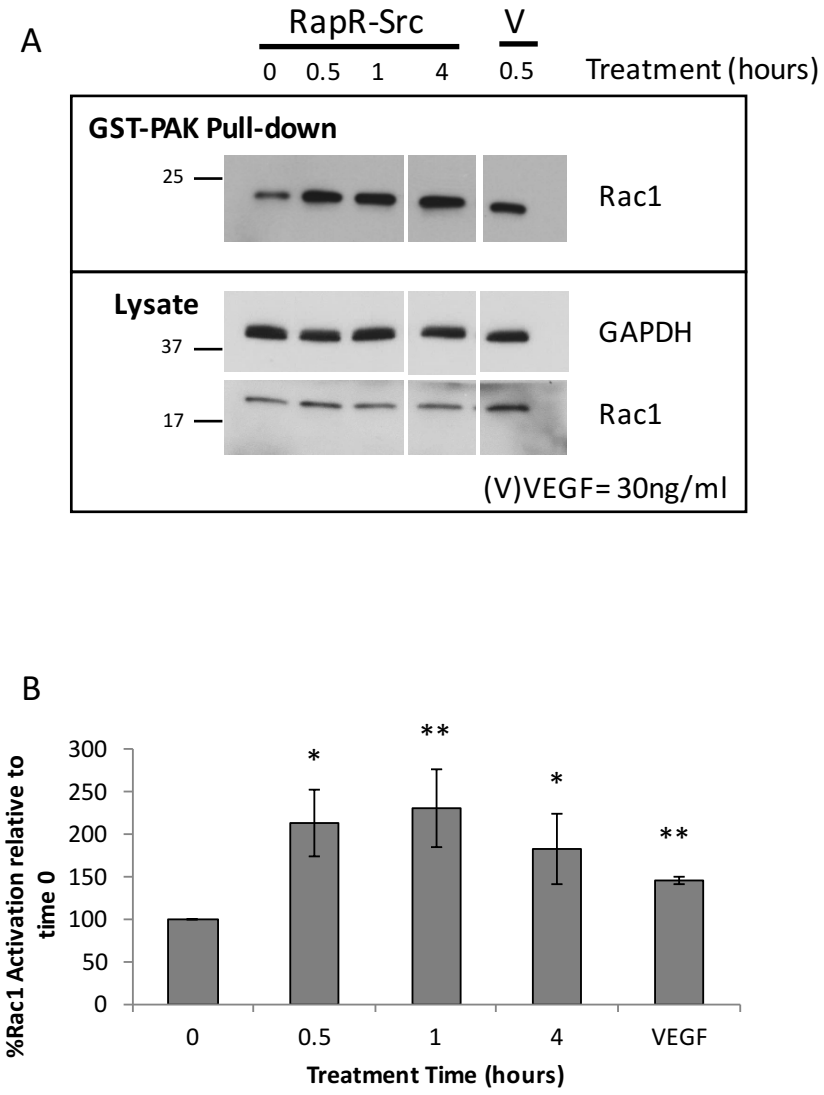

Figure 2.13: Src activates Rac1

(A and B) HPAE cells were infected with adenoviruses expressing RapR-Src-Cerulean-myc and mCherry-FRB and treated with rapamycin (500 nM) for the designated times. GST-PAK-CRIB was used to pull-down Rac1-GTP. VEGF (V) (30ng/ml) was added to HPAE cells for 30 minutes as a positive control for Rac1 activation. (A) Samples were western blotted for the designated proteins. (B) The amount of GTP bound Rac1 was determined by standardizing the pull-down values to their respective lysate values and graphed relative to the 0 min time point with standard deviations (N=4). A two-sample t-test was used to compare significance between time 0 and the other treatments; *P<0.05, **P<0.01.

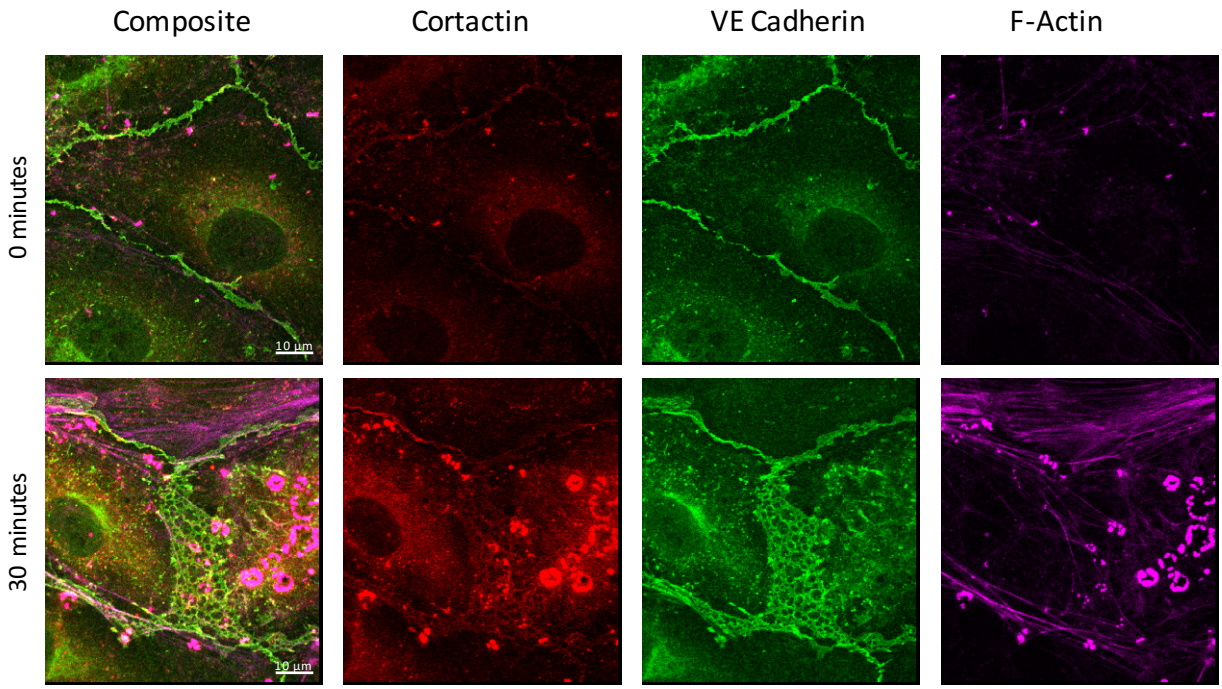

Figure 2.14: Src activation initiates F-actin bundling and rearrangement of cortactin
HPAE cells were infected with adenoviruses expressing RapR-Src-cerulean and GFPY66S-FRB. Cells were activated with rapamycin (500 nM) for 0 or 30 minutes, fixed, and stained for VE cadherin with Rhodamine secondary, cortactin with FITC secondary, and Phalloidin-Alexa647. Images were taken on a Zeiss LSM 880 confocal microscope.

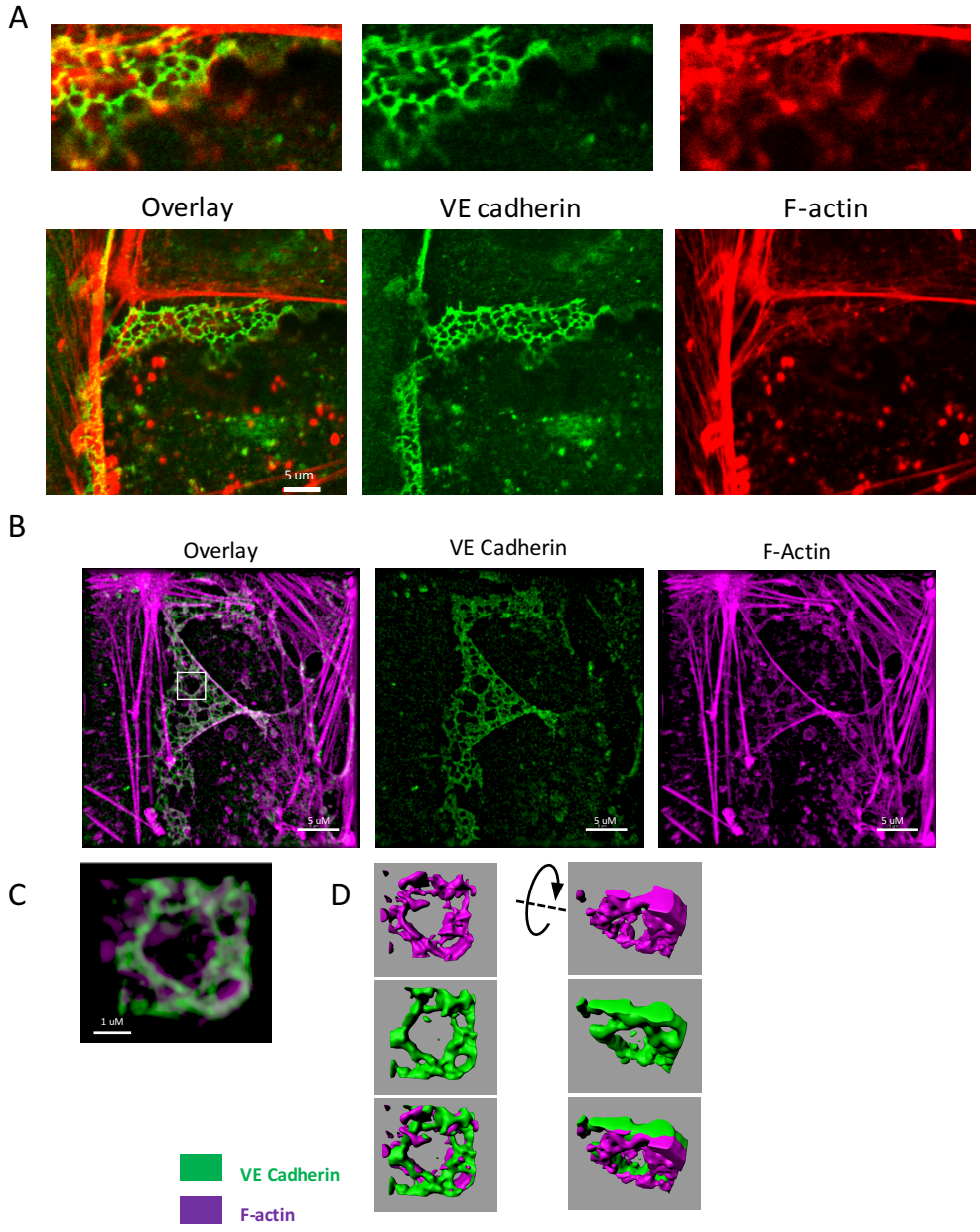

Figure 2.15: F-actin forms a scaffold underneath rearranged VE cadherin
HPAE cells were infected with adenoviruses expressing RapR-Src-cerulean and mCherry-FRB, cells were treated with rapamycin (500 nM) for 30 minutes, fixed, and stained for endogenous VE cadherin and F-actin using VE cadherin with Alexa 488 secondary and Phalloidin-Alexa-647. (A) Immunofluorescence images were collected on a Zeiss LSM 880 confocal microscope. (B-D) Immunofluorescence images were collected on a Nikon SIM. (C) Zoomed in area from the indicated square in part B. (D) Areas showing how F-actin forms the same reticular structure underneath VE cadherin. 3D renderings were generated using IMARIS software.

more detail whether VE cadherin and F-actin re-arranged together into reticular adherens junctions, we imaged reticular adherens junctions and F-actin following 30 minutes of Src activation using confocal and super-resolution microscopy. Both confocal and SIM images revealed that F-actin also re-arranged in reticular adherens junctions directly underneath VE cadherin (Figures 2.15a-d). Thus, the activation of Src increases protrusive activity as well as rearrangement of the actin cytoskeleton and adherens junctions which in turn cause an increase in the endothelial cell barrier function.

Paxillin and VE cadherin complex together during Src mediated endothelial cell barrier enhancement

Src activation has previously been shown to induce the formation and rearrangement of focal adhesions[90]. This suggested to us that Src may be promoting focal adhesions at the leading edge of lamellipodia that may be driving the re-organization of VE cadherin. To test this hypothesis, we stained for endogenous VE cadherin and paxillin (focal adhesion marker) in HPAE cells expressing RapR-Src and FRB which had been activated for 0 and 30 minutes (enhancement phase) and imaged them using confocal microscopy. At 30 minutes paxillin formed focal adhesions within the reticular adherens junctions (Figure 2.16a). To determine whether VE cadherin and paxillin were complexing together following Src activation we performed co-immunonprecipitation of VE cadherin following Src activation. There was an increase in the amount of paxillin which co-immunoprecipitated with VE cadherin following Src activation with the most being pulled-down at 30 minutes (Figure 2.16b). These results support the idea that focal adhesion proteins may be helping to guide the formation of reticular adherens junctions at protrusive fronts by complexing with VE cadherin.

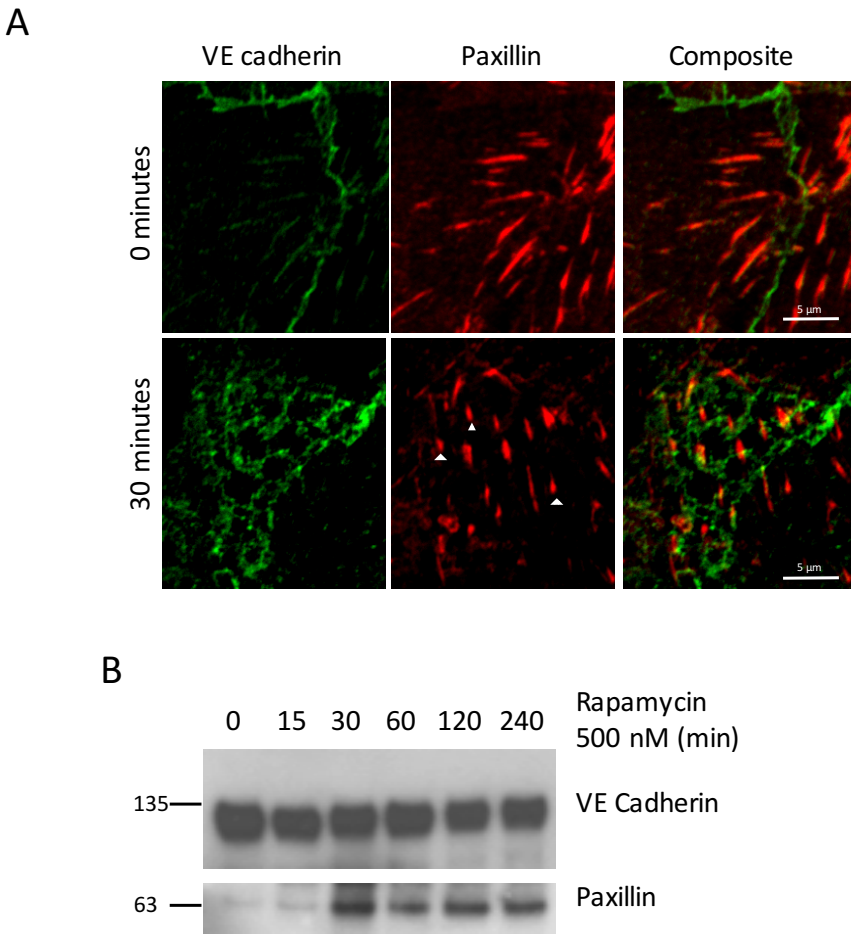

Figure 2.16: Paxillin and VE cadherin following Src activation
HPAE cells were infected with with RapR-Src-cerulean-myc and mCherry-FRB adenoviruses. (A) Cells were treated with rapamycin for 0 or 30 minutes. Cells were fixed and stained for VE cadherin and Paxillin followed by Alexa-488 and Alexa-647 secondary antibodies respectively. Arrowheads indicate non-elongated focal adhesions observed after Src activation. Images were collected on a Zeiss 880 confocal microscope. (B) Cells were treated with rapamycin (500 nM) for the designated amount of time. Cell lysates were collected and VE cadherin was immunoprecipiated. VE cadherin immunoprecipitation samples were immunoblotted with designated antibodies.

VE cadherin is rapidly phosphorylated following Src activation

Despite observing phosphorylation of Src substrate paxillin as early as 15 minutes post-activation, we did not see endothelial cell barrier disruption and gap formation until much later times (Figures 2.3a, 2.3b, 2.4, 2.7, 2.8, 2.9a). The canonical view suggests that Src-mediated phosphorylation of VE cadherin negatively regulates adherens junctions. Phosphorylation of Y658 is proposed to reduce binding to p120-catenin, whereas phosphorylation of Y731 reduces binding to β-catenin[150]. However, it has been also observed that phosphorylation of VE cadherin at these sites is not sufficient to induce internalization and dissociation of the cadherin-catenin complex[47]. To investigate the role of VE cadherin phosphorylation downstream of Src we utilized our RapR-Src construct to temporally monitor VE cadherin phosphorylation and its subsequent association with P120- and β-catenins. Immunoblots of immunoprecipitated endogenous VE cadherin from HPAE cells after activation of Src for various amounts of time revealed phosphorylation of VE cadherin as early as 15 minutes following activation of Src, with the amount of VE cadherin phosphorylation progressively increasing with longer Src activation (Figure 2.17a). Since the different residues of VE cadherin have been reported to regulate different functions of VE cadherin (e.g. permeability, leukocyte extravasation) we also monitored the phosphorylation of the reported Src phosphorylated sites Y658, Y685, and Y731[23,47,53] individually following different durations of Src activation. Phosphorylation of Y658 and Y731 rapidly approached their maximum level, while Y685 progressed over time, comparable to total phospho-Tyrosine (Figures 2.17a-c). Specificities of the commercial phospho-VE cadherin antibodies were verified by expressing GFP tagged VE cadherin constructs for wild-type, Y658F, and Y731F and activating RapR-Src for 0 and 30 minutes. Both of the antibodies were found to be specific and showed little to no signal with their respective

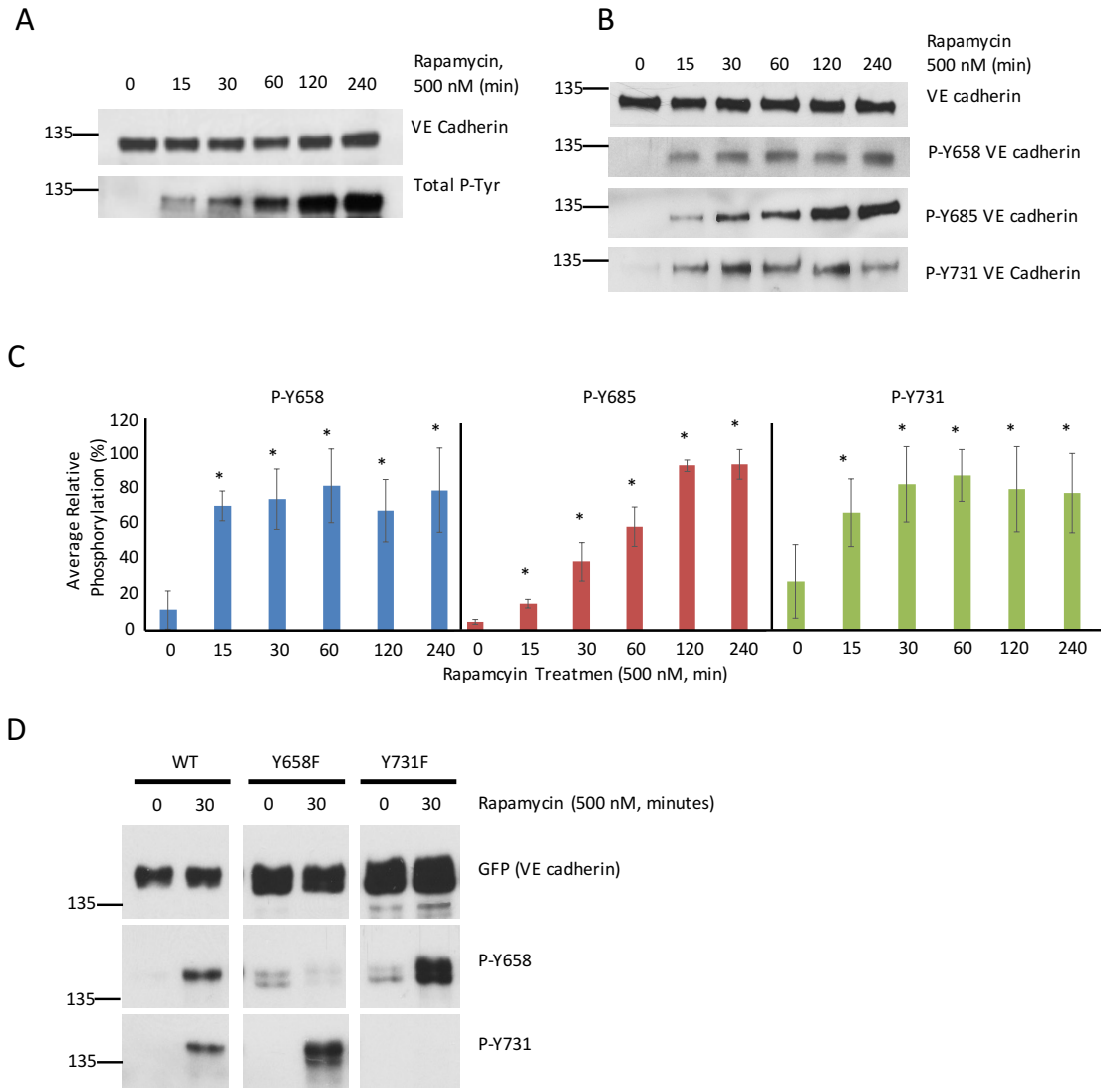

Figure 2.17: Src activation induces phosphorylation at VE cadherin

(A-C) HPAE cells were infected with RapR-Src-as2 and mCherry-FRB. Cells were treated with rapamycin (500 nM) for the designated amount of time. Cell lysates were collected and VE cadherin was immunoprecipiated. (A) Total VE cadherin Tyrosine phosphorylation. (B and C) Phosphorylation of VE cadherin at specific Tyrosine sites: Y658 (n=6), Y685 (n=5), and Y731 (n=6). For each experiment, all time points were normalized to the highest phosphorylation level. Averages for all experiments were graphed with standard deviations between experiments. A two-sample t-test was used to compare each time point for each phosphorylation site to its time 0. *$p<0.05$. (D) HPAE cells were infected with: RapR-Src-as2-mCherry-myc, mCherry-FRB, and GFP tagged VE cadherin (WT, Y658F, or Y731F). Cells were treated with rapamycin (500 nM) for 0 or 30 minutes. Cell lysates were collected GFP tagged VE cadherin constructs were immunoprecipitated via GFP. Immunoprecipitated samples were immunoblotted for GFP, P-Y658, and P-Y731.

**(D) produced by Rima Rebiai (Karginov laboratory).*

phenylalanine mutants (Figure 2.17d). The phospho Y685 antibody was a gift from the Dejana laboratory and has previously been confirmed for specificity[43]. Co-immunoprecipitation of VE cadherin with the catenins P120- and β- revealed that although VE cadherin is rapidly phosphorylated at Y658 and Y731 following Src activation, this does not cause dissociation of P120-catenin from VE cadherin complexes at any of the observed times and a small but significant decrease in the amount of β-catenin at late times (Figures 2.18a and b). In addition, there was no change in expression of VE cadherin, P120-catein, or β-catenin in cell lysates (Figure 2.18c). Therefore, phosphorylation of VE cadherin is not sufficient to drive dissociation of P120- and β-catenins from VE cadherin complexes and phosphorylation of VE cadherin alone is not sufficient to drive permeability.

VE cadherin Y731 is required for Src and S1P mediated endothelial cell barrier enhancement

The rapid induction of phosphorylation of VE cadherin at Y658 and Y731 following Src activation led us to further investigate the roles of these two residues in regulating the localization of VE cadherin and endothelial cell barrier. Both Y658 and Y731 reached their maximum phosphorylation level during Src mediated endothelial cell barrier enhancement (Figures 2.4, 2.7, 2.17b and c). Using GFP tagged constructs for wild-type (WT), Y658F, and Y731F VE cadherin, we imaged live the localization of each of the variants of VE cadherin following Src activation (Figure 2.19). We found that VE cadherin mutant Y731F accumulated more rapidly in the cytoplasm following Src activation than WT VE cadherin (Figures 2.19 and 2.20). Furthermore, we found less Y658F VE cadherin cytoplasmic accumulation following Src activation when compared to WT VE cadherin (Figures 2.19 and 2.20). To determine whether expressing the mutant VE cadherins altered Src mediated endothelial cell barrier, we activated

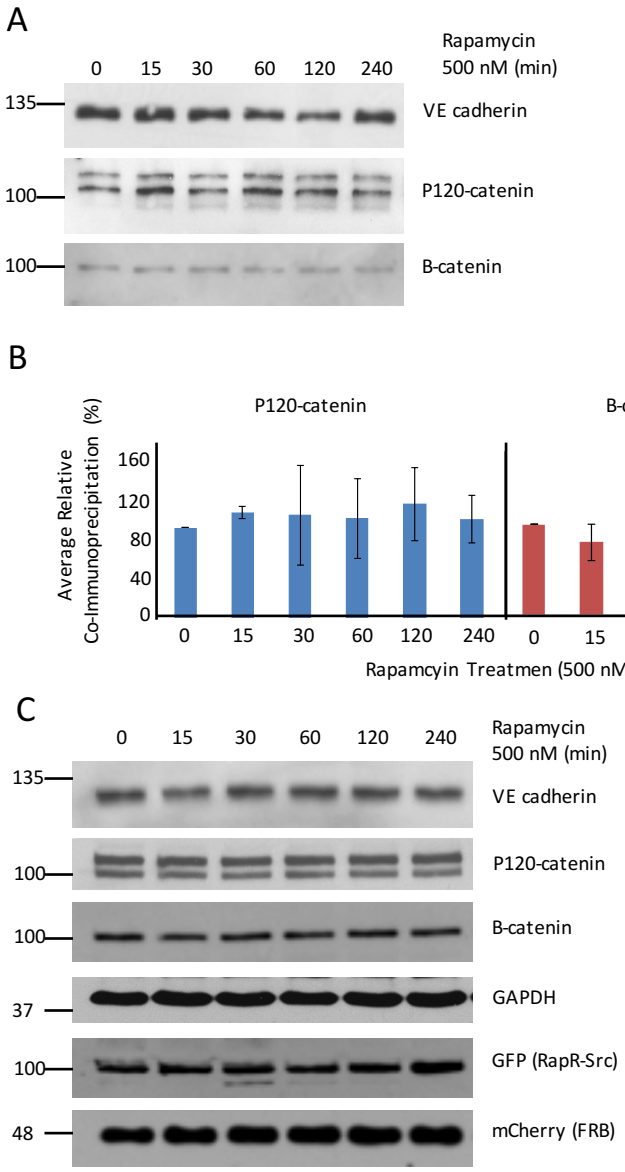

Figure 2.18: Cadherin and Catenin association after Src activation
HPAE cells were infected with: RapR-Src-cerulean-myc and mCherry-FRB. Cells were activated with rapamycin (500 nM) for the specified amount of time. (A and B) Cell lysates were collected and VE cadherin was immunoprecipitated. VE cadherin immunoprecipitation samples were immunoblotted for total VE cadherin as well as P120- and β-catenin. The relative amount of P120- and β-catenin for each time point was standardized to time 0. The average of 4 experiments was graphed with standard deviations. A two-sample t-test was used to compare each time point for each catenin to its time 0. *$p<0.05$. (C) Cell lysates were collected and immunoblotted for the designated proteins.

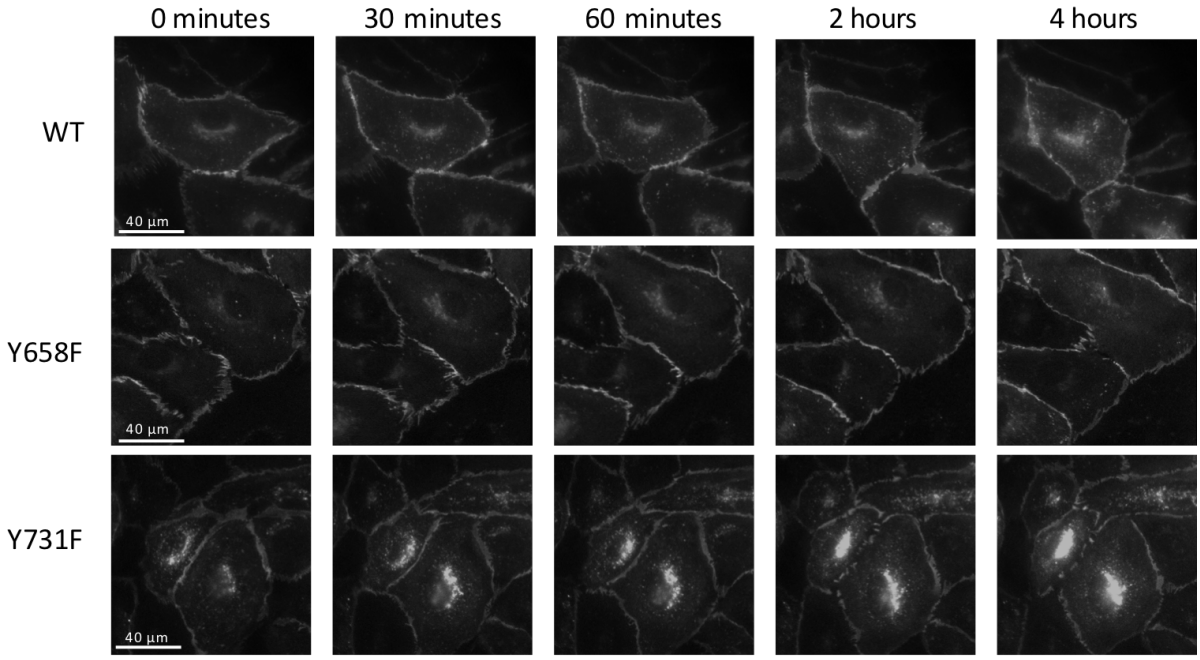

Figure 2.19: P-Y731 and P-Y658 alter Src mediated VE cadherin localization changes
Cells were infected with RapR-Src-as2-cerulean-myc, mCherry-FRB, and the designated VE cadherin-GFP construct, wild-type (WT), Y658F, or Y731F. Cells were imaged live every 2 minutes. Stills taken of VE cadherin at the designated times.

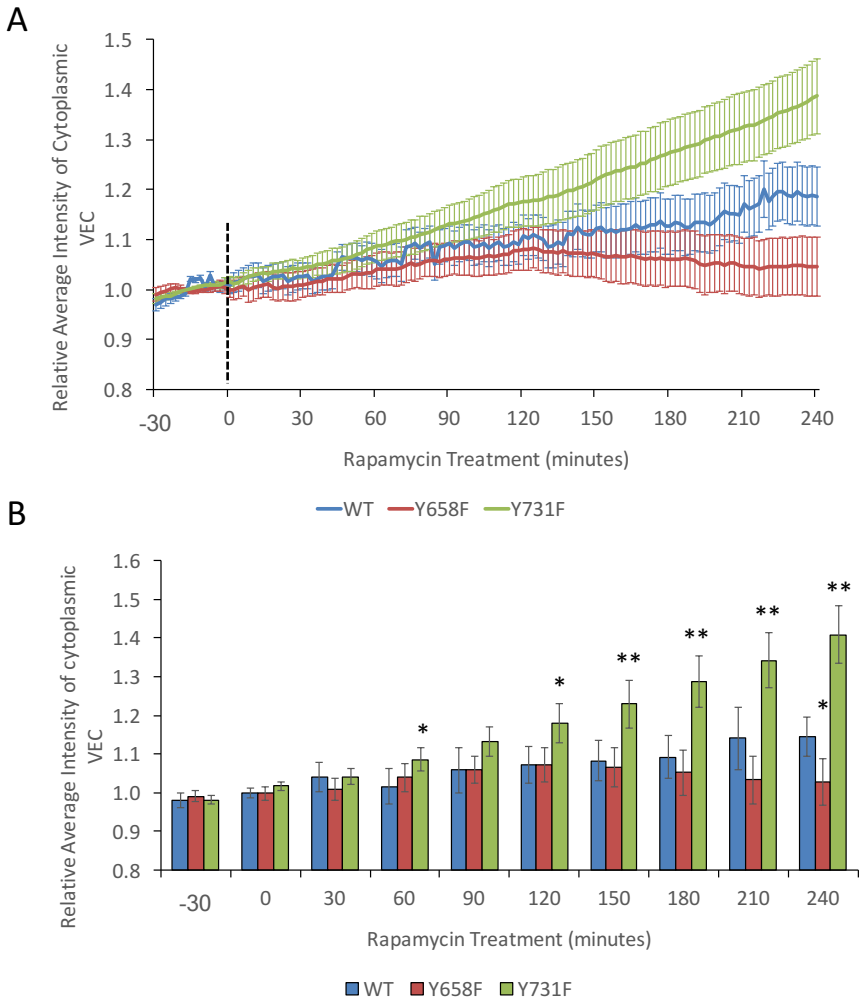

Figure 2.20: Y731F accumulates in the cytoplasm faster than WT VE cadherin
Cells were infected with RapR-Src-as2-cerulean-myc, mCherry-FRB, and the designated VE cadherin-GFP construct. Cells were imaged live every 2 minutes. (A) Rapamycin (500 nM) was added at time point 0. The amount of cytoplasmic VE cadherin was determined by masking with mCherry-FRB (a protein localized predominantly in the cytoplasm), calculating the average intensity of VE cadherin within the mask, and dividing by the total amount of VE cadherin. All frames were normalized to their average cytoplasmic VE cadherin prior to rapamycin treatment. The averages for every 2 minute time point with 90% confidence intervals. (B) Averages of each VE cadherin-GFP construct at 30 minute intervals used for statistical analysis; error bars represent 90% confidence intervals. A two sample t-test was used to compare each of the mutants (Y658F and Y731F) to WT-VE cadherin-GFP at the designated time point. p*<0.05, p**<0.01.

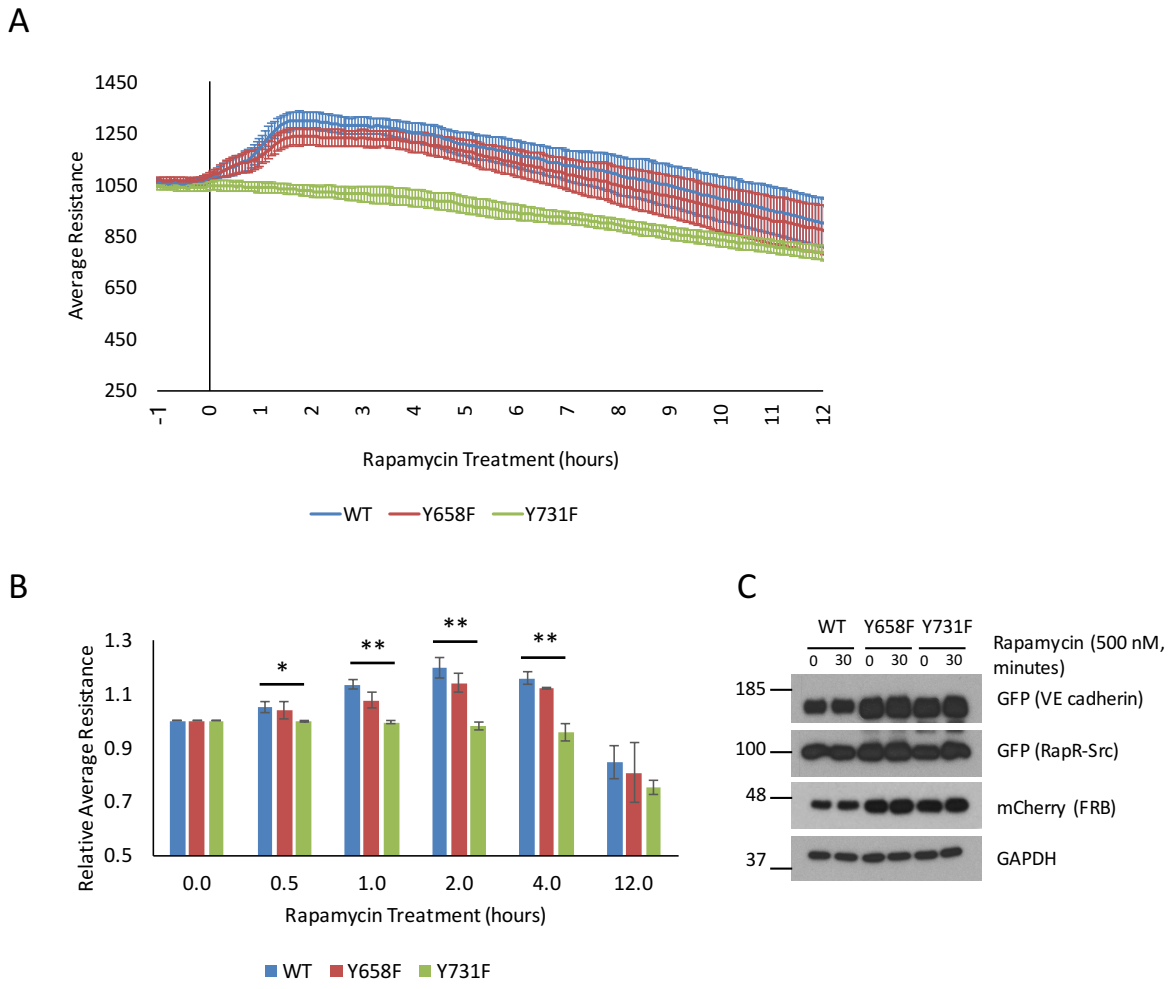

Figure 2.21: Src mediated barrier enhancement requires P-731 on VE cadherin
HPAE cells infected with RapR-Src-as2-cerulean-myc, mCherry-FRB, and the indicated VE cadherin-GFP construct, wild-type (WT), Y658F, or Y731F. (A) Cells were analyzed by TER and were treated with rapamaycin (500 nM) (green triangle) at time 0. Graph represents the average resistance of 3 independent experiments and 90% confidence intervals. (B) The average relative resistance at the indicated time points, Y658F and Y731F were compared to WT using a two sample t-test; graphs depict the average and standard deviation. p**<0.001. (C) Western blots of samples prepared in parallel to TER assay.

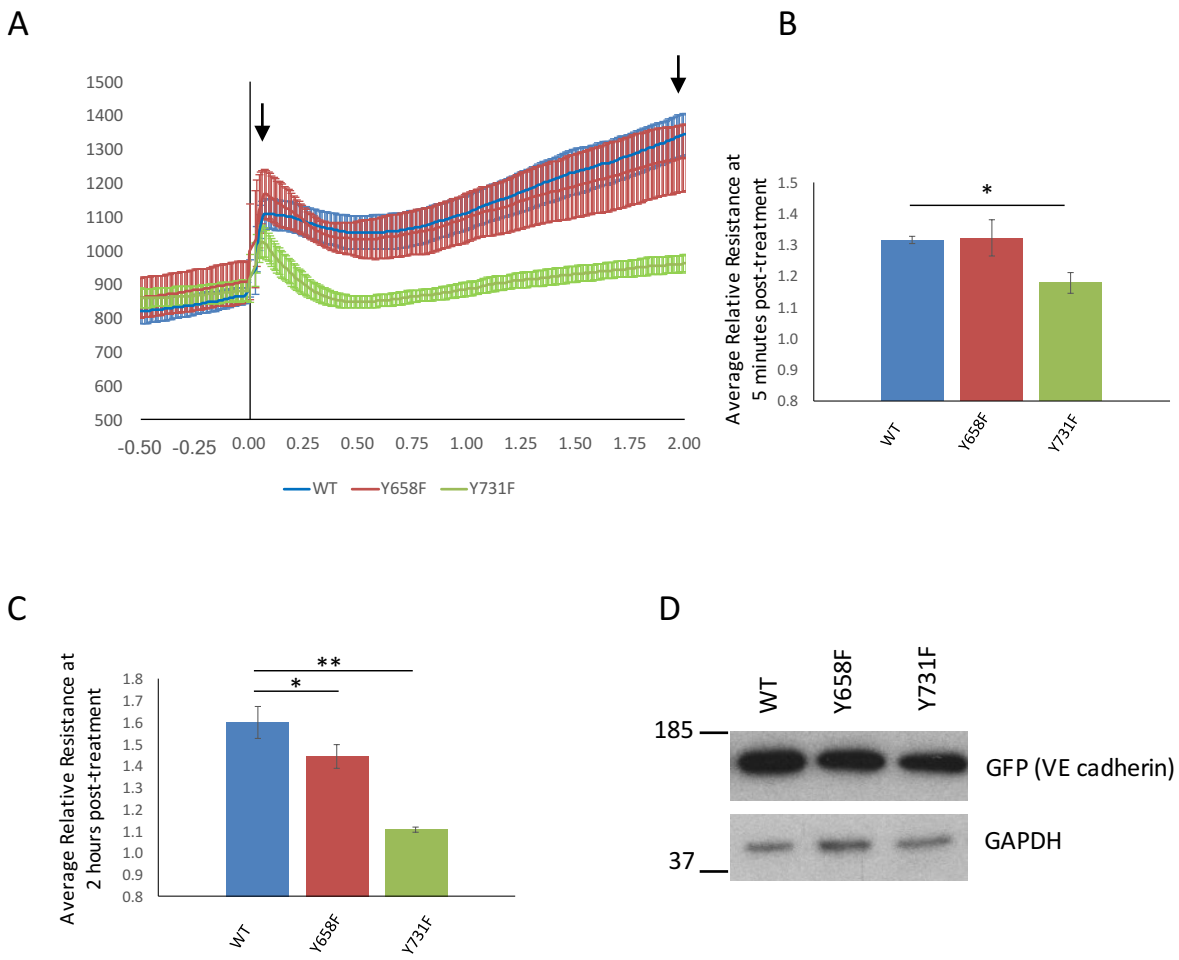

Figure 2.22: VE cadherin Y731-P is required for S1P enhancement
HPAE cells were infected with the indicated VE cadherin-GFP construct, wild-type (WT), Y658F, or Y731F. (A) VE cadherin-GFP expressing cells were analyzed by TER. Samples serum starved for 1 hour and then treated with S1P (1µM), time 0. Graph represents the average resistance from 3 independent experiments and their 90% confidence intervals. (B and C) Average relative resistances for WT, Y658F and Y731F at 5 minutes (B) and 2 hours (C) post S1P treatment. (B-C) The time points analyzed are indicated by the arrows in (A). A two-sample t-test was used to compare Y658F and Y731F to WT, graphs show the average and standard deviations. **$p<0.001$, *$p<0.05$. (D) Western blot comparing expression of the different VE cadherin constructs.

Src with each of the VE cadherin constructs and monitored the effect using TER. WT VE cadherin and Y658 expressing cells both demonstrated Src mediated endothelial cell barrier enhancement. However, cells expressing Y731F did not exhibit the transient increase in the endothelial cell barrier (Figure 2.21). The inability of Y731F cells to exhibit Src mediated enhancement caused us to evaluate what effect expressing these constructs had in the context of S1P mediated enhancement. As with RapR-Src, S1P treatment of cells expressing the Y731F showed much less enhancement than either the WT or Y658F expressing cells (Figure 2.22). Therefore, it appears that phosphorylation of Y731 is required for the retention of VE cadherin at the cell periphery. In addition, phosphorylation at this residue is necessary for both Src- and S1P-mediated endothelial barrier enhancement.

2.4 Discussion

Extensive studies evaluating SFKs have shown that activation of different SFKs exert distinct effects on the endothelial cell barrier[64–66,151]. However, SFK activity is also required for maintenance and recovery of the endothelial barrier[66,70]. We verified these results by demonstrating that SFK inhibition blocks S1P mediated endothelial cell barrier enhancement as well as abrogation of barrier recovery following disruption by α-Thrombin (Figures 2.1a-c and 2.2a-c). In addition, by activating Src and Lyn independently, we demonstrated that Src, but not Lyn, results in a rapid increase in endothelial cell barrier enhancement as well increases the rate of recovery following α-Thrombin disruption (Figures 2.5a-b). Furthermore, we observed that the R175L mutant of Src, which is prohibited SH2 mediated protein interactions, is incapable of initiating Src-mediated endothelial cell barrier enhancement. However, Src-mediated disruption of the endothelial cell barrier was not impeded by the R175L mutation. The inability of R175L-Src to enhance the endothelial cell barrier demonstrates that the SH2 domain of Src is required to

promote enhancement of the endothelial cell barrier. The roles of Src signaling in receptor induced increases in vascular permeability have thoroughly been demonstrated, however, these studies have relied on the use of inflammatory mediators and growth factors to stimulate Src[133,152–155]. The use of inflammatory mediators and growth factors result in the activation of multiple pathways and do not address whether Src signaling alone is sufficient to induce vascular permeability. Previous results, by others, using DN-CSK demonstrated that Src activation and phosphorylation of VE cadherin is not sufficient to drive endothelial cell barrier disruption[47]. Akin to the use of CA-Src, we use an over-expression system for identifying how Src activation independent of upstream stimuli affects the endothelial cell barrier. However, the use of an inducible kinase system also allowed us to temporally monitor the effects of Src activation on the endothelial cell barrier, as well as the localization, conformation, and phosphorylation of VE cadherin. This enabled us to identify transient enhancement of the barrier following Src activation. Prolonged activation of Src by sustained activation of RapR-Src (Figures 2.4 and 2.7) similar to the overexpression of CA-Src[47], initiated disruption of the endothelial cell barrier and induced rearrangement of the actin stress fibers. The biphasic change in endothelial cell permeability we observed supports the concept that it is likely the amount and length of Src activity that determines how it affects the integrity of the endothelial cell barrier[156].

Following Src activation we observed an increase and rearrangement of VE cadherin in the adherens junctions, both of which coincided temporally with Src mediated endothelial cell barrier enhancement (Figures 2.4, 2.7, 2.8, 2.9, 2.14, 2.15, 2.16). Adherens junctions are dynamic structures that form distinct types of junctions, including linear, reticular, and focal adherens junctions[27]. Rearrangement from one structure to another occurs either constitutively or via stimulation[28–30]. Following Src activation there was a distinct shift of VE cadherin from

linear to reticular adherens junctions (Figures 2.8, 2.9, 2.10, 2.14, 2.15, and 2.16) which corroborates previous observations showing their formation following Src activation[47]. Reticular adherens junctions are 3-dimensional mesh-like networks at the interface of two overlapping endothelial cells, composed of platelet endothelial cell adhesion molecule 1 (PECAM-1) interspaced between the cadherin-catenin complex, that are thought to be barrier protective[27,35]. To confirm that they are barrier protective, we compared the amount of permeability directly underneath both linear and reticular adherens junctions in cells under basal conditions in the absence of any other stimuli (Figures 2.10c-d). We found significantly more leakage under linear adherens junctions than reticular adherens junctions. Therefore, Src mediated endothelial cell barrier enhancement is at least partially mediated by the rearrangement of the adherens junctions.

Electron microscopy of reticular adherens junctions clearly shows that they form as the result of two overlapping cells[35]. Therefore, it is reasonable to assume that lamellipodia formation of cells in a confluent monolayer may be driving the formation of the reticular adherens junctions. When cells are sparse, activation of Src shows a transient increase in protrusions and cell spreading[90,137,138]. However, in the context of a confluent monolayer of endothelial cells, we observed sustained lamellipodia formation, with the highest number of protrusions occurring concurrently with Src-mediated endothelial cell barrier enhancement (Figure 2.12). Furthermore, we observed using confocal and SIM that actin also formed a mesh-like network underneath the VE cadherin as well as smaller focal adhesions in these areas (Figures 2.15 and 2.16). Concurrently, we saw an increased association of VE cadherin with focal adhesion protein and an increase in cortactin (Figures 2.14 and 2.16). Interestingly, it has been hypothesized that reticular adherens junctions mediate leukocyte extravasation[27,35].

Src mediates leukocyte extravasation via multiple facets. Binding of the leukocytes to Intercellular adhesion molecule-1 (ICAM-1) stimulates tyrosine phosphorylation of multiple proteins including FAK, paxillin, P130Cas[157], and cortactin[158]. SFK phosphorylation of cortactin is required for ICAM-1 clustering and leukocyte transmigration[158,159]. Following Src activation we see dramatic changes of cortactin, and the bundling of cortactin and actin in reticular adherens junctions during Src mediated endothelial barrier enhancement (Figures 2.4, 2.7, and 2.14). In addition, we see phosphorylation of paxillin as well as an increased association between VE cadherin and paxillin (Figures 2.3 and 2.14). Src activation is also crucial for the phosphorylation of PECAM-1 and PECAM-1-dependent transmigration[160]. Similar to VE cadherin, PECAM-1 also rearranges in reticular adherens junctions forming a predominate component of them[35]. Therefore, it is feasible that Src activation drives the relocalization/rearrangement of paxillin, F-actin, cortactin, VE cadherin, and PECAM-1, initiating the formation of reticular adherens junctions. Furthermore, it is tempting to postulate that the reticular adherens junctions are indeed important for leukocyte extravasation by serving as a barrier protective mechanism while the leukocyte transmigrates through the adherens junctions in an attempt to reduce permeability. However, the stimuli which drive the formation and the function of reticular adherens junctions are not understood and require further investigation.

In addition to rearrangement of VE cadherin, we observed phosphorylation of VE cadherin following Src activation (Figure 2.16). The phosphorylation of VE cadherin and its role in permeability has been studied extensively[8,11,23,38,43,47,48,67–69]. Previous studies demonstrated that Src phosphorylates VE cadherin on multiple residues (Y658, Y685 and Y731)[23,47,53]; therefore, we decided to examine these three sites in more detail. Following Src activation we

found that both Y658 and Y731 were quickly phosphorylated to maximal levels. Conversely, phosphorylation of Y685 steadily increased over two hours, reaching its maximum during the endothelial cell barrier disruption phase (Figures 2.16b-c). The correlation between Y685 phosphorylation and endothelial cell barrier disruption correlates well with previous data[48,53]. Although, it has been demonstrated that blocking Y685 phosphorylation with a phenylalanine mutation blocks vascular permeability, the phosphorylation of this residue alone is not sufficient to induce permeability in the absence of an inflammatory agent[43]. In either case, it is clear that Y685 phosphorylation is closely linked to disruption of the endothelial cell barrier and does not reach maximum levels during Src-mediated endothelial cell barrier enhancement.

The rapid rise of phosphorylation of VE cadherin at Y658 and Y731 during Src mediated enhancement prompted us to evaluate the role of these two residues further (Figures 2.4, 2.7, 2.16b and c). The increase in Y731 phosphorylation was especially intriguing since under basal conditions, Y731 is found to be phosphorylated *in vivo* and it is the de-phosphorylation of this site that is required for leukocyte transmigration, and endothelial cell permeability occurs independently of its phosphorylation[48]. By over-expressing Y731F-VE cadherin-GFP in endothelial cells we found that the Y731F mutation had a dominant negative effect and was capable of blocking Src-mediated endothelial cell barrier enhancement as well as S1P-mediated enhancement (Figures 2.21 and 2.22). Furthermore, we found that following Src activation Y731F VE cadherin-GFP accumulated in the cytoplasm (Figures 2.19 and 2.20). In comparison, Y658F-VE cadherin-GFP did not block Src or S1P mediated endothelial cell barrier enhancement, and accumulated at a significantly slower rate in the cytoplasm than WT-VE cadherin-GFP (Figures 2.19 and 2.20). Our results in combination with previous results from

others suggest that phosphorylation of Y731 is not endothelial cell barrier disruptive but is instead required for Src-mediated endothelial cell barrier enhancement.

In summary, we observed for the first time that direct Src activation leads to a transient increase in endothelial cell barrier enhancement. Furthermore, we demonstrated that Src activation causes an increase in VE cadherin localization to adherens junctions, and the rearrangement of VE cadherin into reticular adherens junctions. We also found that under basal conditions reticular adherens junctions are less leaky than linear adherens junctions. Reticular adherens junction formation occurred concurrently with the highest production of protrusions and bundling of actin-cortactin suggesting that protrusions may be driving the formation of reticular adherens junctions by creating additional cell overlaps. In addition, we found that Y731 phosphorylation of VE cadherin is required for Src-mediated transient enhancement of the barrier. Y731 phosphorylation is also required for S1P barrier enhancement demonstrating its importance downstream of a physiological stimulus. Finally, we demonstrated the utility of using an inducible kinase system to help dissect the functions of specific kinases downstream of complex signaling networks activated by broad acting stimuli. Thorough evaluation of the temporal effects of Src on endothelial cell barrier and VE cadherin localization, rearrangement, and phosphorylation would not have been possible without using an inducible kinase system.

CHAPTER 3: MIMICKING TRANSIENT ACTIVATION OF PROTEIN KINASES IN LIVING CELLS

(Portions of this chapter were originally published in Proceedings of the National Academy of Science and used with permission.)

Klomp, J. E., V. Huyot, A-M Ray, K.B. Collins, A.B. Malik, and A.V. Karginov. Mimicking transient activation of protein kinases in living cells. *Proc. Natl. Acad. Sci.* **113,** 14976–14981 (2016).

**This project was a collaborative project; figures produced by other researchers are indicated in legends.*

3.1 Introduction

Protein phosphorylation by kinases is a critical post-translational modification and an essential mechanism of signal transduction[161]. Phosphorylation is involved in virtually every cellular process, providing cells with the ability to rapidly transduce signals through the cell in a reversible nature [120]. Kinase mediated phosphorylation processes are multistep processes containing complex networks of cross-talk, with feed-forward and feed-back steps. Elucidation of how kinases regulate pathways is only achievable by determining both how these networks connect in space and time and how specific kinases and phosphatases contribute to individual steps of these networks[121].

Aberrations in phosphorylation-mediated signaling have been linked to numerous human diseases[162]. Dissection of kinase function uncovers molecular mechanisms underlying physiological and pathological processes, and guides the development of new therapeutic strategies [163]. However, progress in our understanding of kinase-mediated signaling is often hampered by the limitations of available tools[164]. Pharmacological inhibitors of kinases have been valuable for the study of kinase functions, but they often do not provide desired specificity

and they are not available for the majority of kinases[163,165]. Also, application of inhibitors is limited to identification of processes affected by the inactivation of the kinase. Activation of a kinase is often achieved by the treatment of cells with growth factors or other extracellular stimuli. However, this approach triggers a multitude of parallel signaling pathways, which significantly complicates the analysis of individual kinase functions[166]. Specific activation or inactivation of a kinase can be achieved by genetic modifications. However, this method is susceptible to compensatory artifacts, and does not allow us to control the level and timing of kinase activation. Thus, development of novel tools that combine high specificity and tight temporal control of kinase activity remains a necessity.

Under physiological conditions, kinases are activated for a finite period of time and the duration of this activation is critical for eliciting specific biological outcomes[167,168]. Therefore, to mimic the biological activity of a kinase we need to employ methods that allow for transient activation of a kinase with precise temporal control. An optogenetic approach has been successfully employed for transient regulation of Raf kinase by dimerization[169]. However, this method relies on the fact that Raf dimerization is required for its activation and, thus, has limited applicability to other kinases. Therefore, development of broadly applicable methods for tightly controlled transient activation of a specific kinase remains an important goal.

To achieve efficient and specific control of kinase activation and inactivation we combined two protein engineering strategies. Kinase activation was regulated using a recently developed protein engineering method that employs a rapamycin-regulated allosteric switch, the iFKBP domain[137]. We have previously reported that insertion of iFKBP into the catalytic domain at a specific location renders the modified kinase inactive. Addition of rapamycin or its non-immunosuppressive analogs induces iFKBP heterodimerization with co-expressed FKBP12-

rapamycin-binding (FRB) domain leading to kinase activation[90,131,137]. This strategy provides high specificity and temporal control of kinase activation in living cells. However, this approach results in persistent activation of a kinase without the ability for defined inactivation. To achieve independent control of kinase inactivation, we utilized a strategy developed by Shokat and colleagues that employs a functionally silent mutation that sensitizes the kinase to an allele-specific inhibitor, 1NA-PP1 (1-Naphthyl-PP1 CAS 221243-82-9)[124,126–130,122,123,125]. We hypothesized that the combination of these two methods will enable the transient activation of the engineered kinase and allow us to control the duration of kinase activation. We used c-Src (Src) and p38α (p38) as models of Tyr and Ser/Thr kinases, respectively, to test this hypothesis, optimize the method, and demonstrate its broad applicability. Using this approach, we dissected signaling mediated by transient activation of Src and show that the same pathways play different roles during persistent Src activation.

3.2 Materials and Methods

3.2.1 Antibodies and chemical reagents

The following antibodies were used: anti-GAPDH (Ambion, cat. no. AM4300), anti-phospho-p130Cas (Y249) (BD Pharmigen cat. no. 558401), anti-HA (Biolegends, cat. no. 901502), anti-mCherry (Biovision, cat. no. 5993-100), anti-phospho-Akt (T308) (Cell Signaling, cat. no. 9275), anti-phospho-Akt (S473) (Cell Signaling, cat. no. 9271), anti-Akt (Cell Signaling, cat. no. 9272), anti-GFP (Clontech, cat. no. 632381), anti-paxillin (Fisher Scientific, cat. no. BDB612405), anti-phospho-paxillin (Y118) (Invitrogen, cat. no. 44-722G), anti-c-Src (Santa Cruz, cat. no. sc-8056), anti-Flag (Sigma, cat. no. F3165-1MG), anti-phosphotyrosine (4G10) (Millipore, cat. no 05-321), anti-phospho-ATF-2 (Cell Signaling, cat. no 9221S) and anti-Myc (Millipore, cat. no. 05-724). The following reagents were used: IgG-coupled agarose beads

(Millipore, cat. no. IP04-1.5ML), Rapamycin (LC Laboratories, cat. no. R5000), 1-NA-PP1 (1-Naphthyl-PP1) (Cayman, cat. no. 10954), LY294002 (Cell Signaling, cat. no. 10954), Wortmannin (Millipore, cat. no. CS203298), Rac1 Inhibitor CAS 1177865-17-6 (Calbiochem), ATF-2 substrate (Sigma, cat. no. A2353), Leupeptin hemisulfate (Gold Biotechnology, cat. no. L-010-5), and Aprotinin (Gold Biotechnology, cat. no. A-655-25).

3.2.2 DNA Constructs

The RapR-Src-cerulean-myc was previously described[90], the cerulean tag on RapR-Src-cerulean-myc was changed to mCherry using the modified site-directed mutagenesis with a mCherry mega primer (Supplementary Index A) generating RapR-Src-mCherry-myc[131,137]. RapR-SrcCat-cerulean-myc was made by deleting amino acid residues 1-257 in c-Src sequence of RapR-Src-cerulean-myc using a modified site-directed mutagenesis method[131,137] with a RapR-SrcCat mega primer (Supplementary Index B). CA-Src-cerulean-myc was generated from pUSE-c-Src-cerulean construct[137] by introducing Tyr529Phe mutation using site-directed mutagenesis[131,137] using the mega primers in Supplementary Index C. RapR-Src-as2-cerulean-myc, RapR-SrcCat-as2-cerulean-myc, and RapR-Src-as2-mCherry-myc were generated by introducing a Thr338 to Ala substitution in RapR-Src-cerulean-myc, RapR-SrcCat-cerulean-myc, and RapR-Src-mCherry-myc via site-directed mutagenesis[131,137] using the primers listed in Supplementary Index D. GFP-FRB[90] was changed to mCherry-FRB and mVenus-FRB by modified site-directed mutagenesis[131,137] using the mCherry mega primer (Supplementary Index A) and mVenus mega primer (Supplementary Index E) respectively[131,137]. iPEP-mCherry-FRB and iPEP-mVenus were generated from mCherry-FRB (Supplementary Index E) and mVenus-FRB through modified site-directed mutagenesis[131,137] using the iPEP mega primer (Supplementary Index F). To generate flag-mCherry-p130Cas, mVenus-p130Cas [90] was changed

to mCherry-p130Cas via modified site-directed mutagenesis[131,137] using the mCherry mega primer (Supplementary Index A), and then the Flag peptide sequence was inserted in front of mCherry-p130Cas via a second modified site-directed mutagenesis reaction[131,137] using the CMV-Flag mega primer (Supplementary Index G). iPEP-mVenus-FRB-paxillin was made by first inserting FRB between GFP and paxillin in GFP-paxillin[137] construct through modified site-directed mutagenesis[131,137] using the GFP-FRB-Paxillin mega primer (Supplementary Index H) and then iPEP insertion at the N-terminus of GFP and a simultaneous conversion of GFP into mVenus was done through a second modified site-directed mutagenesis reaction[131,137] using the CMV-iPEP-mVenus mega primer (Supplementary Index I). Stargazin-mVenus was made by replacing mCherry with mVenus using the modified site-directed mutagenesis[131,137] with the mVenus mega primer (Supplementary Index E) in the previously described construct Stargazin-mCherry[90]. The flag tagged mouse p38α was a gift from Dr. Gary Johnson (UNC) and the RapR-p38-flag construct was previously described[137]. RapR-p38-as2-flag was generated by introducing a Thr106 to Ala substitution in RapR-p38-flag using primers listed in Supplementary Index J via modified site-directed mutagenesis[131,137]. HA-Akt1 construct was a gift from Dr. John O'Bryan (UIC). mVenus-ATF2 was generated by inserting mVenus via modified site-directed mutagenesis[131,137] into Flag-ATF2 (a gift from Dr. B. Cuevas, Loyola University) using the CMV-venus-ATFP2 mega primer (Supplementary Index K). iPEP-venuus-FRB-ATF2 was generated using CMV-iPEP-venus-FRB-ATF2 mega primer (Supplementary Index L) via modified site-directed mutagenesis[131,137]. iPEP-GFP(Y66S)-FRB (color-less) was generated via site-directed[131,137] mutagenesis with the GFP(Y66S) mega primer (Supplementary Index M). PH-AKT-mVenus was generated from PH-AKT-GFP, a gift from Dr. W. Cho (UIC), by using modified site-directed mutagenesis[131,137] with the mVenus mega primer (Supplementary Index

E). Rac1-FLARE and the control plasmids expressing Y-PET and Turq[170] were gifts from Dr. Klaus Hahn (UNC). The cerulean-N1 vector is from Add Gene (#54742). Adenoviruses for expression of RapR-Src-as2-Cerulean and iPEP-GFP(Y66S)-FRB were generated by Dr. Jody Martin (Vector Core Facility at University of Illinois – Chicago).

3.2.3 Cell lines

The following cell lines were used: HeLa cells (ATCC, cat. no. CCL-2), human embryonic kidney LinXE cell line (derived from HEK 293 cells)[171], selected for these experiments because they provide higher transfection efficiency and expression levels. Cells were grown in DMEM (Corning, cat. no. 15-013-CV) with L-glutamine and 10-% FBS at 37°C and 5% CO_2. All proteins were expressed via either transient transfection of DNA constructs using Fugene 6 reagent (Promega Corporation, cat. no. E2691) or adenovirus infection; figure legends indicate when adenoviral constructs were used for infecting cells.

3.2.4 Immunoprecipitation and kinase assay

To activate exogenously expressed RapR-Src, cells were treated with either rapamycin or equivalent volumes of ethanol (solvent control) for the indicated amount of time. Cells were then treated with 1NA-PP1 or equivalent volumes of DMSO (solvent control), except in the case of the *in vitro* kinase assay (see below). After treatment, cells were washed with cold PBS and lysed with lysis buffer (20 mM HEPES-KOH, pH 7.8, 50 mM KCl, 100 mM NaCl, 1 mM EGTA, 1% NP40, 1 mM NaF, 0.1 mM Na_3VO_4, 0.033% ethanol, aprotinin 16 μg/ml, and Leupeptin hemisulfate 3.2 μg/mL), and centrifuged at 4,000 rpm, 4°C, for 10 minutes. Cleared cell lysates were immunoprecipitated with the indicated antibody for 1.5 hours at 4°C. Beads were washed (20 mM Tris-HCl, 1 mM DTT, 40 mM NaCl, 30 mM $MgCl_2$, 1 mM NaF, 0.1 mM Na_3VO_4, 0.033% ethanol, aprotinin 16 μg/ml, and Leupeptin hemisulfate 3.2 μg/mL) and then

resuspended in 2X Sample Buffer + 2% 2-Mercaptoethanol. Immunoprecipitation and kinase assays for RapR-Src constructs were performed as previously described[172]. Kinase assays for p38 constructs were performed as previously described[137,173]. Indicated amounts of 1NA-PP1 or solvent control (DMSO) were added to the kinase reactions to test inhibition of activity *in vitro*.

3.2.5 Image collection

HeLa cells were plated on fibronectin-coated coverslips at 5 mg/L and incubated for 2-4 hours. Prior to imaging coverslips were placed into an Attufluor Cell Chamber (Invitrogen, cat. no. A78-16) with Leibovitz (L-15) medium (Sigma Aldrich, cat. no. L1518-500mL) supplemented with 5% FBS. Live cell imaging was done on using an Olympus IX-83 microscope controlled by Metamorph software and equipped with a heated stage (Warner Instruments), Olympus UPlanSAPO 40X (oil, NA 1.25) objective, Xcite 120 LED (Lumen Dynamics) light source, and Image EMX2 CCD (Hamamatsu) camera.

3.2.6 Image Analysis

Cell area and Protrusive Activity Analysis:

Changes in cell area and protrusive activity were calculated following previously described method [90]. Stargazin-mVenus construct was used to label the plasma membrane. Cells expressing desired constructs were selected using epifluorescence imaging. Images were analyzed using Metamorph and CellGeo software[144]. Time-lapse movies were generated by collecting images in 2 minute intervals and analysis was performed using Metamorph and CellGeo software[144]. Stargazin-mVenus images were used to create a binary mask of a cell via MovThresh software[144] and used to assess cell area. The change in cell area was calculated by dividing the cell area at a given time point by the average area of the same cell prior to rapamycin addition. The protrusive activity represents sum of the areas associated with regions

of the cell that undergo local extensions between subsequent movie frames and was analyzed using ProActive software [144]. The change in protrusive activity was determined by dividing the protrusive activity at a given time point by the average protrusive activity prior to rapamycin treatment. For both, cell area and protrusive activity, the average and 90% confidence interval for each time point of all cells treated in the same conditions was calculated, these values were then standardized to the initial time point. The following number of cells (n) were analyzed for each condition: RapR-Src-cerulean-myc (DMSO, 15 minutes) n=18, RapR-Src-cerulean-myc (1NA-PP1, 15 minutes) n=23, RapR-Src-as2-cerulean-myc (DMSO, 15 minutes) n=26, RapR-Src-as2-cerulean-myc (1NA-PP1, 5 minutes) n=22, RapR-Src-as2-cerulean-myc (1NA-PP1, 15 minutes) n=26, RapR-Src-as2-cerulean-myc (1NA-PP1, 35 minutes) n=26, RapR-Src-as2-cerulean-myc (1NA-PP1+LY294002, 15 minutes) n=21, RapR-Src-as2-cerulean-myc (1NA-PP1+Wortmannin, 15 minutes) n=29, RapR-Src-as2-cerulean-myc (1NA-PP1+LY294002, 35 minutes) n=22, RapR-Src-as2-cerulean-myc (1NA-PP1+Wortmannin, 35 minutes) n=24, RapR-Src-as2-cerulean-myc (LY294002, 0 minutes) n=39, RapR-Src-as2-cerulean-myc (LY294002, 15 minutes) n=21, RapR-Src-as2-cerulean-myc (1NA-PP1+Rac1-I, 15 minutes) n=33, RapR-Src-as2-cerulean-myc (Rac1-I, 0 minutes) n=27, and RapR-Src-as2-cerulean-myc (Rac1-I, 15 minutes) n=27.

Rac1 Biosensor:

HeLa cells expressing the Rac1-FLARE [170] were analyzed as previously described. This biosensor works via Forster resonance energy transfer (FRET). When Rac1 is in the inactive form it does not associate with the Cdc42/Rac Interactive Binding (CRIB) region of p21 activated kinase (PAK1). However, when bound to GTP it binds to CRIB-PAK1 and the FRET signal goes up (Figure 3.1). HeLa Cells co-transfected with RapR-Src-as2-mCherry, non-

fluorescent iPEP-GFP(Y66S)-FRB, and bicistronic construct for expression of Rac1 biosensor components[170], were plated on glass coverslips coated with 5mg/ml fibronectin and imaged live with 2 minute intervals. The following combination of filters were used for imaging: 445/10nm excitation and 485/30nm emission filters for the donor, 515/10nm excitation and 540/20nm emission filters for the acceptor, 445/10nm and 540/20nm for raw FRET images. Image analysis was performed as previously described[174]. Cells expressing only Y-PET and Turq proteins were used to determine blead through coefficients as previously described[174]. Number of cells analyzed: DMSO treated n=10 and 1NA-PP1 treated n=10.

PH-AKT-mVenus Translocalization:

Activation of Phosphoinositide 3-Kinase (PI3K) causes the phosphorylation of and re-localization of AKT from the perinuclear region to the cytoplasm (Figure 3.2a). Therefore, to determine how Src activation (transient versus prolonged) temporally affected PI3K activity we measured the translocation of AKT. Using the pleckstrin homology (PH) domain of AKT fused to a fluorescent protein, we were capable of tracking, the location of AKT over-time and thus monitor the activity of PI3K (Figure 3.2b). HeLa cells co-transfected with PH-AKT-mVenus, RapR-Src-as2-cerulean and iPEP-mCherry-FRB constructs were plated on class coverslips coated with 5mg/ml fibronectin. Cells were imaged live every 2 min. Average intensity of mVenus signal was determined for each frame for perinuclear region (12 μm around the nucleus) and the peripheral region (beyond 12 μm region around the nucleus. Analysis was performed using Metamorph software. For each cell, ratio of average peripheral to average perinuclear mVenus intensity was normalized to the average value before addition of rapamycin. Number of cells analyzed: DMSO treated n=14 and 1NA-PP1 treated n=15.

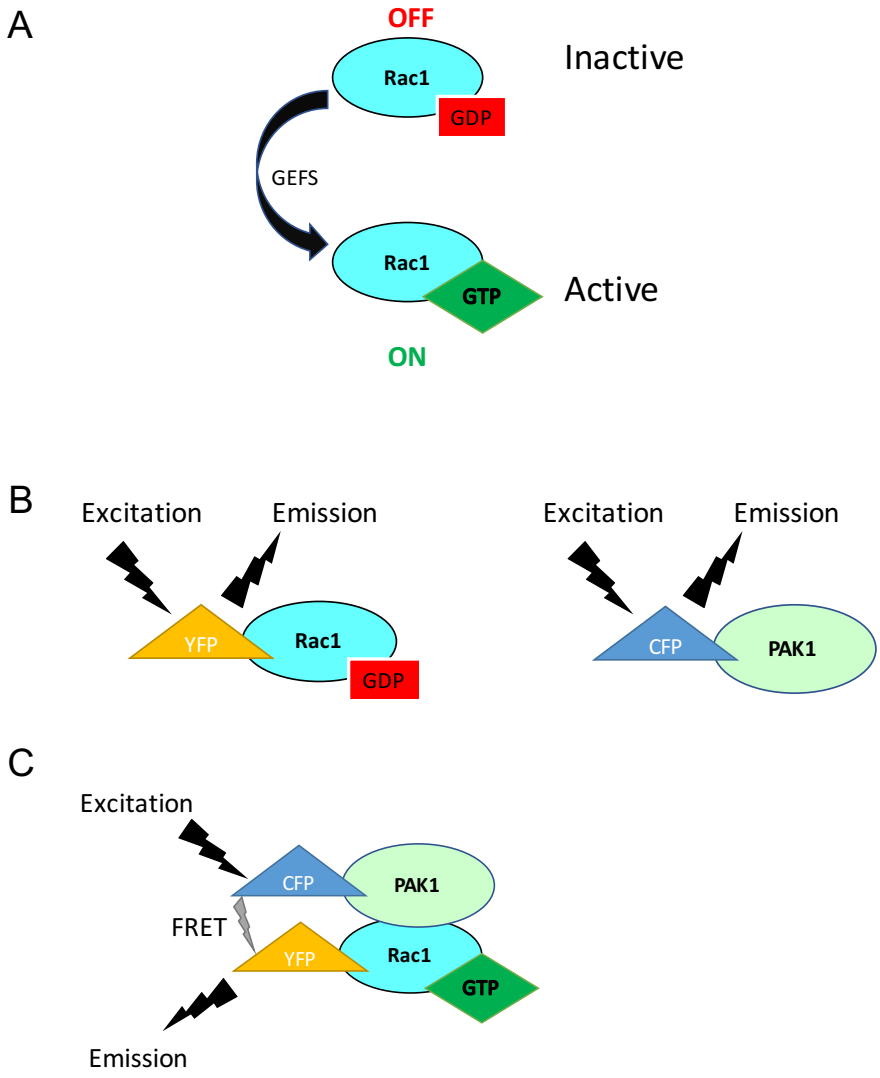

Figure 3.1: Detecting Rac1 activity
(A) Rac1 is a RhoGTPase which cycles between the inactive form, GDP-bound, and the active form, GTP bound. (B and C) To detect changes in Rac1 activity following Src activation we utilized a Rac1 FRET biosensor[1,2]. (B) When Rac1 is inactive excitation Rac1 does not interact with the CRIB domain of PAK1 and excitation of CFP and emission of YFP produces a very low FRET signal. (C) However, when Rac1 is activated it interacts with PAK1 bringing the CFP and YFP close together and the FRET signal increases.

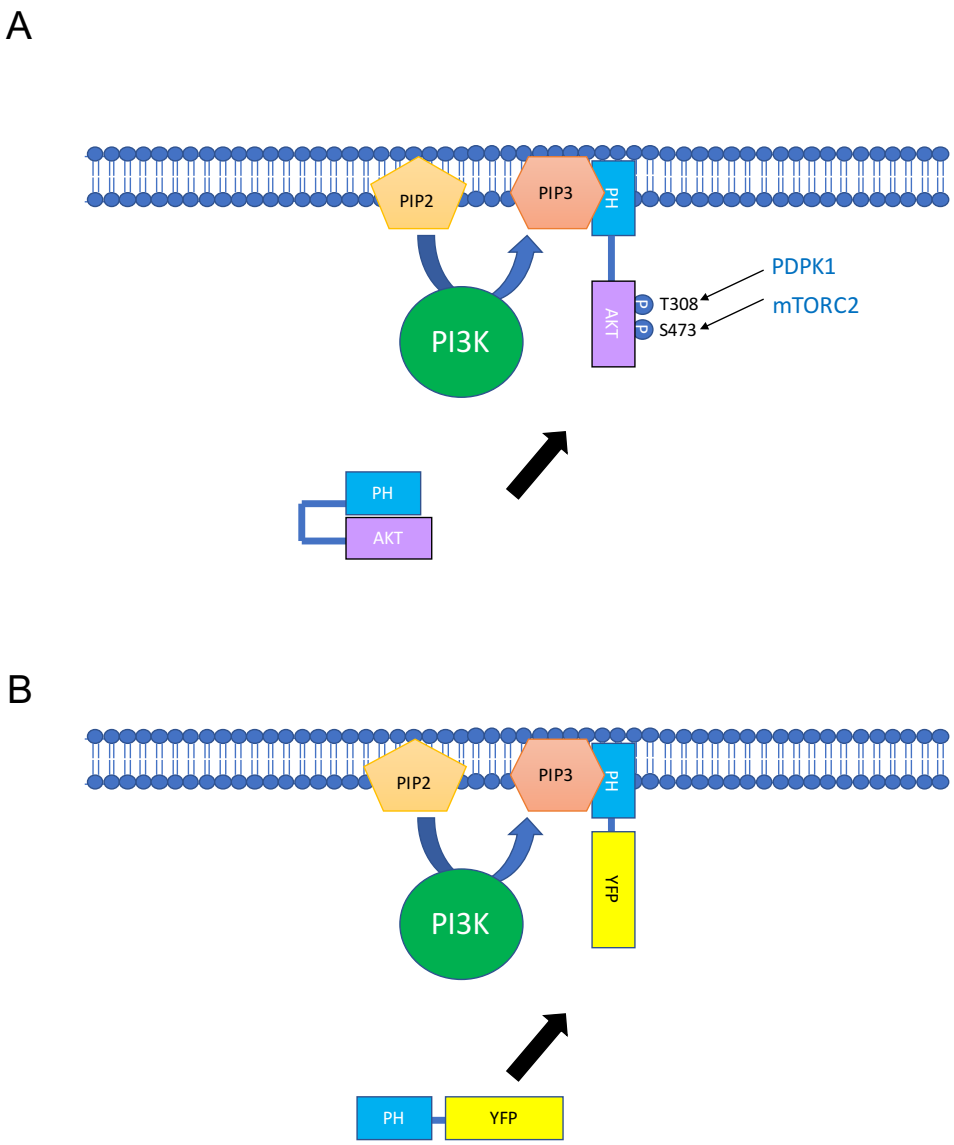

Figure 3.2: Detecting PI3K activity
(A) Activation of PI3K results in the phosphorylation of AKT at T308 and S473 and its recruitment to the plasma membrane through its PH (pleckstrin homology) domain. Therefore, PI3K activity in the cell can be detected either by the re-localization of AKT or its phosphorylation. (B) To detect re-localization of AKT its PH domain was fused to YFP. Monitoring of PH-YFP localization allows for the temporal monitoring of PI3K activity.

Data Analysis:

To analyze secondary cell spreading that follows inactivation of Src, we determined the change in cell area starting from 10 minutes after addition of 1NA-PP1. The average cell area was standardized to the value for the initial (10 minute) time point. The spreading rate was determined by calculating the slope of cell area increase following addition of 1NA-PP1. A Student's t-test (two-sample, unequal variances) was used to compare the spreading rates between each treatment. Cell area and protrusive activity statistics were calculated using the mean cell area of each cell during the indicated time periods to compare treatment groups using a Student's t-test (two-sample, unequal variances). A Student's t-test (two-sample, equal variances) was used to compare the phosphorylation levels of ATF between each treatment.

3.3 Results

Engineering Src kinase with independent activation and inactivation controls

Activation of Src was accomplished by using an engineered RapR-Src kinase construct which can be activated in living cells by addition of rapamycin or its non-immunosuppressive analogs [90,131,137]. RapR-Src contains tyrosine 529 to phenylalanine mutation making it insensitive to inhibitory regulation by endogenous factors[90,137]. Introduction of this mutation in wild type Src prevents inhibitory phosphorylation by Csk kinase leading to generation of constitutively active Src [175]. In the context of RapR-Src, this property enables us to control Src activity only through engineered components. To gain independent control of kinase inactivation, we introduced a Thr338 to an Ala mutation in RapR-Src. The equivalent mutation (I338A) renders v-Src sensitive to 1NA-PP1 inhibitor[122–125]. Thus, we hypothesized that the T338A mutant of RapR-Src (RapR-Src-as2) will be sensitive to 1NA-PP1 inhibition and reverse rapamycin induced activation (Figure 3.3a). Indeed, RapR-Src-as2 is activated by rapamycin, and subsequent 1NA-PP1

treatment efficiently inhibits its activity (Figure 3.3b). These data demonstrate that RapR-Src-as2 successfully combines two orthogonal regulatory switches: stimulation by rapamycin and inactivation by 1NA-PP1.

RapR-Src-as2 activation, however, was not as robust as activation of RapR-Src (Figure 3.3b). This is consistent with previous observations where a similar reduction in catalytic activity was reported for analog-sensitive mutants of v-Src[176]. We therefore sought to improve the catalytic activity of RapR-Src-as2 by modifying our approach for kinase activation. Prior studies suggested that iFKBP inactivates RapR-Src by increasing conformational dynamics of the catalytic domain, whereas interaction with rapamycin and FRB stabilizes RapR-Src and rescues its activity[137]. Decreased activity of RapR-Src-as2 suggests that the T338A mutant may further destabilize the RapR-Src catalytic domain, reducing its activity even in the presence of rapamycin. We hypothesized that tighter binding of FRB to iFKBP would stabilize RapR-Src-as2 and improve its catalytic activity. The iFKBP domain was initially engineered by deletion of the first 15 amino acids of FKBP12 that comprise an additional β-strand in the structure[137] (Figure 3.4a). We predicted that addition of these residues to the N-terminus of FRB might enhance the interaction between FRB and iFKBP and lead to improved activation of RapR-Src and RapR-Src-as2 (Figure 3.4a). FRB bearing the first 15 amino acids of FKBP12 at the N-terminus (iPEP-FRB) dramatically improved activation of RapR-Src-as2 (Figure 3.4b). Importantly, RapR-Src-as2 was still efficiently inhibited by 1NA-PP1 (Figure 3.4b). Addition of iPEP to FRB significantly improved binding to RapR-Src-as2 and resulted in higher kinase activity at lower rapamycin concentrations (Figure 3.5a) suggesting that T338A mutation affected RapR-Src-as2 activity by reducing affinity to rapamycin and/or FRB. In addition, iPEP-FRB was able to activate unmodified RapR-Src at lower doses of rapamycin than FRB without

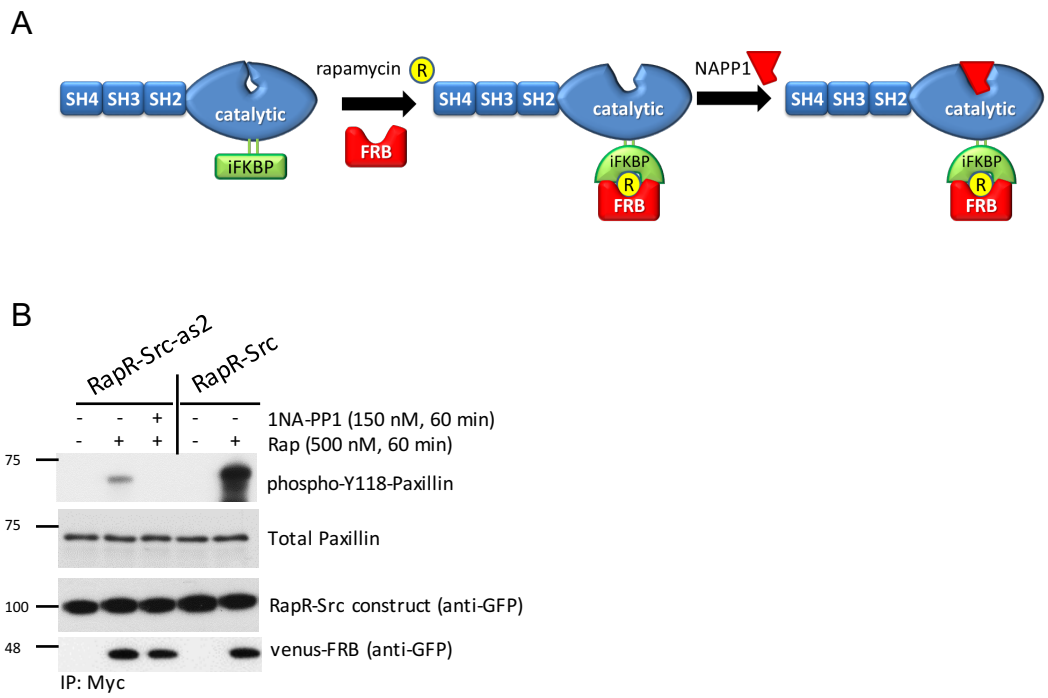

Figure 3.3: Transient activation of engineered Src kinase
(A) Schematic of RapR-Src-as2 regulation. (B) *In vitro* kinase assay of immunoprecipitated Src constructs. LinXE cells we co-transfected with mVenus-FRB and indicated Src constructs bearing cerulean (recognized by GFP antibody) and myc tags in. Cells were treated with rapamycin (Rap, 500 nM) or ethanol (solvent) for 1 hour and immunoprecipitated. Kinase assays were carried out in the presence of equivalent volumes of either DMSO (solvent) or 1NA-PP1 (150 nM). The purified N-terminal fragment of paxillin was used as a substrate. Data are representative of at least three independent experiments.

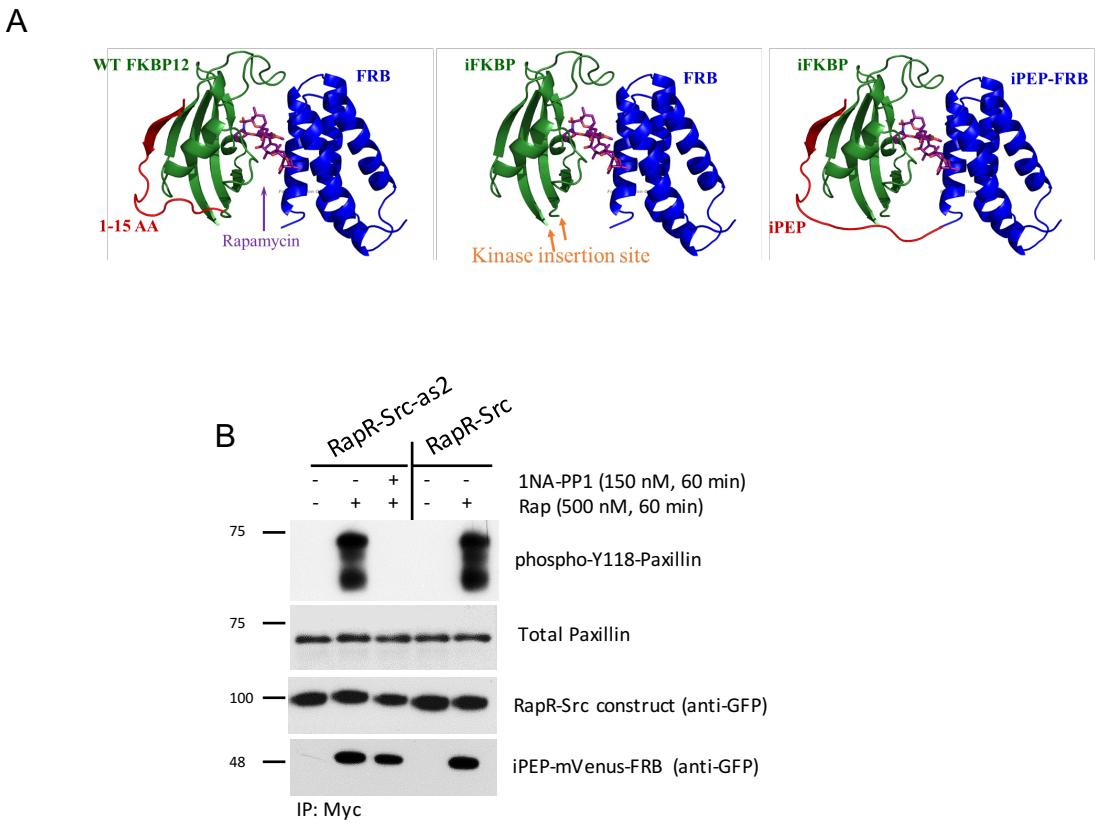

Figure 3.4: Transient activation of engineered Src is improved by FRB modification
(A) Tertiary protein structure schematic of FRB modification to generate iPEP-FRB. (B) *In vitro* kinase assay of immunoprecipitated Src constructs. LinXE cells we co-transfected with iPEP-mVenus-FRB and indicated Src constructs bearing cerulean (recognized by GFP antibody) and myc tags in. Cells were treated with rapamycin (Rap, 500 nM) or ethanol (solvent) for 1 hour and immunoprecipitated. Kinase assays were carried out in the presence of equivalent volumes of either DMSO (solvent) or 1NA-PP1 (150 nM). The purified N-terminal fragment of paxillin was used as a substrate. Data are representative of at least three independent experiments.
** Figure 3.4A was generated by Dr. Anne-Marie Ray (Karginov laboratory)*

the iPEP, (Figure 3.5b) further supporting our hypothesis that iPEP improves interaction between FRB and iFKBP. Thus, we chose to use RapR-Src-as2 and iPEP-FRB for our studies since this newly engineered system enables both the robust activation and inactivation of Src signaling. We chose to use 500 nM rapamycin to ensure efficient activation of RapR-Src-as2 and to keep our experiments consistent with previously published studies[90,137].

Next, we characterized the efficiency and the selectivity of RapR-Src-as2 regulation *in vitro* and in living cells. An *in vitro* analysis revealed complete inactivation of RapR-Src-as2 was achieved with concentrations of 1NA-PP1 as low as 50 nM (Figure 3.6a). Importantly, similar doses of 1NA-PP1 did not affect activity of non-modified RapR-Src or a constitutively active mutant of c-Src (Figures 3.6b and 3.6c). Activation of RapR-Src-as2 in living cells led to a dramatic increase in phosphorylation of the endogenous Src substrate paxillin and an increase in the level of tyrosine phosphorylated proteins (Figures 3.7a and b). RapR-Src-as2 was overexpressed at a higher level than endogenous Src (Figure 3.8). A substantial reduction in phosphorylation was observed upon addition of 250 and 500 nM 1NA-PP1, indicating efficient inactivation of RapR-Src-as2 (Figures 3.7a and b). Importantly, similar concentrations did not reduce the activity of unmodified RapR-Src, demonstrating that the selected doses only affect the analog-specific mutant kinase (Figures 3.7a and b). Inactivation of RapR-Src-as2 was fast. Treatment with 1NA-PP1 for only 5 minutes reduced protein phosphorylation to the levels preceding Src activation (Figure 3.7b). Phosphorylation levels of paxillin and p130Cas, and total protein phosphorylation remained at the same reduced levels for at least 1 hour after addition of 1NA-PP1 (Figures 3.7b and 3.9), indicating sustained inactivation of RapR-Src-as2. These data demonstrate efficient regulation of Src activity *in vitro*

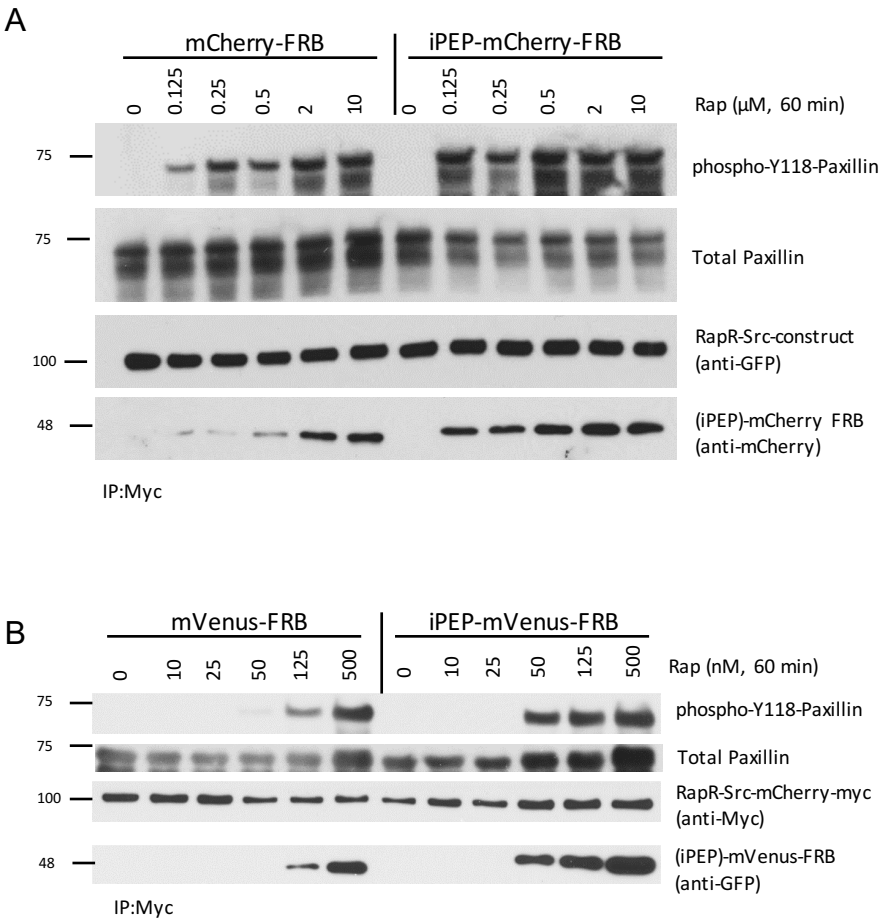

Figure 3.5: Activation of RapR-Src and RapR-Src-as2 with FRB versus iPEP-FRB
(A) LinXE cells transfected with RapR-Src-as2-cerulean-myc and either iPEP-mCherry-FRB or mCherry-FRB were treated with the indicated amount of rapamycin or ethanol (solvent) for 1 hour. (B) LinXE cells transfected with RapR-Src-mCherry-myc and either iPEP-mVenus-FRB or mVenus-FRB were treated with the indicated amount of rapamycin or ethanol (solvent) for 1 hour. (A and B) RapR-Src constructs were immunoprecipitated and analyzed by an *in vitro* kinase assay using the N-terminal fragment of paxillin as a substrate. Data are representative of at least three independent experiments.
** Figure 3.5B was generated by Dr. Anne-Marie Ray (Karginov laboratory)*

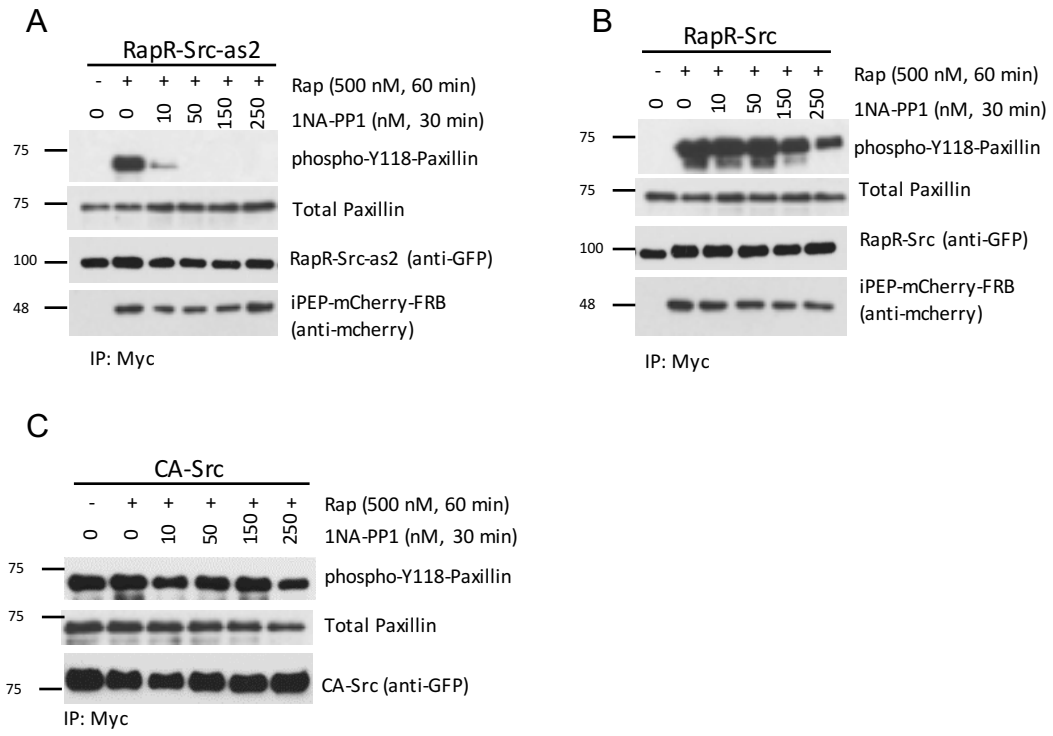

Figure 3.6: Characterization of RapR-Src-as2 *in vitro*
(A-C) LinXE cells transfected with the indicated Src construct tagged with cerulean-myc and iPEP-mCherry-FRB were activated with rapamycin (500 nM) for 1 hour. Src was immunoprecipitated and analyzed by an *in vitro* kinase assay using the N-terminal fragment of paxillin as a substrate. Equal volume of either 1NA-PP1 or DMSO (solvent) was added to the kinase reactions with: RapR-Src-as2 (A), RapR-Src (B), and CA-Src (constitutively active mutant of Src, Y529F) (C) at the indicated dose. (A-C) Data are representative of at least three independent experiments.

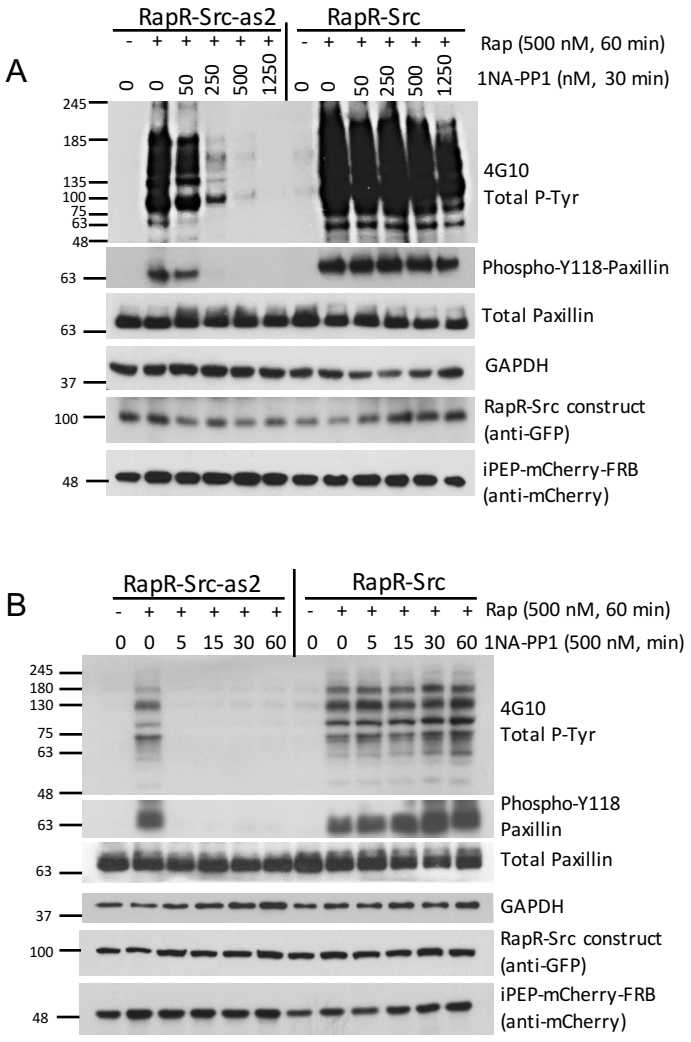

Figure 3.7: RapR-Src-as2 activation and inactivation in living cells
LinXE cells, transfected with iPEP-mCherry-FRB and either RapR-Src-as2-cerulean-myc or RapR-Src-cerulean-myc, were activated with rapamycin (500 nM) for 1 hour. (A)Cells were then treated with either the indicated amount of 1NA-PP1 or DMSO (solvent) for 30 minutes. (B) Cells were treated for the indicated amount of time with 1NA-PP1 (500 nM). (A and B) Cell lysates were collected and analyzed for protein phosphorylation. Data are representative of at least three independent experiments.
** Figure 3.7A was generated by Kerrie B. Collins (Karginov Laboratory)*

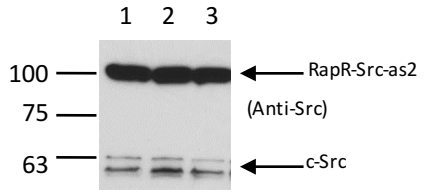

Figure 3.8: RapR-Src-as2 expression relative to endogenous Src expression
Cell lysates were collected from three independent samples of LinXE cells transfected with RapR-Src-as2-cerulean-myc and iPEP-mCherry-FRB. Lysates were analyzed to compare levels of RapR-Src-as2 expression to endogenous Src expression levels.

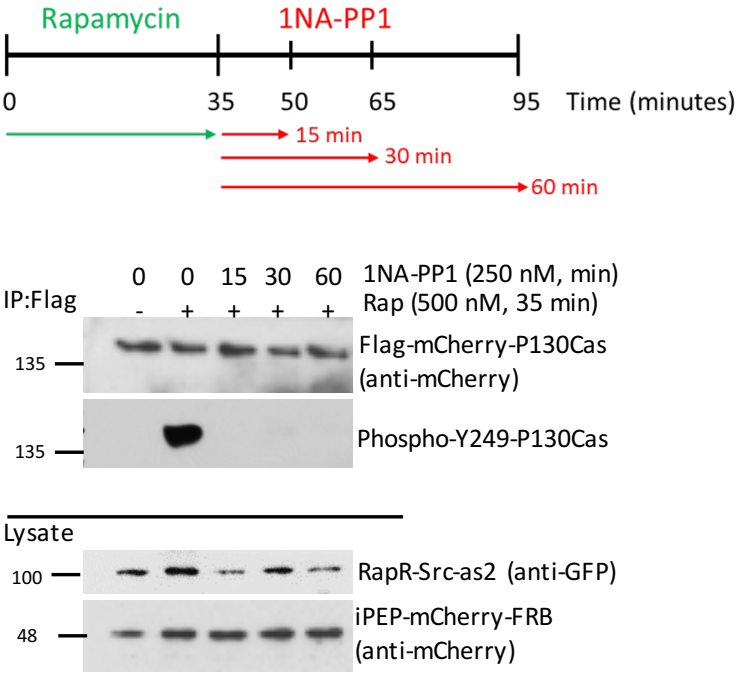

Figure 3.9: Inactivation of RapR-Src-as2 in HeLa cells
HeLa cells transfected with: RapR-Src-as2-cerulean-myc, iPEP-mCherry-FRB, and Flag-mCherry-p130Cas were treated with rapamycin (500 nM) for 35 minutes and then with 1NA-PP1 (250 nM) for the indicated amount of time. Flag-mCherry-p130Cas was immunoprecipitated and its phosphorylation on Tyr249 was assessed by western blot. Data are representative of at least three independent experiments.

and in living cells using RapR-Src-as2 and iPEP-FRB. Therefore, RapR-Src-as2 can be used to evaluate the effects of transient Src activation in cells.

Transient regulation of Src activity in specific signaling complexes

RapR-Src can be activated in specific protein complexes when the FRB domain is fused to a selected protein using the "rapamycin-regulated targeted activation of pathways" (RapRTAP) method[90]. This approach enables activation of individual signaling pathways downstream of Src. However, subsequent inactivation of these pathways was not achievable with the RapRTAP approach. Therefore, we evaluated whether RapR-Src-as2 could be used to turn on and off Src activity in a specific complex. As a model system, we tested targeted activation of Src in complex with its known binding partner and substrate, paxillin (Figure 3.10a). Association of Src with other proteins is primarily mediated by domains N-terminal to its catalytic domain (SH2, SH3, SH4) [94,177]. Src interaction with endogenous binding partners was prevented by using only the catalytic domain of RapR-Src-as2 (RapR-SrcCat-as2). This approach limits Src signaling only to the paxillin complex. iPEP-FRB was added to the N-terminus of paxillin to mediate binding and activation of RapR-SrcCat-as2 (Figure 3.10a). Targeted activation of RapR-SrcCat-as2 induced phosphorylation iPEP-FRB-paxillin (Figures 3.10b and c), and subsequent addition of 1NA-PP1 led to de-phosphorylation of the targeted paxillin (Figures 3.10b and c). Thus, RapR-SrcCat-as2 can be used for activation and inactivation of Src-mediated signaling in specific protein complexes.

Engineered transient activation of p38 kinase

To explore the general applicability of this method, we tested whether it could be utilized for transient regulation of Ser/Thr kinases. We demonstrated previously that activation of p38 can be achieved using the RapR method[137]. To achieve independent control of inactivation we

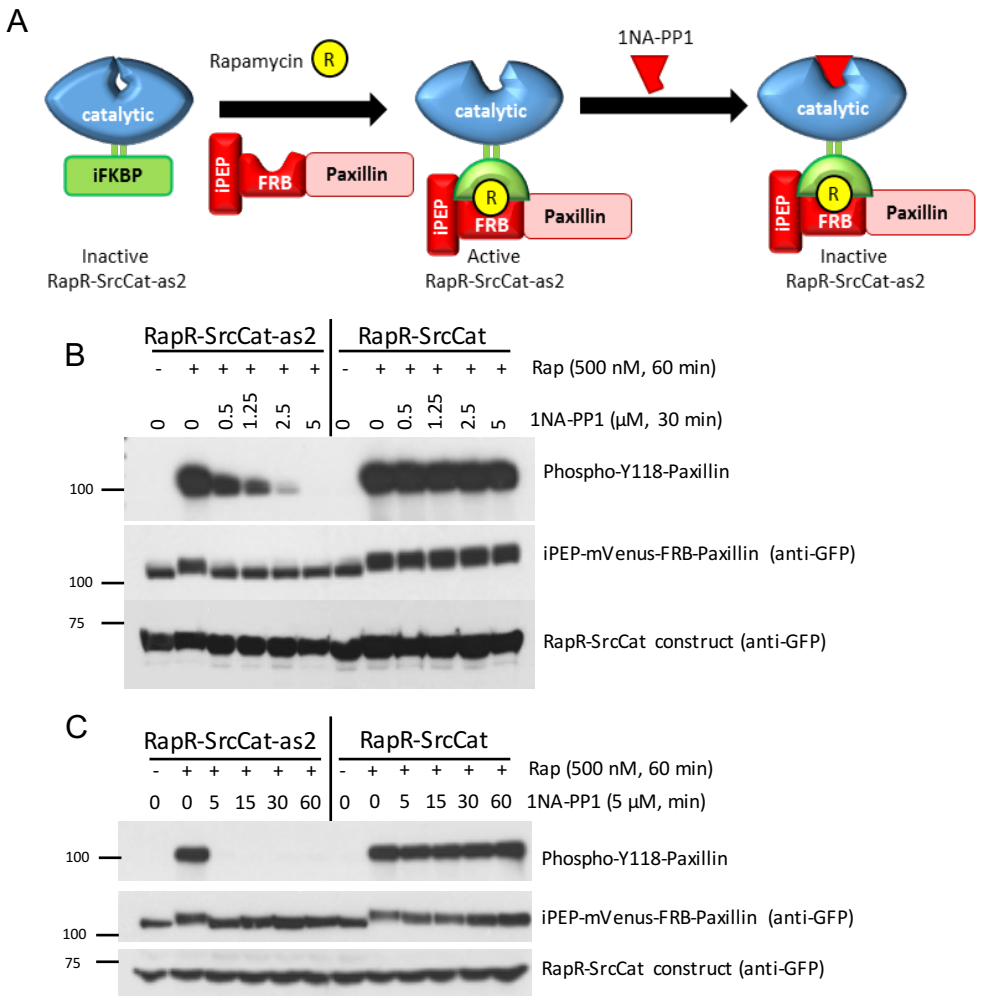

Figure 3.10: Transient activation with RapR-SrcCat-as2
(A) Schematic of RapR-SrcCat-as2 regulation in complex with paxillin. (B and C) Regulation of Src activity targeted to complex with paxillin in living cells. LinXE cells transfected with iPEP-mVenus-FRB-paxillin and either RapR-SrcCat-as2-cerulean-myc or RapR-SrcCat-cerulean-myc, were treated with rapamycin (500 nM) or ethanol (solvent) for 1 hour, and subsequently with 1NA-PP1; at the indicated dose for 30 minutes (B) or with (5 μM) for the designated amount of time (C). Cell lysates were analyzed for phosphorylation of iPEP-mVenus-FRB-paxillin. Data are representative of at least three independent experiments.

mutated residue Thr106 to an Ala in RapR-p38 generating RapR-p38-as2. To our knowledge, analog sensitive p38 has not been generated previously, and its inhibition by 1NA-PP1 has not been demonstrated. Activation and inactivation of RapR-p38-as2 was tested *in vitro* using purified ATF-2 as a known p38 substrate[137,173]. The *in vitro* kinase assay shows that RapR-p38-as2 activity was specifically inactivated by 1NA-PP1 (Figure 3.11a). Importantly, activity of RapR-p38 and wild-type p38 was not affected using similar concentrations of 1NA-PP1 (Figures 3.11b and c). Activation of RapR-p38-as2 in living cells led to elevated levels of phosphorylated ATF2, whereas subsequent inactivation reduced ATF2 phosphorylation (Figure 3.12a). These results demonstrate successful transient activation of engineered p38 *in vitro* and in living cells, and suggest that this tool can be applied for regulation of both Tyr and Ser/Thr kinases.

To demonstrate targeted regulation of RapR-p38-as2 in living cells we generated ATF2 construct bearing iPEP-FRB at the N-terminus (iPEP-mVenus-FRB-ATF2). Treatment of cells with rapamycin induced binding of RapR-p38-as2 to the engineered ATF2, and stimulated its phosphorylation. Addition of 1NA-PP1 resulted in significant reduction in phospho-ATF2 levels (Figure 3.12b). These results demonstrate transient activation of p38 in complex with ATF2 in living cells.

Regulation of morphological changes using transient stimulation of Src

Previously developed technologies did not allow us to assess the effect of transient Src activation on cell morphological changes. We can overcome this limitation by using RapR-Src-as2. Therefore, we evaluated how activation and inactivation of RapR-Src-as2 affects Src-induced cell morphological changes. Prior studies demonstrated that RapR-Src localization is not perturbed by the engineered modification[90]. RapR-Src-as2 also exhibited similar localization patterns to RapR-Src and wild type Src. Inactive Src localized primarily to the perinuclear area,

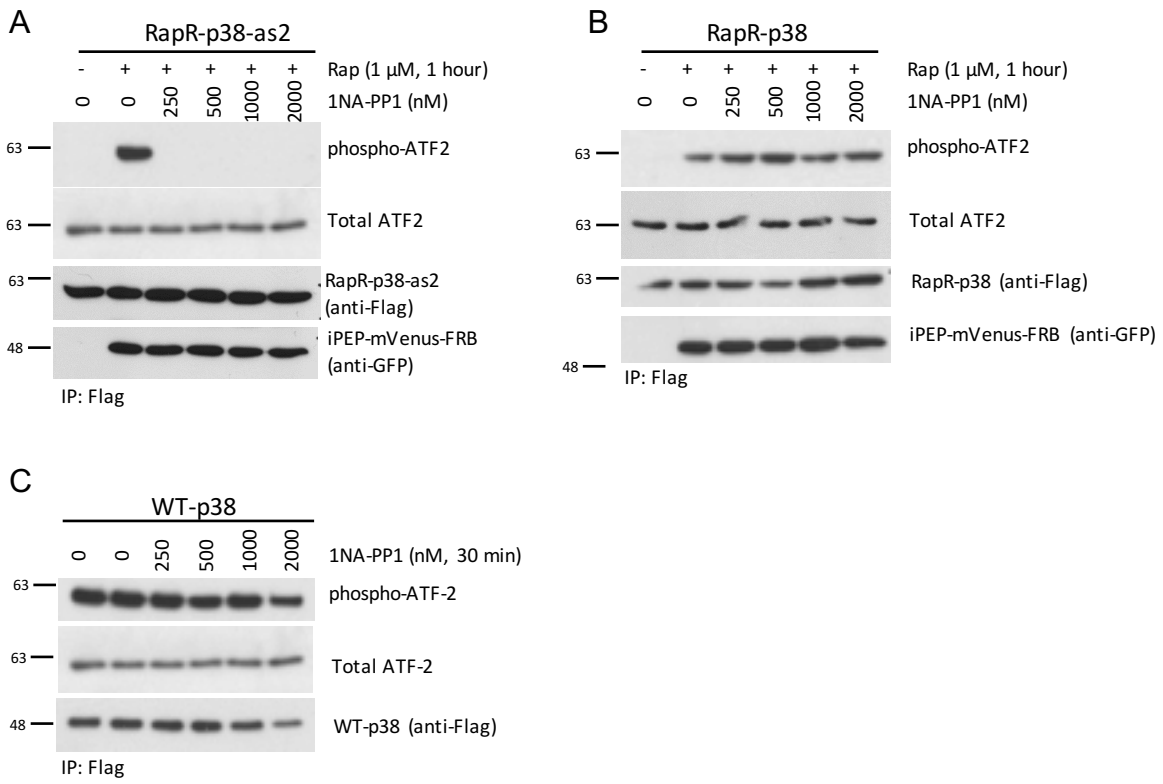

Figure 3.11: Development and characterization of RapR-p38-as2 System *in vitro*
LinXE cells transfected with flag-tagged: RapR-p38-as2 (A), RapR-p38 (B), or wild-type (WT) p38 (C) and iPEP-venus-FRB were treated with rapamycin (1 µM) or ethanol (solvent) for 1 hour. Five minutes prior to collection cells were exposed to 30 seconds of UV. Flag tagged p38 constructs were immunoprecipitated and analyzed by an *in vitro* kinase assay using ATF-2 as a substrate. Equal volume of either 1NA-PP1 or DMSO (solvent) was added to the kinase reactions at the indicated dose. Data is representative of three independent experiments.
**Experiments in this figure were performed by Vincent Huyot (Karginov lab)*

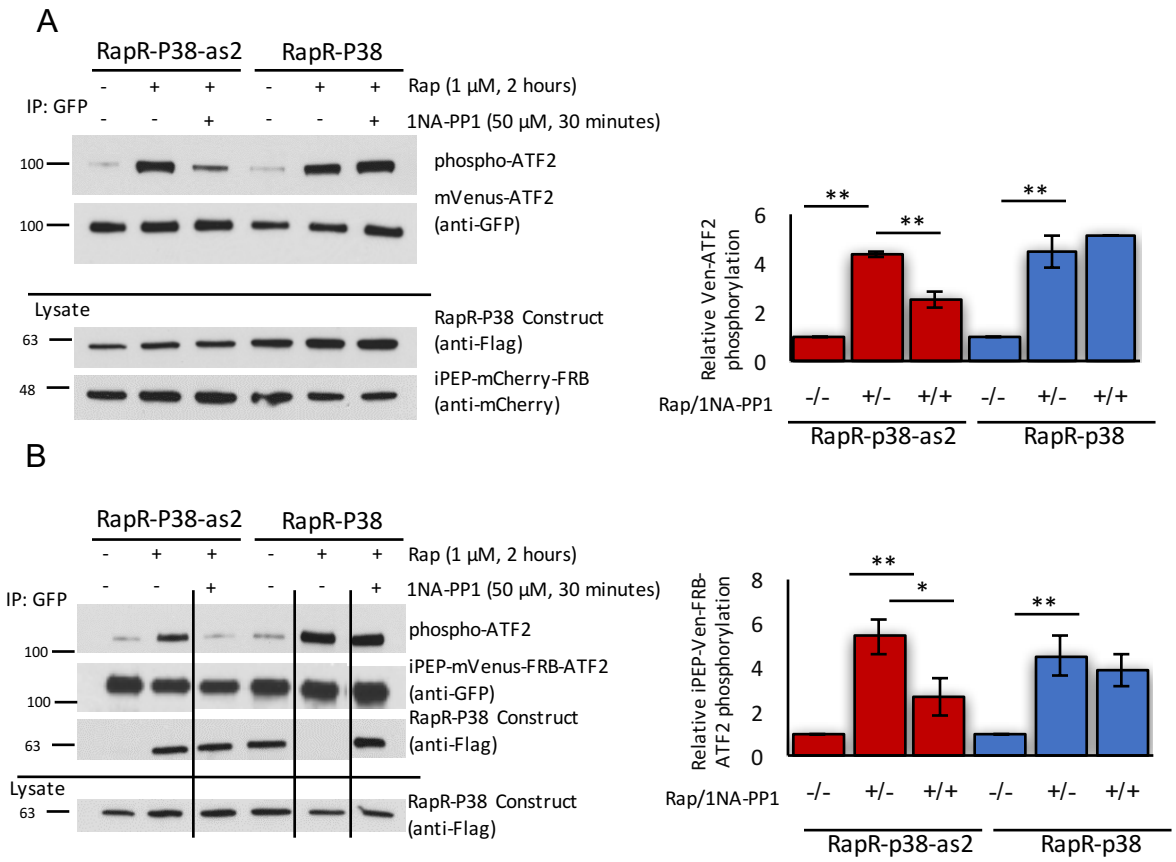

Figure 3.12: RapR-p38-as2 System in living cells

(A) LinXE cells transfected with either flag-tagged RapR-p38-as2 or RapR-p38, iPEP-mCherry-FRB, and mVenus-ATF2 were activated for 2 hours with rapamycin (1 µM) and then treated with either 1NA-PP1 (50 µM) or DMSO (solvent) for 30 minutes. mVenus tagged ATF2 was immunoprecipitated and analyzed via Western Blot for its phosphorylation status. (B) Activation and inactivation of RapR-p38-as2 targeted to ATF2. LinXE cells transfected with flag-tagged RapR-p38-as2 or RapR-p38 and iPEP-mVenus-FRB-ATF2 were activated for 2 hours with rapamycin (1 µM) and then treated with either 1NA-PP1 (50 µM) or DMSO (solvent) for 30 minutes. mVenus tagged ATF2 was immunoprecipitated and analyzed via Western Blot for its phosphorylation status. (A and B) Graphs show average relative phosphorylation levels of mVenus tagged ATF2 constructs from three experiments and error bars indicate standard deviations. A two-sample Student's T-Test was used compare pre- versus post-rapamycin treatment and DMSO versus 1NA-PP1 treatment (*$p<0.05$ and **$p<0.005$).

whereas activation of Src stimulated its translocation to plasma membrane and focal adhesions (Figure 3.13). Sustained activation of RapR-Src-as2 in HeLa cells induced robust cell spreading and transient stimulation of protrusive activity (Figures 3.14a-e) in agreement with our previously published results[90,137]. A substantial increase in paxillin phosphorylation was detected 5 minutes after addition of rapamycin indicating fast activation of RapR-as2 in living cells (Figure 3.14f). Treatment with 1NA-PP1 after rapamycin resulted in an immediate reduction in cell area and inhibition of protrusive activity (Figures 3.14c-e; 3.15a-c). By adding 1NA-PP1 at different time points after Src activation we were capable of inducing Src-mediated cell spreading and protrusive activity for different periods of time (Figures 3.14c-e; 3.15a-c). These results demonstrate the capability of our approach to regulate the extent and duration of Src-mediated morphological changes. Treatment of cells expressing RapR-Src-as2 with DMSO (solvent control) (Figure 3.14a), or treatment of cells expressing unmodified RapR-Src with 1NA-PP1 (Figure 13.14b) did not affect Src-induced cell area changes, indicating that the reversal of morphology was specific to inactivation of RapR-Src-as2

Inactivation of RapR-Src-as2 by 1NA-PP1 reversed Src-induced phenotypes. However, initial reduction in cell area and protrusive activity was followed by a slow and steady cell spreading and increased protrusive activity (Figure 3.15a and b). These secondary morphological changes were not caused by restoration of RapR-Src-as2 activity after inhibition (Figures 3.7b and 3.9). Additionally, the extent of secondary changes depended on the duration of Src activation. Activation of RapR-Src-as2 for 15 minutes was followed by significantly faster cell spreading and greater protrusive activity than stimulation for 5 or 35 minutes (Figures 3.14c-e; 3.15b and c; 3.16a and b). Thus, using this novel methodology for controlling the duration of

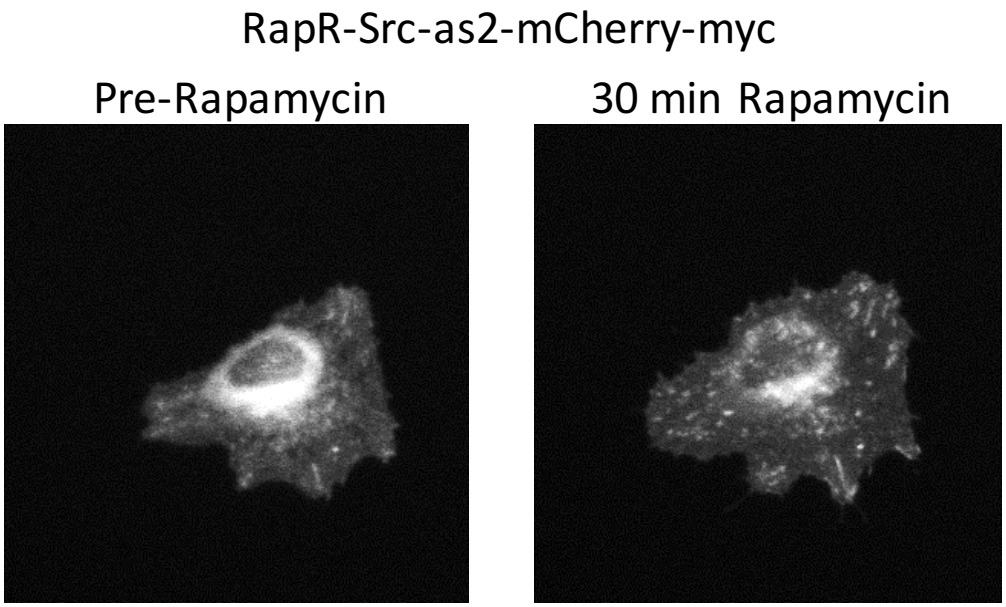

Figure 3.13: RapR-Src-as2 localization in HeLa cells
HeLa cells, transfected with RapR-Src-as2-mCherry-myc and infected with iPEP-GFP(Y66S)-FRB, were imaged live to analyze RapR-Src-as2 localization both before and after activation via rapamycin (500 nM). RapR-Src-as2 prior to rapamycin treatment is localized predominantly in the perinuclear area. However, after rapamycin treatment Src localizes to the plasma membrane and focal adhesions.

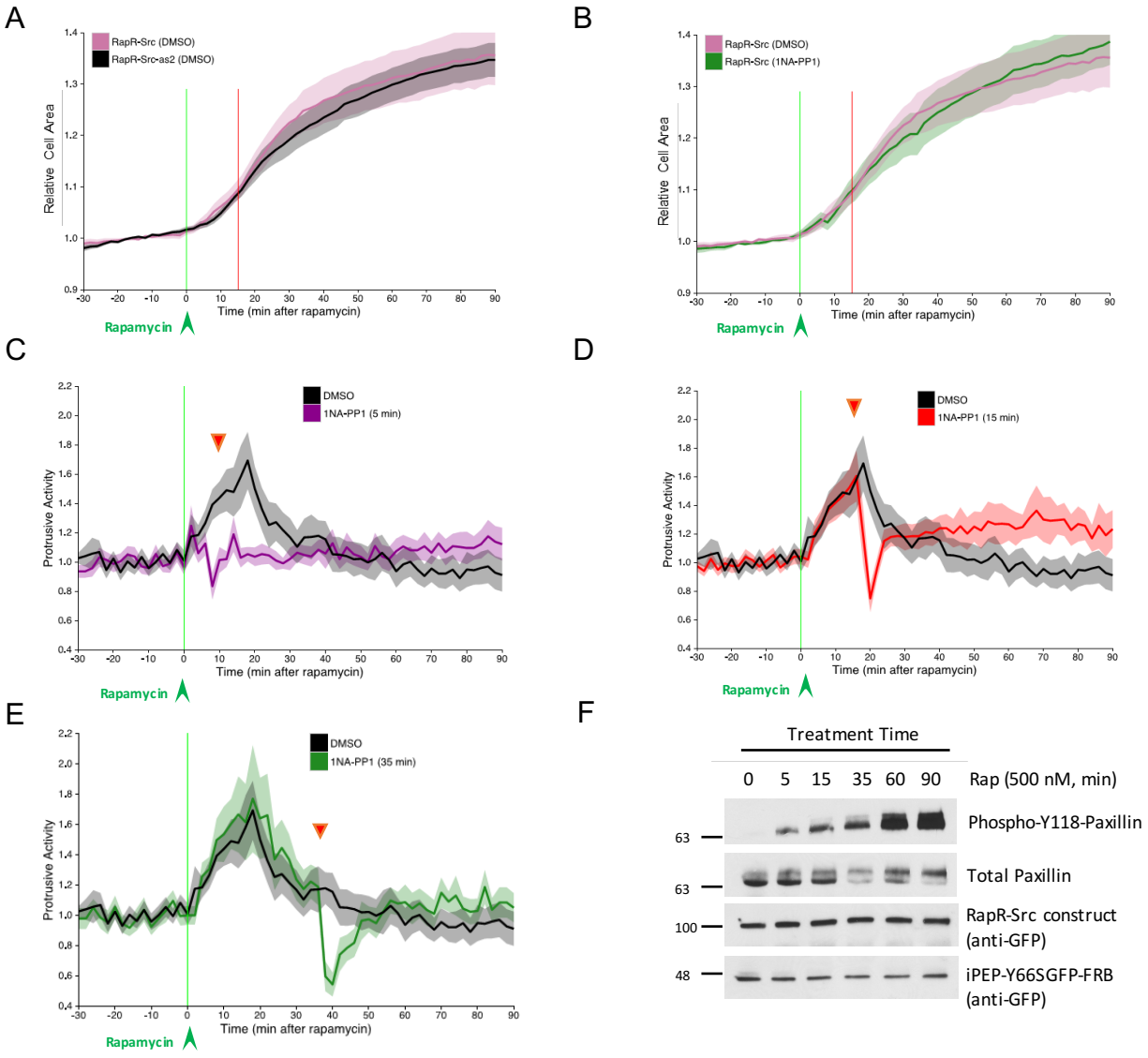

Figure 3.14: Effect of prolonged versus transient Src activity on cell morphodynamics
(A-E) HeLa cells, transfected with: the indicated Src construct tagged with cerulean-myc, iPEP-mCherry-FRB, and Stargazin-mVenus, were imaged live. Cell area and protrusive activity were calculated using Stargazin-mVenus images. (A) Cell area changes upon treatment with rapapmycin (500 nM) (green line), and then subsequent treatment with DMSO 15 min later (red line). (B) Cell area changes upon treatment with rapamycin (500 nM) (green line) and then treatment with DMSO (solvent) or 1NA-PP1 (250 nM) 15 min later (red line). (C-E) Protrusive activity for cells expressing RapR-Src-as2 treated with DMSO at 15 minutes compared to cells treated with 1NA-PP1 (250 nM) (red triangle) at (C) 5 minutes, (D) 15 minutes, and (E) 35 minutes. All error bars/shading represent 90 percent confidence intervals; *p<0.05, **p<0.005. (F) HeLa cells infected with RapR-Src-as2-cerulean-myc and iPEP-Y66SGFP-FRB were activated with rapamycin (500 nM) for the designated amount of time. Cell lysates were collected and analyzed for phosphorylation of paxillin on Tyr118.

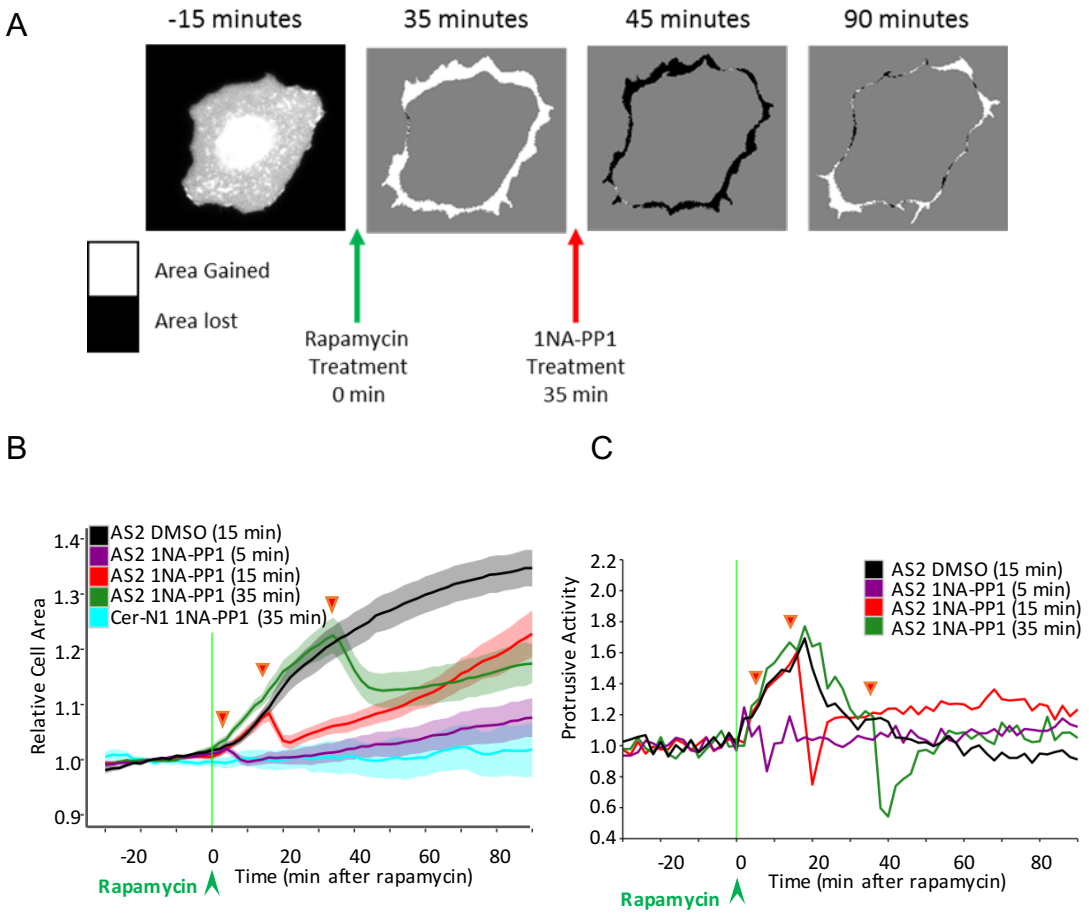

Figure 3.15: Regulation of Src mediated morphological changes
Hela cells transfected with: cerulean-myc tagged RapR-Src-as2, iPEP-mCherry-FRB, and Stargazin-mVenus were imaged live. Stargazin-mVenus imaging was used to evaluate cell area and protrusive activity changes. Cells were treated with rapamycin (500 nM) (green arrow/line) and then treated with either DMSO (15 minutes) or 1NA-PP1 (250 nM) at the indicated time (red arrow/triangles). (A) Changes in cell area for a representative cell. (B) Quantification of cell area changes. (C) Quantification of changes in protrusive activity. Confidence intervals were omitted for clarity, but they are presented in Figure 3.14.

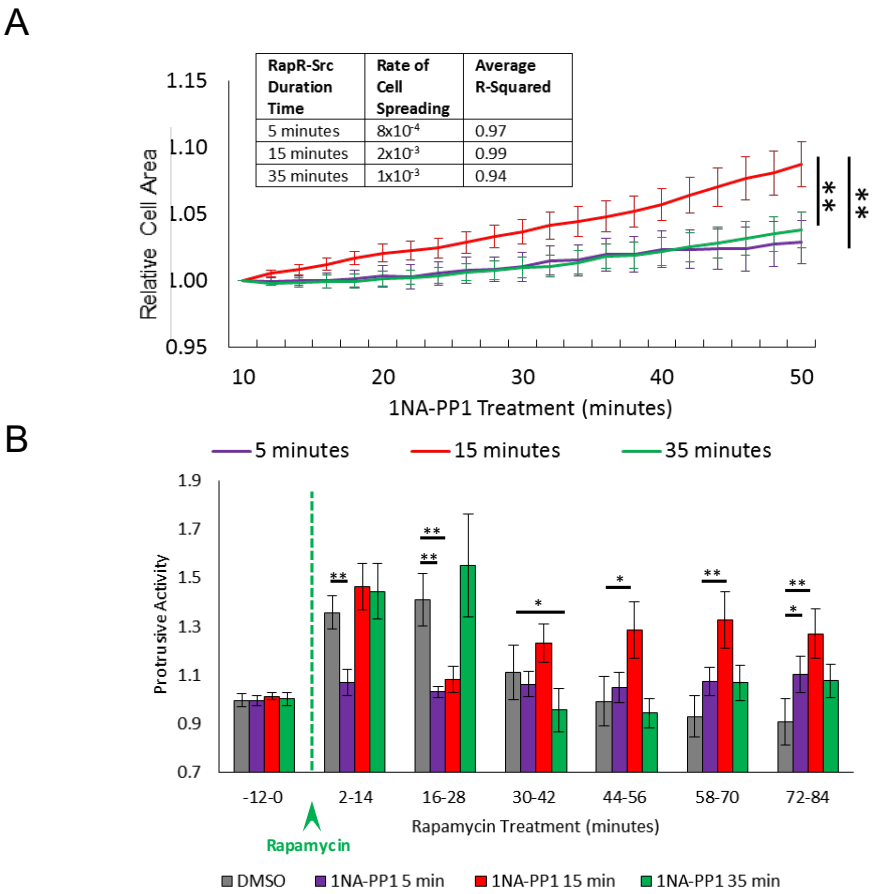

Figure 3.16: Regulation of Src mediated morphological changes
Hela cells transfected with: cerulean-myc tagged RapR-Src-as2, iPEP-mCherry-FRB, and Stargazin-mVenus were imaged live. Stargazin-mVenus imaging was used to evaluate cell area and protrusive activity changes. Cells were treated with rapamycin (500 nM) and then treated with either DMSO (15 minutes) or 1NA-PP1 (250 nM) at the indicated time. (A) Cell spreading rates following inactivation of RapR-Src-as2 (10 to 50 minutes post-1NA-PP1 treatment) in cells where Src was activated for 5, 15, and 35 minutes. The average correlation coefficients (R-squared) for relative cell area versus time are based on individual cells in each experiment. R-squared values close to 1 suggest a linear relationship between cell spreading and time. (B) Average protrusive activity over 12-minute time intervals, standardized by average protrusive activity before addition of rapamycin, a two-sample T-Test was used for comparisons between the 3 sample groups. All error bars/shading represent 90 percent confidence intervals; *p<0.05, **p<0.005.

kinase signaling, we identified conditions optimal for the induction of specific morphological changes independent of continuous kinase activation.

Dissecting Src-mediated signaling pathways using engineered transient activation of Src

Our results suggest that transient Src activation induces additional signaling pathways capable of stimulating slow cell spreading and protrusive activity independently of Src activity. Slow spreading that follows transient Src activation could be mediated by increased formation of membrane protrusions. One of the key pathways for stimulation of membrane protrusions is signaling through small GTPase Rac1[178,179]. To determine changes in Rac1 activity mediated by regulation of RapR-Src-as2 we employed previously described biosensor for Rac1[116,170,180] (Figure 3.1). Our studies show that activation of RapR-Src-as2 leads to robust stimulation of Rac1 at the cell periphery (Figure 3.17). Inactivation of RapR-Src-as2 caused fast downregulation of Rac1 activity that was partially restored at the later time points (Figure 3.17). Importantly, secondary increase in Rac1 activity following 1NA-PP1 treatment occurred concurrently with the increase in protrusive activity (Figures 3.14d; 3.15c, 3.16b). These data demonstrate regulation of Rac1 by RapR-Src-as2 and show a dynamic correlation between Src-induced changes in Rac1 activity and cell morphodynamics.

To test the role of Rac1-induced protrusive activity we treated cells with an inhibitor of Rac1 activation, CAS 1177865-17-6[181]. Rac1 inhibition at the time of Src inactivation suppresses protrusive activity (Fig. 3.18a and b). However, inhibition of protrusive activity did not affect cell spreading that followed transient Src activation (Figure 13.18c). Strikingly, inhibition of Rac1 at the time of Src activation had the opposite effect: protrusive activity was not affected,

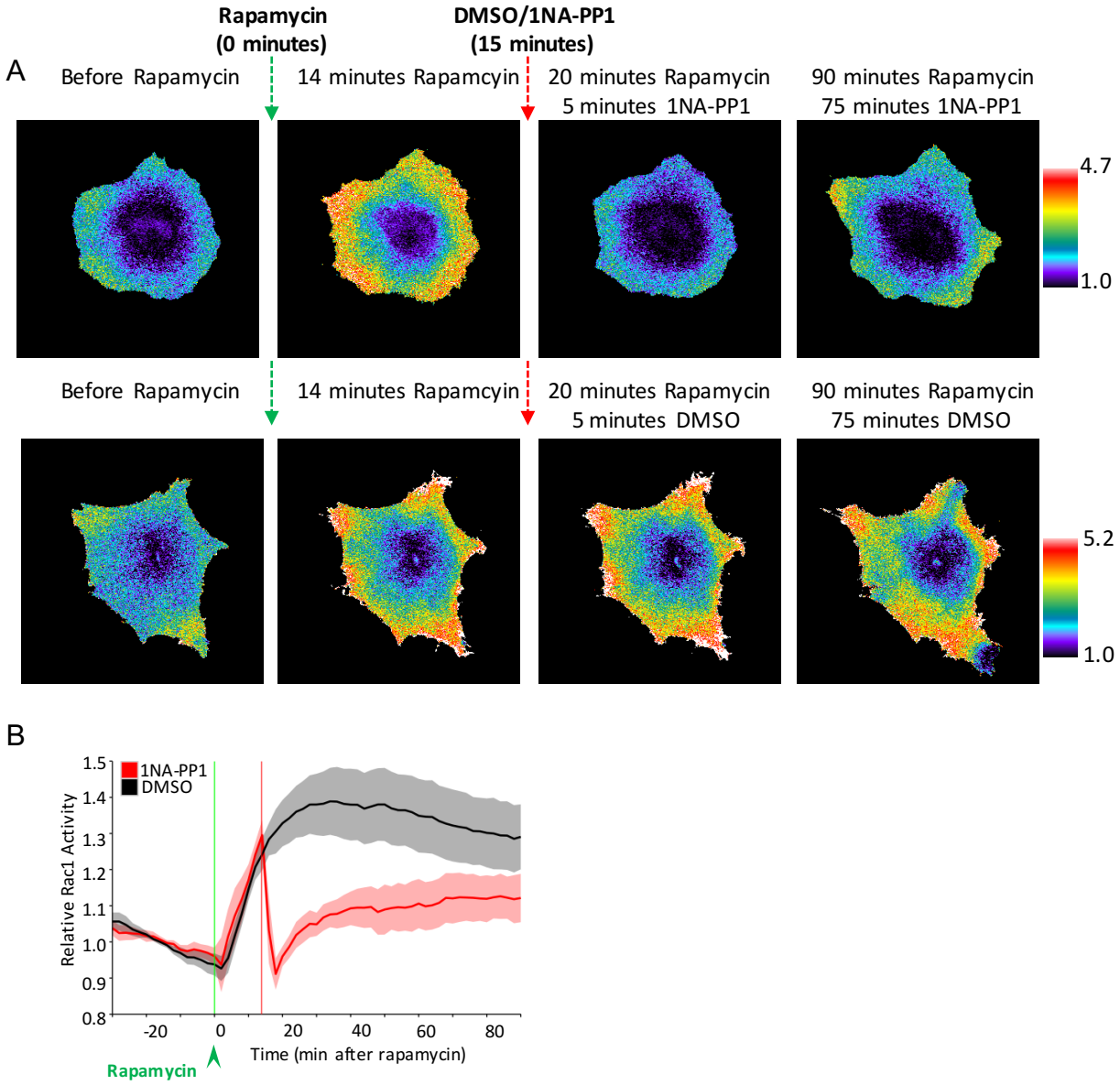

Figure 3.17: Regulation of Rac1 activity by RapR-Src-as2
HeLa cells transfected with RapR-Src-as2-mCherry-myc, Rac1 FLARE biosensor, and infected with adenovirus expressing iPEP-GFP(Y66S)-FRB (non-fluorescent GFP mutant) were imaged live. Cells were treated with rapamycin (500 nM) (green line) and 15 minutes later cells were treated with either DMSO (solvent) or 1NA-PP1 (250 nM). (A) Rac1 activity assessed via Rac1 FLARE biosensor (FRET/CFP signal) in cells upon either transient activation (1NA-PP1 treated, top panel) or prolonged activation (DMSO treated, bottom panel) of Src. Color scales show dynamics range of FRET/CFP signal ratio. (B) Quantification of Rac1 activity over time. Shading represents 90 percent confidence intervals.

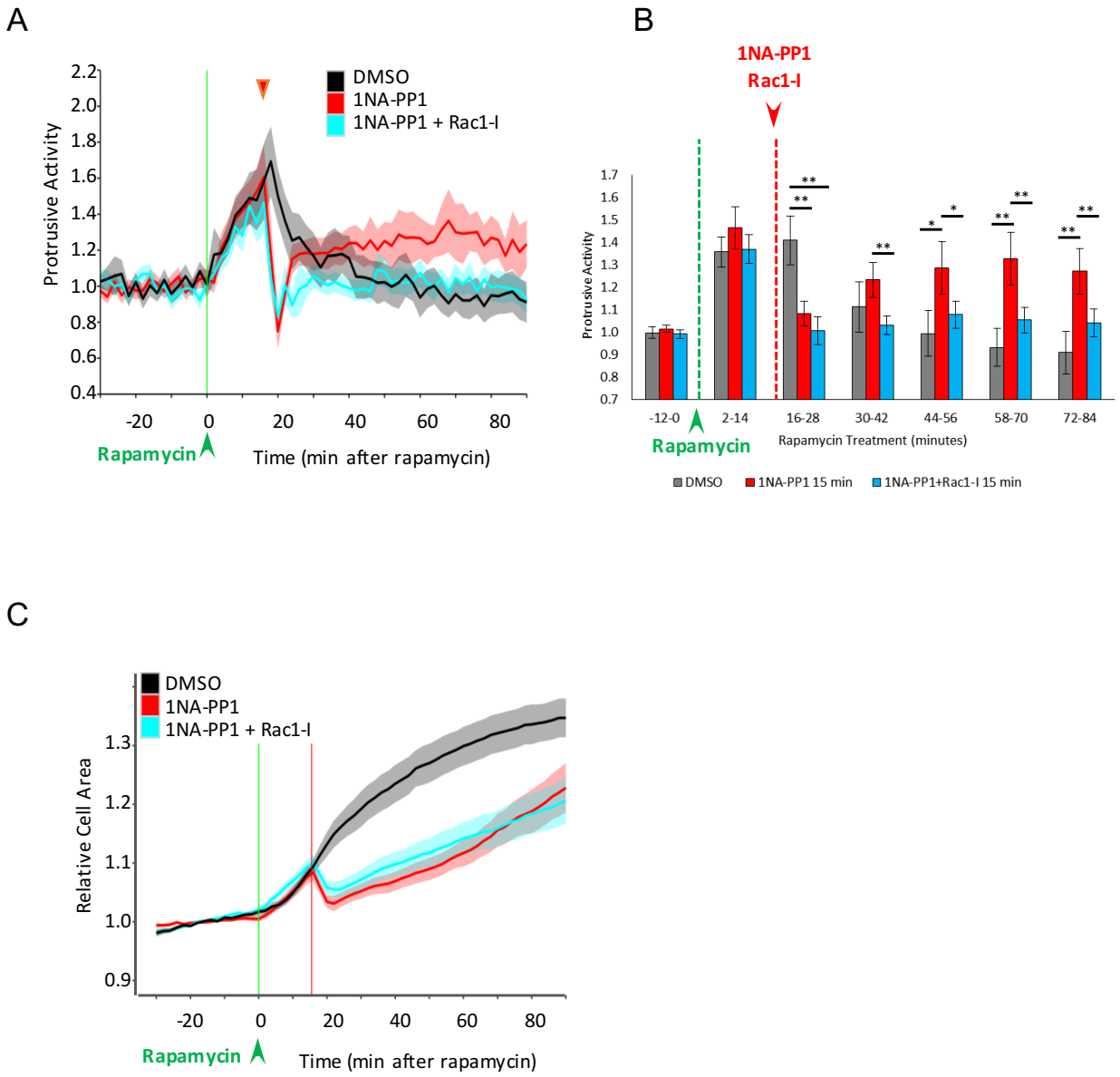

Figure 3.18: Effect of Rac1 inhibition on Src induced morphological changes
Effect of Rac1 inhibition on Src mediated (A and B) protrusive activity and (C) cell spreading. HeLa cells transfected with: RapR-Src-as2-cerulean-myc, iPEP-mCherry-FRB, and Stargazin-mVenus were imaged live. Stargazin-mVenus images were used to assess cell area and protrusive activity. (A and C) Cells were treated with rapamycin (500 nM) (green line), and 15 minutes later cells were treated with either DMSO (solvent), 1NA-PP1 (250 nM), or 1NA-PP1+Rac1-I (1NA-PP1+CAS 1177865-17-6, 250 nM + 100 µM) as indicated by red triangle or line. (B) Statistical analysis of protrusive activity averaged over 12 minute intervals. A two-sample T-Test was used compare the amount of protrusive activity between the three different treatment groups. All error bars/shading represent 90 percent confidence intervals; *p<0.05, **p<0.005.

whereas cell spreading was significantly inhibited (Figures 3.19a-d). Inhibition of Rac1 15 minutes after activation of Src did not have a significant effect on either cell spreading or protrusive activity, suggesting that during Src activation, Rac1 is only needed to maintain the initial rate of spreading (Figures 3.19a-d). These data demonstrate that Rac1 plays different roles during Src activation and following transient stimulation of Src (Figure 3.20). During Src activation Rac1 activity is important for cell spreading at the initial stages, but it is not involved in increased protrusion formation and it is dispensable for cell spreading at the later stages. Following Src inactivation, Rac1 mediates increased membrane protrusion formation, but it is dispensable for cell spreading.

Our data suggest that signaling events upstream of Rac1 control cell spreading that follows transient activation of Src. The PI3-kinase/AKT pathway is known to be stimulated by Src and plays an important role in the regulation of cell morphology[115,182]. PI3-kinase (PI3K) also stimulates Rac1 and membrane protrusions[183–185]. Furthermore, the PI3K/AKT pathway can induce cell spreading independently of Src[182]. We detected a significant increase in AKT phosphorylation following activation of RapR-Src-as2 indicating stimulation of PI3K/AKT signaling[186–188] (Figure 3.21a). Cells lacking RapR-Src-as2 did not exhibit changes in AKT phosphorylation after rapamycin treatment, verifying that PI3K/AKT stimulation was specific to the activation of Src (Figure 3.21b). AKT phosphorylation was not affected by treatment with 1NA-PP1, suggesting that transient activation of Src induces sustained PI3K/AKT signaling following Src inactivation (Figure 3.21a). To elucidate dynamic changes in PI3K activity in living cells we monitored distribution of AKT pleckstrin homology (PH) domain upon activation and inactivation of RapR-Src-as2. Previous studies demonstrated that translocation of AKT PH domain from cytoplasmic/perinuclear to peripheral/plasma membrane re-localization indicate

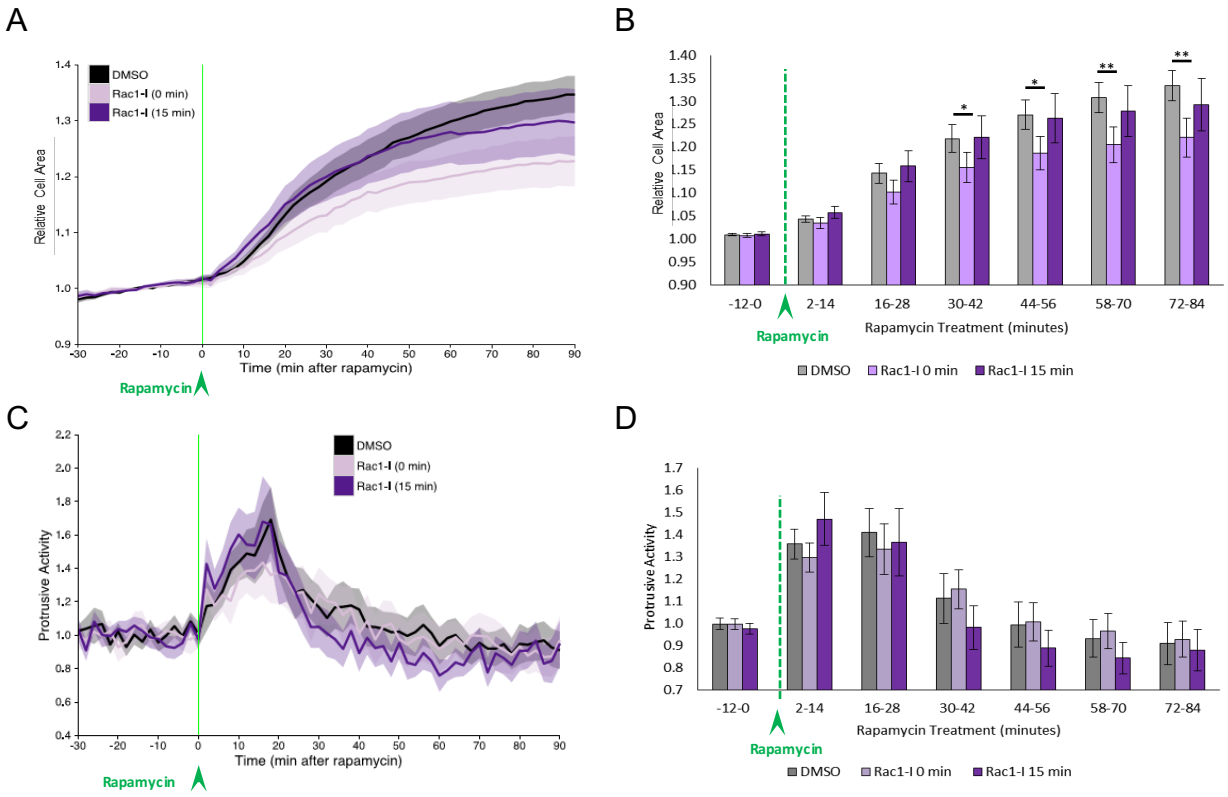

Figure 3.19: Src and Rac1 mediated morphological changes
HeLa cells, transfected with: RapR-Src-as2-cerulean-myc, iPEP-mCherry-FRB, and Stargazin-mVenus, were imaged live. Cell area (A and B) and protrusive activity (C and D) were analyzed using Stargazin-mVenus images. Cells were treated with: DMSO 15 minutes post rapamycin (500 nM) (DMSO), Rac1-I (CAS 1177865-17-6) (100 µM) simultaneously with rapamycin (500 nM) (Rac1-I 0 min), or with Rac1-I (CAS 1177865-17-6) (100 µM) 15 minutes post rapamycin treatment (500 nM) (Rac1-I 15 min). (B and D) A two-sample T-Test was used compare the DMSO treated cells with the two groups of Rac1-I treated cells, cells were averaged over 12 minute intervals. All error bars/shading represent 90 percent confidence intervals; *p<0.05, **p<0.005.

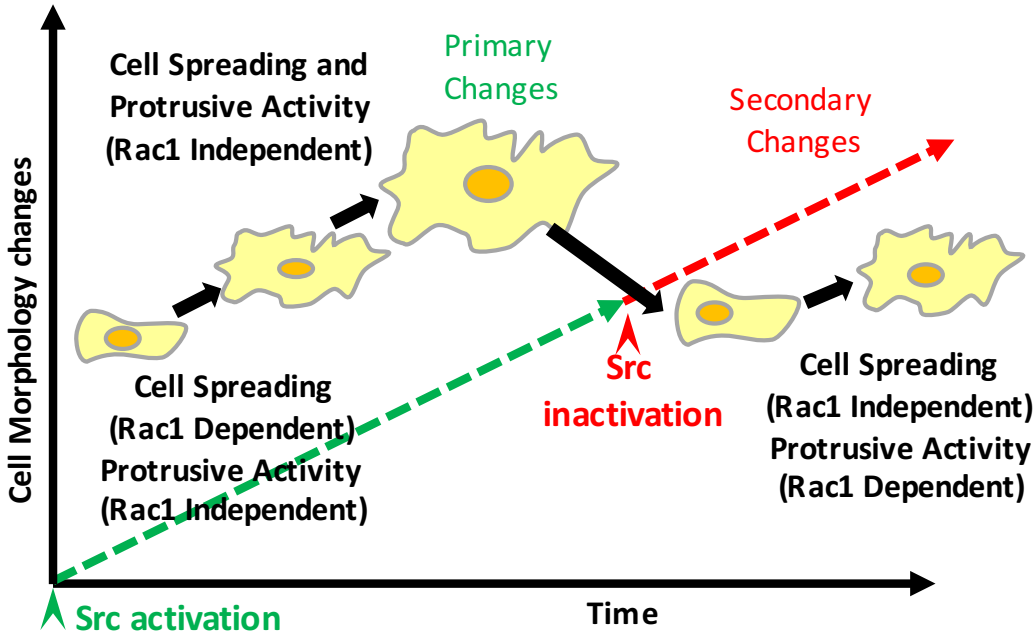

Figure 3.20: The role of Rac1 in the regulation of Src mediated morphological changes
Schematic depicting different roles for Rac1 signaling at different stages upon transient/prolonged activation of Src.

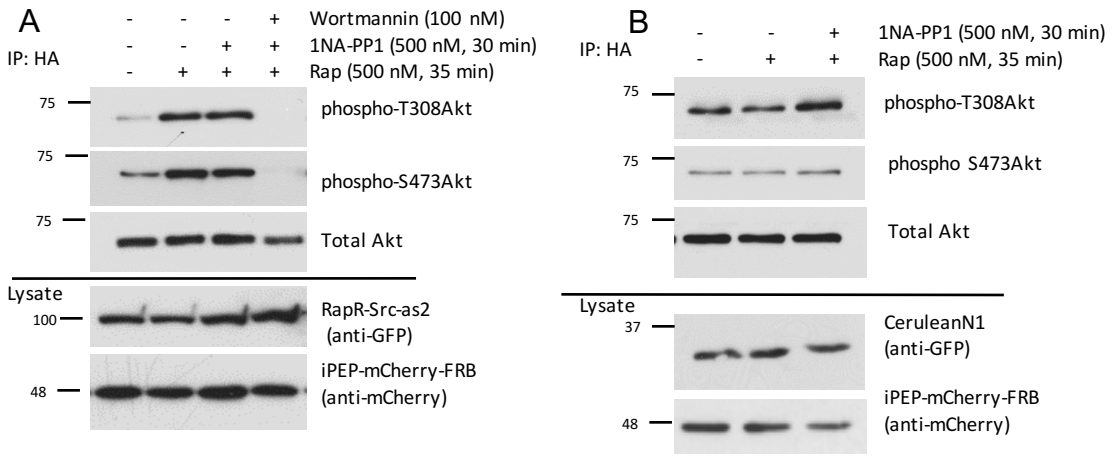

Figure 3.21: PI3K remains active following Src inactivation
Activation of PI3K signaling was assessed by phosphorylation levels and localization of AKT. LinXE cells co-expressing cerulean-myc tagged RapR-Src-as2, iPEP-mCherry-FRB, and HA-Akt were treated with rapamycin (500 nM) or ethanol (solvent) and then with either 1NA-PP1 (500 nM), 1NA-PP1 + Wortmannin (500 nM, 100 nM), or DMSO. HA-AKT was immunoprecipitated via its HA-tag and analyzed for phosphorylation at Thr308 and Ser473. Data is representative of three independent experiments.

production of phosphatidylinositol (3,4,5) trisphosphate PtdIns(3,4,5)P_3 generated by activated PI3K[189] (Figure 3.2). Our results show that activation of RapR-Src-as2 stimulates redistribution of AKT PH domain from perinuclear to peripheral location supporting our biochemical evidence demonstrating PI3K activation (Figure 3.22). Subsequent inactivation of RapR-Src-as2 leads to transient perinuclear accumulation of AKT PH domain that is followed by redistribution to the cell periphery (Figure 3.22). Quantitative analysis of AKT PH domain localization supports this observation (Figure 3.22b), and suggests that transient activation of RapR-Src-as2 is followed by partial reduction in PtdIns(3,4,5)P_3 levels that is later restored. Interestingly, dynamics of AKT PH domain localization mirrors the changes observed in cell spreading (Figures 3.15b; 3.16a; 3.22b) demonstrating correlation between PI3K signaling and Src-induced morphological changes.

To test if PI3K/AKT pathway mediates cell spreading after Src inhibition, HeLa cells were treated with the PI3K inhibitors Wortmannin and LY294002[190,191]. Addition of these inhibitors at the same time as 1NA-PP1 dramatically reduced AKT phosphorylation, abolished cell spreading, and reduced protrusive activity after Src inactivation (Figures 3.21a; 3.23a-d). These data demonstrate that transient activation of Src induces downstream PI3K/AKT signaling, which mediates cell spreading after Src inactivation. Thus, this new approach for Src kinase activation enabled us to define the role of sequential Src-PI3K signaling in the regulation of cell morphology. We also found that PI3K plays different roles during Src activation. Inhibition of PI3K at the time of Src activation prevented Src-mediated cell spreading and delayed stimulation of protrusive activity (Figures 3.24a-d). Addition of PI3K inhibitor 15 minutes after Src activation had no effect on either cell spreading or protrusive activity (Figures

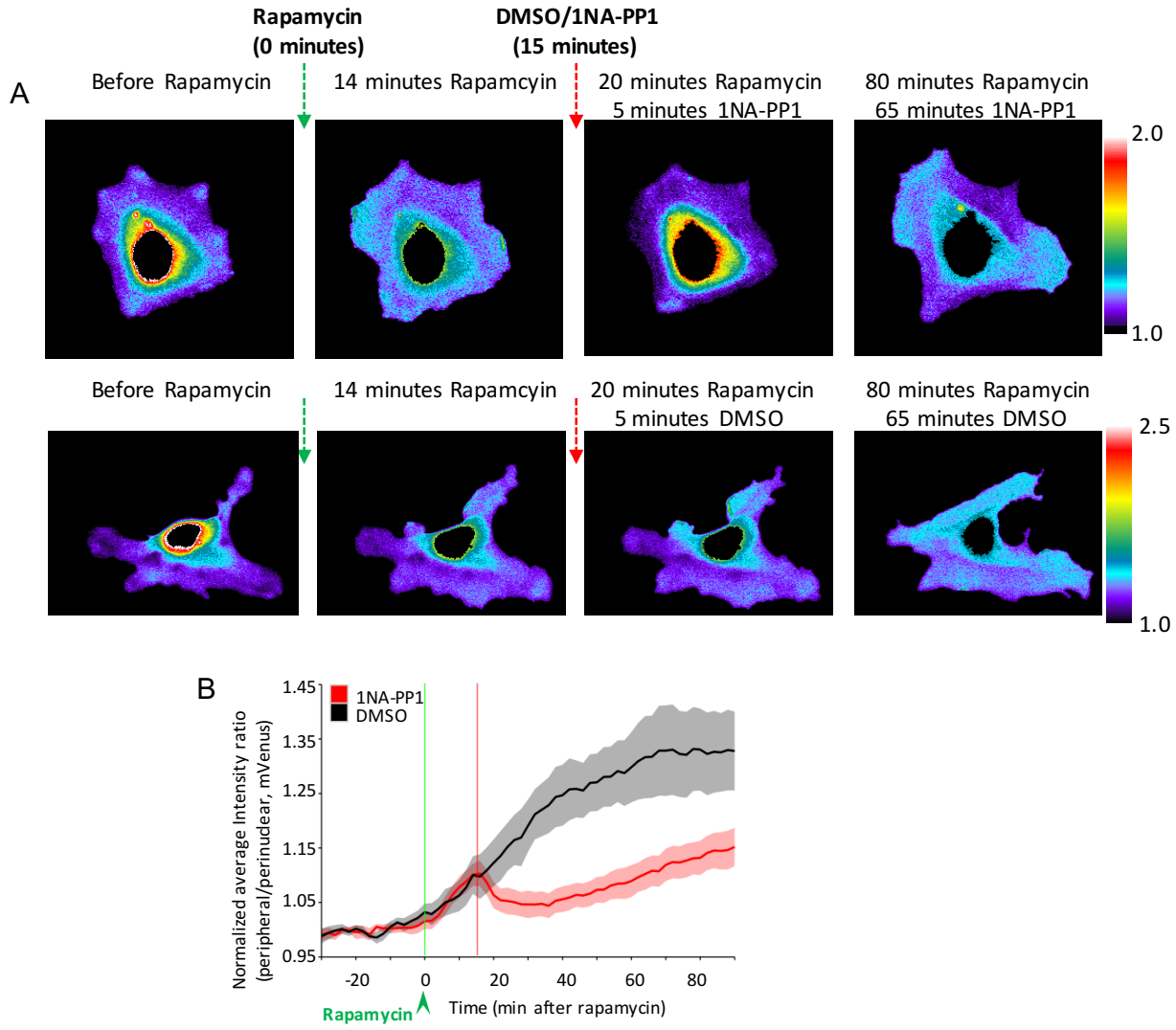

Figure 3.22: Regulation of PI3K signaling by RapR-Src-as2

HeLa cells, infected with an adenovirus expressing RapR-Src-as2-cerulean-myc and transfected with mVenus-PH-AKT and iPEP-mCherry-FRB, were imaged live. Cells were treated with rapamycin (500 nM) (green line) and 15 minutes later cells were treated with either DMSO (solvent) or 1NA-PP1 (250 nM) (red line). (A) Localization of mVenus-PH-AKT upon either transient activation (1NA-PP1 treated, top panel) or prolonged activation (DMSO treated, bottom panel) Src activation. The nucleus was masked to show changes in perinuclear/peripheral localization. Color scale bar shows dynamic range of mVenus fluorescence signal. (B) Quantification of mVenus-PH-AKT localization over time. Shading represents 90 percent confidence intervals.

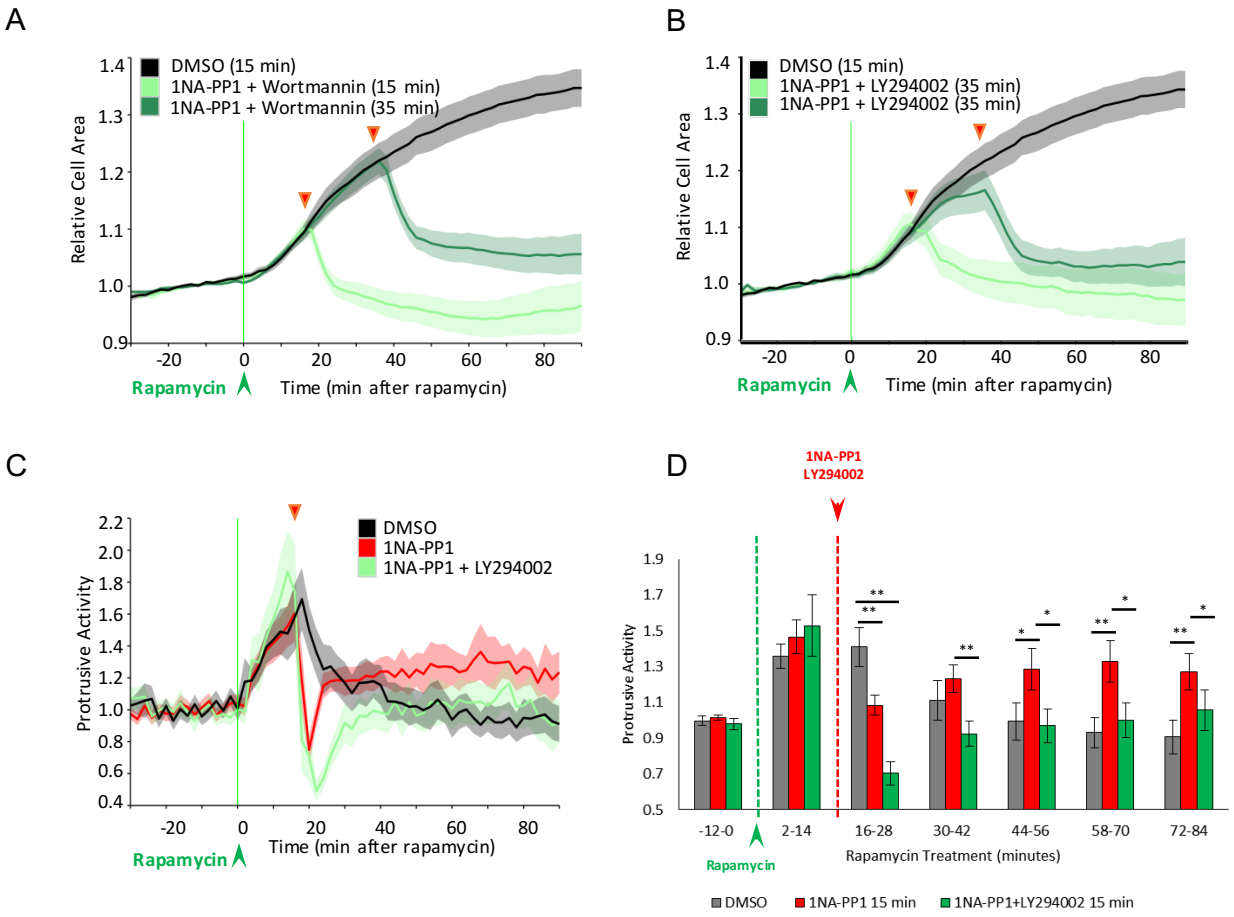

Figure 3.23: Effect of PI3K inhibition on Src induced morphological changes
Effect of PI3K inhibitor on (A and B) cell spreading and (C and D) protrusive activity. (A-D) HeLa cells transfected with: RapR-Src-as2-cerulean-myc, iPEP-mCherry-FRB, and Stargazin-mVenus were imaged live before and after the addition of rapamycin (green line). Stargazin-mVenus images were used to evaluate changes in cell area and protrusive activity. (A) Cells were treated with DMSO (solvent) or 1NA-PP1+Wortmannin (250 nM, 100 nM) at the indicated time points (red triangles) after addition of rapamycin. (B) Cells were treated with DMSO (solvent) or 1NA-PP1+LY294002 (250 nM, 50 µM) at the indicated time points (red triangles) after addition of rapamycin. (C and D) Cells were treated with the DMSO (solvent), 1NA-PP1 (250 nM), or 1NA-PP1+LY294002 (250 nM + 50 µM) (red triangle) 15 minutes after rapamycin treatment. (D) Statistical analysis of protrusive activity averaged over 12 minute intervals. A two-sample T-Test was used compare the amount of protrusive activity between the three different treatment groups. All error bars/shading represent 90 percent confidence intervals; *p<0.05, **p<0.005.

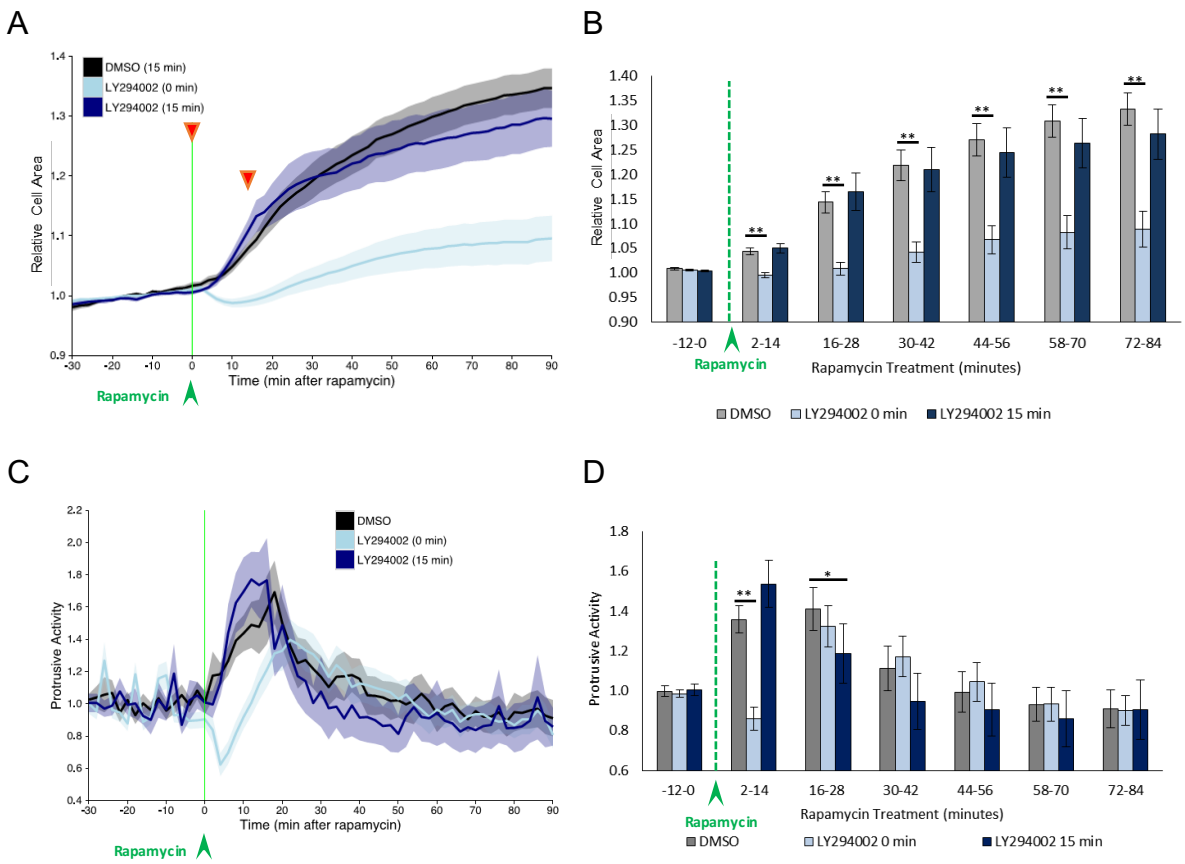

Figure 3.24: Src and PI3K mediated morphological changes
HeLa cells, transfected with: RapR-Src-as2-cerulean-myc, iPEP-mCherry-FRB, and Stargazin-mVenus, were imaged live. Cell area (A and B) and protrusive activity (C and D) were analyzed using Stargazin-mVenus images. Cells were treated with: DMSO 15 minutes post rapamycin (500 nM) (DMSO), LY294002 (50 µM) simultaneously with rapamycin (500 nM) (LY294002 0 min), or with LY294002 (50 µM) 15 minutes post rapamycin treatment (500 nM) (LY294002 15 min). (B and D) A two-sample t-test was used compare the DMSO treated cells with the two groups of LY294002 treated cells, the cells were averaged over 12 minute intervals. All error bars/shading represent 90 percent confidence intervals; *p<0.05, **p<0.005.

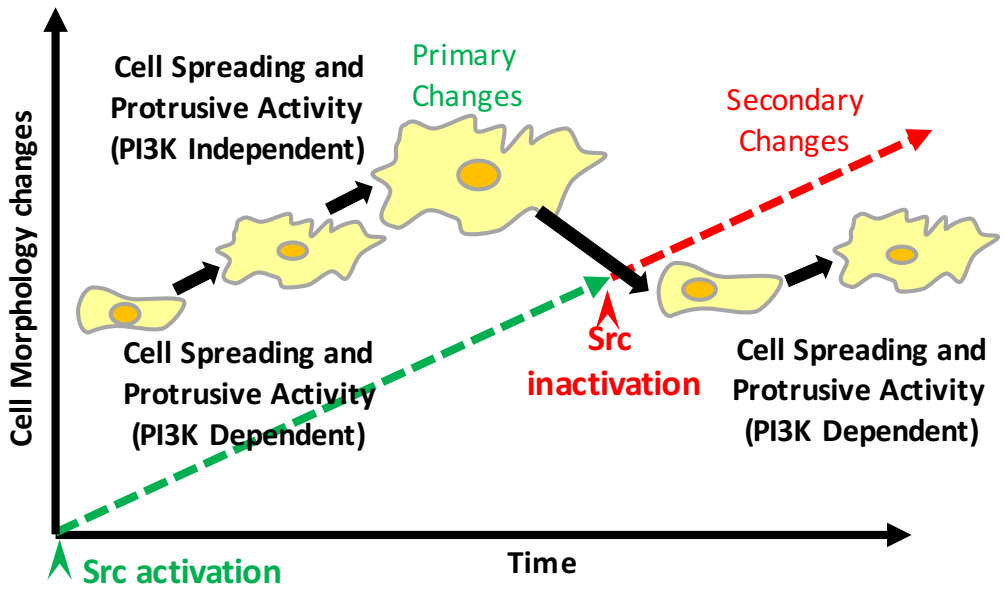

Figure 3.25: The role of PI3K in the regulation of Src mediated morphological changes
Schematic depicting different roles for PI3K signaling at different stages upon transient/prolonged activation of Src.

3.24a-d). Combined, our data suggest that PI3K plays different roles at three different stages during transient Src activation (Figure 3.25). At the time of Src activation PI3K is required for stimulation of cell spreading and protrusive activity. Once Src has been active for at least 15 minutes, PI3K becomes dispensable for Src-mediated morphological changes. Following Src inactivation, PI3K takes control of secondary morphological changes.

3.4 Discussion

Our results describe a new approach for transient activation of kinases in living cells. This method enables the precise temporal regulation of kinase activation and inactivation. Furthermore, this method allows for control of the duration of kinase activation and identification of optimal conditions for specific kinase-induced morphological effects. Using this approach, we identified distinct roles for Rac1 and PI3K signaling in mediating Src-induced morphological changes during Src activation and following its inactivation. By regulating Src catalytic activity in complex with paxillin and p38 activity in complex with ATF2 we demonstrated that this approach allows us to induce transient activation of specific signaling complexes. Successful regulation Tyr kinase Src and serine/threonine kinase p38 suggests that this strategy could be broadly applicable for regulation of different kinases.

Current strategies for manipulation of kinase activity are primarily limited to either activation or inactivation of a kinase. We have developed a novel approach that enables precise control of both aspects of kinase function. Previous studies suggest broad applicability of this strategy for regulation of kinases in living cells. Analog sensitive approach has been successfully employed for more than eighty different kinases from different classes and different species[125]. RapR analogs of six different Tyr and Ser/Thr kinases have been reported[137]. Importantly, activation and inactivation directly targets the catalytic domain without affecting other functions

of the protein[137,131,90]. The main components of this system are genetically encoded and regulation is achieved by using cell permeable compounds. Our previous studies show that activation of RapR-kinases can be achieved using non-immunosuppressive analogs of rapamycin[137,131]. Because 1NA-PP1 has very low affinity towards endogenous kinases, this approach will have minimal off-target effects on endogenous signaling pathways[122–130].

We demonstrate that this new approach for regulating kinases can be used to dissect dynamics of signaling processes mediated by transient kinase activation. Our studies show the changes in Rac1 activity following inactivation of Src emulated changes in protrusive activity (Figures 3.14d; 3.15c; 3.16b; 3.17b). Interestingly, changes in activity of PI3K occurred with slower kinetics, and mirrored changes in cell spreading (Figures 3.15c; 3.16a; 3.22b). Also, inactivation of Src induced only partial reduction in PI3K activity. We show that PI3K signaling is required for Rac1-mediated increase in protrusive activity (Figure 3.23c and d), suggesting that PI3K activity remaining after inactivation of Src regulates secondary activation of Rac1. However, faster kinetics of Rac1 regulation indicates that parallel signaling pathways also contribute to this process. These data suggest a potential mechanism where PI3K regulates overall restoration of Rac1 activity following Src inactivation, whereas other factors, such as GTPase activating proteins and GTPase exchange factors, control fast dynamic changes of Rac1 activity.

Our studies show that the same signaling component can play different roles at different stages during kinase activation and following its inactivation. Upon Src activation Rac1 signaling preferentially affects cell spreading and not protrusive activity suggesting that at the initial stage of Src activation, Rac1 is more important for establishing cell contacts with the extracellular matrix. This result correlates with previously reported observations of Rac1-

independent protrusion formation in MTLn3 and Rac1-dependent focal adhesion formation and migration[192–194]. Our results show that the function of PI3K is important for Src-induced cell spreading and protrusive activity upon Src activation and following its inactivation. However, neither Rac1 nor PI3K activity was critical at later stages during Src activation (15 minutes) suggesting that prolonged activation can drive morphological transformation independently of Rac1 and PI3K. This is in agreement with previously reported studies showing that inhibition of PI3K signaling does not block v-Src-induced transformation[195]. A different report suggests that Rac1 activity is required for v-Src-mediated transformation[196]. However, in these experiments dominant negative Rac1 was co-transfected together with v-Src supporting our evidence that inhibition of Rac1 at the time of Src activation suppresses Src-induced morphological changes.

Nearly all eukaryotic physiological events are regulated by protein kinases. Aberrations in function of different kinases are linked to numerous diseases. Significant progress has been made in dissecting the role of many kinases. However, understanding how specific kinases orchestrate complex signaling events remains challenging. The method we present here allows for the ability to control the timing and the duration of kinase activity. This system provides the ability to mimic physiologically relevant transient activation of a kinase.

3.5 Supplementary Index

A. mCherry Mega Primer

GTGAGCAAGGGCGAGGAGGATAACATGGCCATCATCAAGGAGTTCATGCGCTTCAAGGTGCACATGGAG
GGCTCCGTGAACGGCCACGAGTTCGAGATCGAGGGCGAGGGCGAGGGCCGCCCCTACGAGGGCACCCAG
ACCGCCAAGCTGAAGGTGACCAAGGGTGGCCCCCTGCCCTTCGCCTGGGACATCCTGTCCCCTCAGTTCA
TGTACGGCTCCAAGGCCTACGTGAAGCACCCCGCCGACATCCCCGACTACTTGAAGCTGTCCTTCCCCGA
GGGCTTCAAGTGGGAGCGCGTGATGAACTTCGAGGACGGCGGCGTGGTGACCGTGACCCAGGACTCCTC
CCTGCAGGACGGCGAGTTCATCTACAAGGTGAAGCTGCGCGGCACCAACTTCCCCTCCGACGGCCCCGTA
ATGCAGAAGAAGACCATGGGCTGGGAGGCCTCCTCCGAGCGGATGTACCCCGAGGACGGCGCCCTGAAG
GGCGAGATCAAGCAGAGGCTGAAGCTGAAGGACGGCGGCCACTACGACGCTGAGGTCAAGACCACCTA
CAAGGCCAAGAAGCCCGTGCAGCTGCCCGGCGCCTACAACGTCAACATCAAGTTGGACATCACCTCCCA
CAACGAGGACTACACCATCGTGGAACAGTACGAACGCGCCGAGGGCCGCCACTCCACCGGCGGCATGGA
CGAGCTGTACAAG

B. RapR-Src-Cat-cerulean-myc Mega Primer

FORWARD: GAGCGGCCGCCACTGTGCTGGATCATGGGAGATGCGTGGGAGATCCCCCGGGAGTCCCTG
REVERSE: CAGGGACTCCCGGGGGATCTCCCACGCATCTCCCATGATCCAGCACAGTGGCGGCCGCTC

C. CA-Src primers

FORWARD: CTTTACGTCCACTGAGCCACAGTTCCAGCCCGGGGAGAACCTATAGGG
REVERSE: CCCTATAGGTTCTCCCCGGGCTGGAACTGTGGCTCAGTGGACGTAAAG

D. T338A primers

FORWARD: GTGTCGGAAGAACCCATTTACATTGTG**GCA**GAGTACATGAACAAGGGGAGTCTGCTGGAC
REVERSE: GTCCAGCAGACTCCCCTTGTTCATGTACTC**TGC**CACAATGTAAATGGGTTCTTCCGACAC

E. mVenus Mega Primer

GTGAGCAAGGGCGAGGAGCTGTTCACCGGGGTGGTGCCCATCCTGGTCGAGCTGGACGGCGACGTAAAC
GGCCACAAGTTCAGCGTGTCCGGCGAGGGCGAGGGCGATGCCACCTACGGCAAGCTGACCCTGAAGTTG
ATCTGCACCACCGGCAAGCTGCCCGTGCCCTGGCCCACCCTCGTGACCACCCTCGGCTACGGCCTGCAGT
GCTTCGCCCGCTACCCCGACCACATGAAGCAGCACGACTTCTTCAAGTCCGCCATGCCCGAAGGCTACGT
CCAGGAGCGCACCATCTTCTTCAAGGACGACGGCAACTACAAGACCCGCGCCGAGGTGAAGTTCGAGGG
CGACACCCTGGTGAACCGCATCGAGCTGAAGGGCATCGACTTCAAGGAGGACGGCAACATCCTGGGGCA
CAAGCTGGAGTACAACTACAACAGCCACAACGTCTATATCACCGCCGACAAGCAGAAGAACGGCATCAA
GGCAAACTTCAAGATCCGCCACAACATCGAGGACGGCGGCGTGCAGCTCGCCGACCACTACCAGCAGAA
CACCCCCATCGGCGACGGCCCCGTGCTGCTGCCCGACAACCACTACCTGAGCTACCAGTCCAAACTGAGC
AAAGACCCCAACGAGAAGCGCGATCACATGGTCCTGCTGGAGTTCGTGACCGCCGCCGGGATCACTCTC
GGCATGGACGAGCTGTACAAG

F. iPEP Mega Primer

TCAGATCCGCTAGCGCTACCGGTCGCCACCATGGGAGTGCAGGTGGAGACTATCTCCCCAGGAGACGGG
CGCACCTTCGGTAGCGGCTCTGGTTCCGGTAGTGGCAGCATGGTGAGCAAGGGCGAGGAGCTGTTCACC

G. CMV-Flag Mega Primer

GTAATCAATTACGGGGTCATTAGTTCATAGCCCATATATGGAGTTCCGCGTTACATAACTTACGGTAAAT
GGCCCGCCTGGCTGACCGCCCAACGACCCCCGCCCATTGACGTCAATAATGACGTATGTTCCCATAGTAA
CGCCAATAGGGACTTTCCATTGACGTCAATGGGTGGAGTATTTACGGTAAACTGCCCACTTGGCAGTACA
TCAAGTGTATCATATGCCAAGTACGCCCCCTATTGACGTCAATGACGGTAAATGGCCCGCCTGGCATTAT
GCCCAGTACATGACCTTATGGGACTTTCCTACTTGGCAGTACATCTACGTATTAGTCATCGCTATTACCAT
GGTGATGCGGTTTTGGCAGTACATCAATGGGCGTGGATAGCGGTTTGACTCACGGGGATTTCCAAGTCTC
CACCCCATTGACGTCAATGGGAGTTTGTTTTGGCACCAAAATCAACGGGACTTTCCAAAATGTCGTAACA
ACTCCGCCCCATTGACGCAAATGGGCGGTAGGCGTGTACGGTGGGAGGTCTATATAAGCAGAGCTGGTTT
AGTGAACCGTCAGATCCGCTAGCACCATGGACTATAAGGACGATGATGACAAAATGGTGAGCAAGGGCG
AGGAG

H. GFP FRB Paxillin Mega Primer

GACGAGCTGTACAAGTCCGGACTCAGATCTGGCCCCGGATGGCATGAGATGTGGCATGAAGGCCTGGAA
GAGGCATCTCGTTTGTACTTTGGGGAAAGGAACGTGAAAGGCATGTTTGAGGTGCTGGAGCCCTTGCATG
CTATGATGGAACGGGGCCCCCAGACTCTGAAGGAAACATCCTTTAATCAGGCCTATGGTCGAGATTTAAT
GGAGGCCCAAGAGTGGTGCAGGAAGTACATGAAATCAGGGAATGTCAAGGACCTCCTCCAAGCCTGGGA
CCTCTATTATCATGTGTTCCGACGAATCTCAAAGACTAGTGGACCCGGTGCTCAAGCTTCGAATTCAGAC
GACCTCGACGCCC

I. CMV-iPEP-mVenus Mega Primer

GTAATCAATTACGGGGTCATTAGTTCATAGCCCATATATGGAGTTCCGCGTTACATAACTTACGGTAAAT
GGCCCGCCTGGCTGACCGCCCAACGACCCCCGCCCATTGACGTCAATAATGACGTATGTTCCCATAGTAA
CGCCAATAGGGACTTTCCATTGACGTCAATGGGTGGAGTATTTACGGTAAACTGCCCACTTGGCAGTACA
TCAAGTGTATCATATGCCAAGTACGCCCCCTATTGACGTCAATGACGGTAAATGGCCCGCCTGGCATTAT
GCCCAGTACATGACCTTATGGGACTTTCCTACTTGGCAGTACATCTACGTATTAGTCATCGCTATTACCAT
GGTGATGCGGTTTTGGCAGTACATCAATGGGCGTGGATAGCGGTTTGACTCACGGGGATTTCCAAGTCTC
CACCCCATTGACGTCAATGGGAGTTTGTTTTGGCACCAAAATCAACGGGACTTTCCAAAATGTCGTAACA
ACTCCGCCCCATTGACGCAAATGGGCGGTAGGCGTGTACGGTGGGAGGTCTATATAAGCAGAGCTGGTTT
AGTGAACCGTCAGATCCGCTAGCGCTACCGGTCGCCACCATGGGAGTGCAGGTGGAGACTATCTCCCCA
GGAGACGGGCGCACCTTCGGTAGCGGCTCTGGTTCCGGTAGTGGCAGCATGGTGAGCAAGGGCGAGGAG
CTGTTCACCGGGGTGGTGCCCATCCTGGTCGAGCTGGACGGCGACGTAAACGGCCACAAGTTCAGCGTGT
CCGGCGAGGGCGAGGGCGATGCCACCTACGGCAAGCTGACCCTGAAGTTGATCTGCACCACCGGCAAGC
TGCCCGTGCCCTGGCCCACCCTCGTGACCACCCTCGGCTACGGCCTGCAGTGCTTCGCCCGCTACCCCGA

CCACATGAAGCAGCACGACTTCTTCAAGTCCGCCATGCCCGAAGGCTACGTCCAGGAGCGCACCATCTTC
TTCAAGGACGACGGCAACTACAAGACCCGCGCCGAGGTGAAGTTCGAGGGCGACACCCTGGTGAACCGC
ATCGAGCTGAAGGGCATCGACTTCAAGGAGGACGGCAACATCCTGGGGCACAAGCTGGAGTACAACTAC
AACAGCCACAACGTCTATATCACCGCCGACAAGCAGAAGAACGGCATCAAGGCAAACTTCAAGATCCGC
CACAACATCGAGGACGGCGGCGTGCAGCTCGCCGACCACTACCAGCAGAACACCCCCATCGGCGACGGC
CCCGTGCTGCTGCCCGACAACCACTACCTGAGCTACCAGTCCAAACTGAGCAAAGACCCCAACGAGAAG
CGCGATCACATGGTCCTGCTGGAGTTCGTGACCGCCGCCGGGATCACTCTCGGCATGGACGAGCTGTACA
AG

J. T106A Primers

FORWARD: GGAATTCAATGACGTGTACCTGGTGGCCCATCTCATGGGGGCGGACCTGAACAACATC
REVERSE: GATGTTGTTCAGGTCCGCCCCCATGAGATGGGCCACCAGGTACACGTCATTGAATTCC

K. CMV-venus-ATF2 Mega Primer

GTGAGCAAGGGCGAGGAGCTGTTCACCGGGGTGGTGCCCATCCTGGTCGAGCTGGACGGCGACGTAAAC
GGCCACAAGTTCAGCGTGTCCGGCGAGGGCGAGGGCGATGCCACCTACGGCAAGCTGACCCTGAAGTTG
ATCTGCACCACCGGCAAGCTGCCCGTGCCCTGGCCCACCCTCGTGACCACCCTCGGCTACGGCCTGCAGT
GCTTCGCCCGCTACCCCGACCACATGAAGCAGCACGACTTCTTCAAGTCCGCCATGCCCGAAGGCTACGT
CCAGGAGCGCACCATCTTCTTCAAGGACGACGGCAACTACAAGACCCGCGCCGAGGTGAAGTTCGAGGG
CGACACCCTGGTGAACCGCATCGAGCTGAAGGGCATCGACTTCAAGGAGGACGGCAACATCCTGGGGCA
CAAGCTGGAGTACAACTACAACAGCCACAACGTCTATATCACCGCCGACAAGCAGAAGAACGGCATCAA
GGCAAACTTCAAGATCCGCCACAACATCGAGGACGGCGGCGTGCAGCTCGCCGACCACTACCAGCAGAA
CACCCCCATCGGCGACGGCCCCGTGCTGCTGCCCGACAACCACTACCTGAGCTACCAGTCCAAACTGAGC
AAAGACCCCAACGAGAAGCGCGATCACATGGTCCTGCTGGAGTTCGTGACCGCCGCCGGGATCACTCTC
GGCATGGACGAGCTGTACAAGGGACCAAGCTTGAGTGATGACAAACCCT

L. CMV-iPep-venus-FRB-ATF2 Mega Primer

GTGAGCAAGGGCGAGGAGCTGTTCACCGGGGTGGTGCCCATCCTGGTCGAGCTGGACGGCGACGTAAAC
GGCCACAAGTTCAGCGTGTCCGGCGAGGGCGAGGGCGATGCCACCTACGGCAAGCTGACCCTGAAGTTG
ATCTGCACCACCGGCAAGCTGCCCGTGCCCTGGCCCACCCTCGTGACCACCCTCGGCTACGGCCTGCAGT
GCTTCGCCCGCTACCCCGACCACATGAAGCAGCACGACTTCTTCAAGTCCGCCATGCCCGAAGGCTACGT
CCAGGAGCGCACCATCTTCTTCAAGGACGACGGCAACTACAAGACCCGCGCCGAGGTGAAGTTCGAGGG
CGACACCCTGGTGAACCGCATCGAGCTGAAGGGCATCGACTTCAAGGAGGACGGCAACATCCTGGGGCA
CAAGCTGGAGTACAACTACAACAGCCACAACGTCTATATCACCGCCGACAAGCAGAAGAACGGCATCAA
GGCAAACTTCAAGATCCGCCACAACATCGAGGACGGCGGCGTGCAGCTCGCCGACCACTACCAGCAGAA
CACCCCCATCGGCGACGGCCCCGTGCTGCTGCCCGACAACCACTACCTGAGCTACCAGTCCAAACTGAGC
AAAGACCCCAACGAGAAGCGCGATCACATGGTCCTGCTGGAGTTCGTGACCGCCGCCGGGATCACTCTC
GGCATGGACGAGCTGTACAAGTCCGGACTCAGATCTCGAGCTCAAGCTTCGAATTCAATGGCTTCTAGAA
TCCTCTGGCATGAGATGTGGCATGAAGGCCTGGAAGAGGCATCTCGTTTGTACTTTGGGGAAAGGAACGT
GAAAGGCATGTTTGAGGTGCTGGAGCCCTTGCATGCTATGATGGAACGGGGCCCCCAGACTCTGAAGGA
AACATCCTTTAATCAGGCCTATGGTCGAGATTTAATGGAGGCCCAAGAGTGGTGCAGGAAGTACATGAA
ATCAGGGAATGTCAAGGACCTCCTCCAAGCCTGGGACCTCTATTATCATGTGTTCCGACGAATCTCAAAG
ACTAGTGGACCAAGCTTGAGTGATGACAAACCCTTTCTATGCAC

M. GFP(Y66S) Mega Primer

GTGAGCAAGGGCGAGGAGCTGTTCACCGGGGTGGTGCCCATCCTGGTCGAGCTGGACGGCGACGTAAAC
GGCCACAAGTTCAGCGTGTCCGGCGAGGGCGAGGGCGATGCCACCTACGGCAAGCTGACCCTGAAGTTC
ATCTGCACCACCGGCAAGCTGCCCGTGCCCTGGCCCACCCTCGTGACCACCCTGACCTCCGGCGTGCAGT
GCTTCAGCCGCTACCCCGACCACATGAAGCAGCACGACTTCTTCAAGTCCGCCATGCCCGAAGGCTACGT
CCAGGAGCGCACCATCTTCTTCAAGGACGACGGCAACTACAAGACCCGCGCCGAGGTGAAGTTCGAGGG
CGACACCCTGGTGAACCGCATCGAGCTGAAGGGCATCGACTTCAAGGAGGACGGCAACATCCTGGGGCA
CAAGCTGGAGTACAACTACAACAGCCACAACGTCTATATCATGGCCGACAAGCAGAAGAACGGCATCAA
GGTGAACTTCAAGATCCGCCACAACATCGAGGACGGCAGCGTGCAGCTCGCCGACCACTACCAGCAGAA
CACCCCCATCGGCGACGGCCCCGTGCTGCTGCCCGACAACCACTACCTGAGCACCCAGTCCGCCCTGAGC
AAAGACCCCAACGAGAAGCGCGATCACATGGTCCTGCTGGAGTTCGTGACCGCCGCCGGGATCACTCTC
GGCATGGACGAGCTGTACAAG

CHAPTER 4: FUTURE DIRECTIONS

4.1 Summary of objectives

In chapter 2, our objective was to investigate how direct activation of the non-receptor tyrosine kinase c-Src (Src) affected the endothelial cell barrier. The direct activation of Src, independent of upstream stimuli, was achieved by employing an inducible kinase system (RapR-kinase)[90,131,137]. By using RapR-Src we dissected how the activation of the Src temporally altered the endothelial cell barrier. Furthermore, we determined how Src activation altered the localization, arrangement, and phosphorylation of the adherens junction protein VE cadherin. The use of the RapR-kinase method allowed us to temporally identify key phosphorylation and cell morphological changes altered the endothelial cell barrier via direct Src activation. However, one limitation we identified using the RapR-kinase system was the inability to inactivate our kinase of interest, Src, and determine how the length of catalytic activity affected the endothelial cell barrier.

Our objective in chapter 3, was to generate a protein engineering strategy which allowed for both the specific activation and inactivation of a kinase. Shokat and colleagues had previously provided the ability to rapidly and specifically inhibit a variety of kinases via chemical-genetic inhibition[122–130]. This method had addressed many of the concerns of inhibiting kinase activity using non-specific inhibitors or classical genetic approaches. However, due to the dynamic nature of phosphorylation, a system which allows for both specific and rapid activation and inhibition is needed for more accurate re-capitulation and dissection of specific kinases in signaling cascades. The previously described RapR-kinase system[90,131,137] had allowed for an efficient, specific, and broadly applicable method for controlling kinase activity. Therefore, we combined it with Shokat and colleagues' chemical genetic-inhibition[122–130].

4.2 Src regulation of the endothelial barrier

The application of the RapR-kinase method to investigate how direct activation of a kinase effects the endothelial cell barrier has revealed multiple possibilities for future work. The most obvious being to evaluate the direct activation of other kinases. The dramatic differences between two SFKs, Src and Lyn, begs the question of how do two similar kinases have different effects on the endothelial cell barrier. We have preliminary data demonstrating that activation of Lyn causes a more rapid internalization of VE cadherin than Src (Figure 4.1). However, the mechanisms driving the differences of Src and Lyn regulation of the endothelial cell barrier are currently unclear and require further investigation.

One possibility for the different responses between Src and Lyn activation may be differences in the localization and targeting of these two kinases. All SFKs are co-translationally myristoylated at glycine 2[199]. Lyn is also palmitoylated on cysteine 3, causing it to associate with Golgi pools of caveolin and to be transported to the plasma membrane through the secretory pathway[200]. Conversely, Src is not palmitoylated and instead moves between the plasma membrane and late endosomes[201]. The palmitoylation site on Lyn is necessary for altering its localization and prevents Lyn from localizing to the focal adhesions, with mutation of cysteine 3 causing it to localize and traffic like Src[201]. Therefore, one interesting experiment would be to make chimeras of Lyn and Src; by disrupting palmitoylation of Lyn and causing it to be transported like Src, we could determine whether their differences endothelial cell barrier regulation are the result of differences in trafficking. The absence of Lyn from focal adhesions hints at an additional possible mechanism for Src regulation of the endothelial cell barrier. In our studies, we focused on how Src regulates the adherens junctions and how they contribute to the Src mediated changes in the endothelial cell barrier. However, the focal adhesions are another

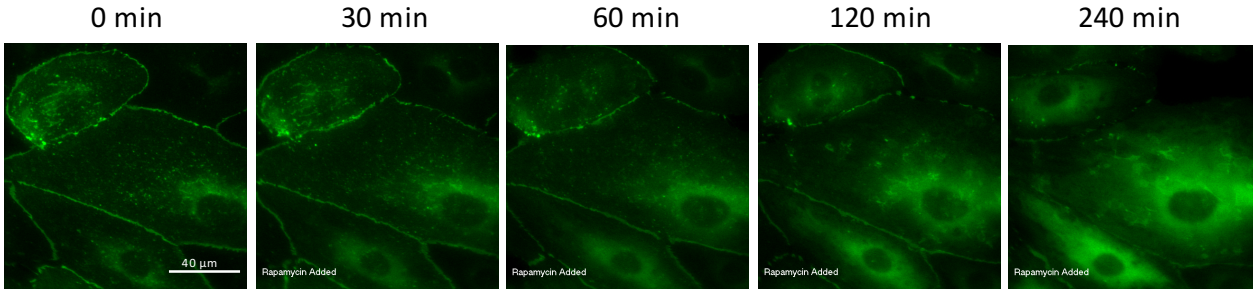

Figure 4.1: Lyn activation induces internalization of VE cadherin
Cells were infected with RapR-Lyn-cerulean-myc, mCherry-FRB, and VE cadherin-GFP construct. Cells were imaged live every 2 minutes in CFP, mCherry, and YFP channels. Stills taken of VE cadherin at the designated times following rapamycin treatment.

important avenue for regulating the endothelial cell barrier[1]. Previously published work demonstrates that activation of Src in complex with p130Cas stimulates new focal adhesions, whereas activation of Src in complex with focal adhesion kinase (FAK) leads to rearrangement of existing focal adhesions[90]. Thus, by targeting Src activation to p130Cas or FAK, we would be able to dissect how formation of new focal adhesions and rearrangement of existing focal adhesions affect the endothelial cell barrier. Specific activation of Src in complex with each of these proteins could be achieved using the RapR targeted activation of pathways (RapRTAP) method (Figure 1.6)[90]. Furthermore, Src myristoylation mutant, Glycine 2 Alanine,[202] was previously found to induce membrane protrusions but was incapable of stimulating *de novo* focal adhesion formation[90]. Using this mutant of RapR-Src, would allow us to determine whether focal adhesion formation is necessary for Src regulation of the endothelial cell barrier.

The use of the RapR-TAP system would also enable us to direct Src activity to the VE cadherin complex. By fusing FRB to VE cadherin and using the SH2 mutant of RapR-Src (R175L) (Figure 1.6), we could determine whether Src is predominantly exerting its endothelial cell barrier effects through VE cadherin. Furthermore, using live cell imaging and directing Src activity to VE cadherin, we could determine whether activation of Src in complex with VE cadherin is sufficient to induce the formation of reticular adherens junctions. This combined with the targeting of Src to FAK, P130Cas, and blocking the formation of focal adhesions via the Src-G2A mutant, would allow us to determine how much of the Src mediated changes to the endothelial cell barrier are due to its regulation of the adherens junctions versus the focal adhesions.

We also demonstrated that activation of Src caused a shift from linear to reticular adherens junctions. The link between SFK activation and reticular adherens junction was

previously observed by others using a DN-CSK[47]. Reticular adherens junctions are intriguing structures that are not very well understood. The molecular composition, structure, and mechanism of formation of reticular junctions all remain to be elucidated. The investigation of these junctions is of interest because we identified that the strengthening of the endothelial cell barrier following Src activation correlates with their formation. In addition, we found that in basal HPAE cells reticular adherens junctions were less leaky than linear adherens junctions. This further suggests that the formation of reticular junctions may be a barrier enhancing phenotype exhibited by endothelial cells.

Reticular junction formation appears to occur in the Src-stimulated membrane protrusions. These protrusions also contain newly formed peripheral focal adhesions. In addition, we see a biochemical association between VE cadherin and paxillin during the endothelial cell barrier enhancement period. We hypothesize that actin-mediated connections between reticular adherens junctions and focal adhesions contributes to the Src driven enhancement of endothelial cell barrier. Using live cell imaging and the RapRTAP system to direct Src activation to VE cadherin or to the focal adhesions, we could determine how each of these components contributes to their formation. In addition, we could determine temporally whether PECAM-1 arrival to reticular adherens junctions is necessary for their formation or it arrives and incorporates after VE cadherin has already rearranged. Currently, reticular adherens junction formation has been associated with leukocyte extravasation[27,35]. A thorough analysis of how Src activation leads to the formation, recruitment, and organization of proteins in reticular adherens junctions would help elucidate the role they play in the regulation of the endothelium.

The differences between Src and Lyn and the distinct phases of Src activation on the endothelial cell barrier that could be regulated through differential control of RhoGTPases. The

function of Rac1 and Cdc42 is thought to maintain and stabilize adherens junctions while activation of RhoA is believed to have a negative effect on endothelial barrier[76,203]. We detected global activation of the RhoGTPase of Rac1 following Src activation. In addition, preliminary studies showed no activation of RhoA, even at very late time periods (Figure 4.3). We did not investigate how Src activation altered Cdc42 activity nor did we evaluate how Lyn activation affected any of these RhoGTPases. Furthermore, we did not evaluate the spatiotemporal changes in RhoGTPase following Src or Lyn activation. Using live cell imaging with biosensor probes for Rac1, Cdc42, and RhoA[116,180,204,205] would allow for spatiotemporal monitoring of Rho GTPase activation via Src and Lyn. Using this approach, we could determine whether Rho GTPase resides in close proximity to the adherens junctions and focal adhesions following Src and Lyn activation. Furthermore, we could determine how the spatiotemporal activation of the RhoGTPases differs between the Src mediated endothelial cell barrier enhancement phase and disruption phase.

The differences in regulation of the endothelial cell barrier between Src and Lyn or the two phases of Src activation might not be dependent on which RhoGTPases are activated but rather the temporal activation of specific Guanine Exchange Factors (GEFs) that result in the activation of RhoA, Rac1 and Cdc42[80,81,83]. The timing and the sequence of Src regulation of GEFs has not been previously described in endothelial cells. In addition, virtually nothing is known about Lyn regulation of GEFs or subsequent activation of Rho GTPases. By isolating active GEFs using RhoA(G17A), Rac1(G15A) and Cdc42(G15A)[206] nucleotide-free mutant pull-downs, we could identify the temporal activation of GEFs by Src and Lyn. The temporal activation of GEFs may indicate which SFK mediated GEFs lead to endothelial cell barrier enhancement and which lead to disruption.

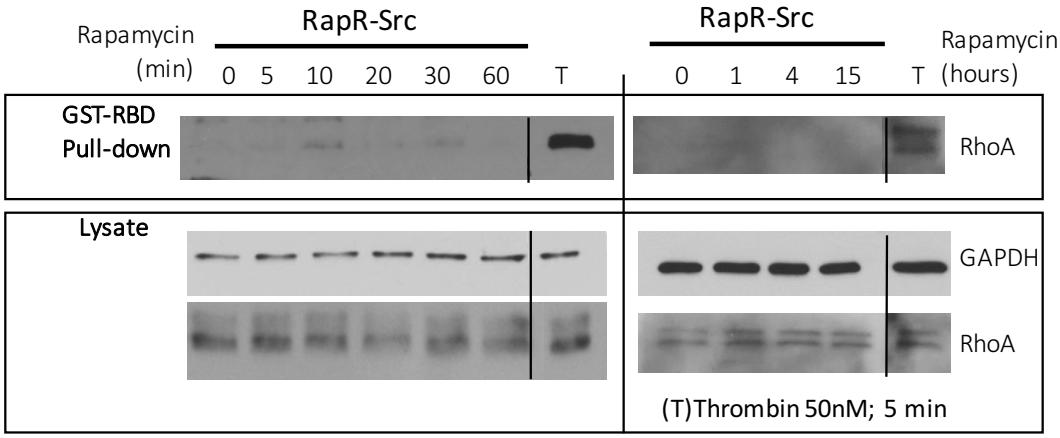

Figure 4.2: Src does not activate RhoA

HPAE cells were infected with adenoviruses expressing RapR-Src-Cerulean-myc and mCherry-FRB and treated with rapamycin (500 nM) for the designated times. GST-Rhotekin-RBD was used to pull-down RhoA-GTP. α-Thrombin (T) (50 nM) was added to HPAE cells for 5 minutes as a positive control for RhoA activation.

** This figure was produced by Dr. Maulik Patel*

One of the most dramatic effects we observed following Src activation were the changes in the actin-cytoskeleton. During the early enhancement phase, we saw the formation of actin foci and during the disruption phase we saw the formation of centripetal actin stress fibers. Understanding the mechanisms behind the formation of each of these actin structures would be quite interesting. The formation of the centripetal actin stress fibers in an endothelial cell monolayer has been previously described using an over-expressed constitutively-active (CA) c-Src[47]. The authors hypothesized that it was the drastic rearrangement of the actin that drove the Src mediated disruption of the endothelial cell barrier. Further investigation of how Src-mediated actin rearrangement drives endothelial cell barrier changes could be enlightening to pursue.

4.3 Transient activation of kinases

Using the RapR-kinase system we investigated how Src activation temporally alters the endothelial cell barrier. However, we were incapable of investigating how activating Src for different amounts of time affected downstream signaling. To enable transient activation of a kinase, we decided to modify the RapR-kinase scheme. The RapR-kinase-as2 method was developed to provide a way to activate kinases for a finite amount of time. We were successful in our endeavor and demonstrated that transient versus prolonged activation of Src had differing effects on cell morphology. The intention of this project was to provide a broadly applicable tool that could be used by others to assist them in dissecting complex signaling pathways. For this reason, we intentionally chose methods of kinase activation and inactivation that had previously been applied to multiple kinases. It is our hope that this tool can be used in the future by others to answer important biological and physiological questions.

A slightly unexpected result and potential application of our tool was the observation that transient activation of Src is followed by a rapid drop in the phosphorylation level of Src

substrates and other proteins. This observation suggests that Src signaling may stimulate high levels of tyrosine phosphatase activity. Indeed, we detected a rapid decrease in paxillin phosphorylation following 1NA-PP1 inhibition of RapR-Src-as2. Therefore, engineered transient activation of Src can be used as a new platform for identification of tyrosine phosphatases that are activated by Src and mediate de-phosphorylation of Src substrates. Selective inhibition or downregulation of specific tyrosine phosphatases will reveal their role in the signaling processes following Src inactivation. Furthermore, the broad applicability of this method should enable identification of phosphatases that de-phosphorylate substrates for other kinases.

This method can be used to control kinase activity in specific protein complexes and to identify novel downstream signaling pathways. It allows for the identification of pathways that cannot be identified with conventional experimental approaches relying on persistent kinase activation that mask the significance of sequential signaling cascades. We described a new approach that enables transient activation of a kinase in living cells and demonstrated that the duration of kinase signaling can be tightly controlled in living cells by specific activation and inhibition. The ability to manipulate kinase activity for a finite amount of time provides the opportunity for a biologically relevant method of dissecting individual kinase functions and their effects on downstream signaling pathways.

4.4 Using RapR-Src-as2 to investigate Src mediated endothelial barrier changes

A large motivator behind designing a reversible kinase activation system was to address questions such as whether transient activation of Src stimulates endothelial cell barrier enhancement without subsequent disruption. By activating Src with rapamycin and subsequently inactivating Src with 1NA-PP1 after different amounts of time, we could determine how the length of Src activity affects Src-mediated changes on the endothelial cell barrier. During the

endothelial cell barrier enhancement phase, we saw an accumulation and broadening of VE cadherin in the adherens junctions. Conversely, during the disruption phase we saw internalization of VE cadherin and gap formation. Therefore, Src activation has temporally distinct effects on VE cadherin by initially causing it to accumulate at the adherens junctions and then leading to its internalization following prolonged activation of Src. The ability to transiently activate Src would allow us to determine whether transient activation of Src was sufficient to drive the accumulation and broadening of the junctions and whether these phenotypes persisted following inactivation of Src or whether they required continuous Src activation. In HeLa cells, we identified signaling pathways stimulated by Src activation which persisted following Src inactivation, driving secondary cell morphological changes. Identifying similar pathways in endothelial cells that may lead to sustained endothelial cell barrier enhancement is an especially interesting prospect for the future.

Both the phosphorylation status of VE cadherin and the specific residue phosphorylated are critical for Src-mediated endothelial cell barrier enhancement. VE-Protein Tyrosine Phosphatase (VE-PTP) de-phosphorylates residue Y685[41] and Src homology 2-domain phosphatase (Shp2) dephosphorylates VE cadherin[53]. In addition, Protein Tyrosine Phosphatase 1B (PTP1B)[54], density-enhanced phosphatase-1 (DEP-1)[55], and protein tyrosine phosphatase receptor type M (PTP-μ)[56] also all appear to affect the phosphorylation status of VE cadherin[22]. RapR-Src-as2 is a perfect tool for answering which phosphatases are necessary for the de-phosphorylation of VE cadherin at each residue. By individually decreasing the expression of each of the phosphatases and evaluating the phosphorylation status of each of the VE cadherin residues and the permeability of the barrier following Src inactivation, it would be possible to identify the role each of these phosphatases play in regulating the permeability of the barrier and phosphorylation

of VE cadherin following Src activation. Moreover, a certain amount of Src activity combined with repression of a specific phosphatase could promote persistent Src-mediated enhancement.

4.5 Conclusion

By employing an inducible kinase system, we temporally monitored key phosphorylation events and cellular changes that in turn regulated the endothelial cell barrier downstream of Src. Our results demonstrate the utility of using an inducible kinase system to dissect key pathways in complex physiological processes. Furthermore, we adapted our kinase system to enable transient activation of a specific kinase. By using our reversible-inducible kinase, we determined that the length of Src activation altered the subsequent cellular morphological changes. The use of engineered-kinases has opened new opportunities to evaluate how specific kinases regulate complex physiological systems. The advent of new optogenetic strategies to regulate kinases and RhoGTPases also provide exciting new opportunities for dissecting signaling pathways in live cells[207–212]. However, in order for these tools to have meaningful results, they need to be able to answer important biological questions.

CHAPTER 5: CITED LITERATURE

1. Mehta, D. & Malik, A. B. Signaling mechanisms regulating endothelial permeability. *Physiol. Rev.* **86,** 279–367 (2006).
2. Dejana, E., Tournier-Lasserve, E. & Weinstein, B. M. The Control of Vascular Integrity by Endothelial Cell Junctions: Molecular Basis and Pathological Implications. *Dev. Cell* **16,** 209–221 (2009).
3. Nagy, J. A., Benjamin, L., Zeng, H., Dvorak, A. M. & Dvorak, H. F. Vascular permeability, vascular hyperpermeability and angiogenesis. *Angiogenesis* **11,** 109–119 (2008).
4. Nagy, J. A. *et al.* Pathogenesis of Ascites Tumor Growth: Vascular Permeability Factor, Vascular Hyperpermeability, and Ascites Fluid Accumulation. *Cancer Res.* **55,** 360–368 (1995).
5. Dvorak, H. F. *et al.* Distribution of vascular permeability factor (vascular endothelial growth factor) in tumors: concentration in tumor blood vessels. *J. Exp. Med.* **174,** 1275–1278 (1991).
6. Dvorak, H. F. How Tumors Make Bad Blood Vessels and Stroma. *Am. J. Pathol.* **162,** 1747–1757 (2003).
7. Pappenheimer, J. R., Renkin, E. M. & Borrero, L. M. Filtration, diffusion and molecular sieving through peripheral capillary membranes; a contribution to the pore theory of capillary permeability. *Am. J. Physiol.* **167,** 13–46 (1951).
8. Komarova, Y. & Malik, A. B. Regulation of endothelial permeability via paracellular and transcellular transport pathways. *Annu. Rev. Physiol.* **72,** 463–493 (2010).
9. Frank, P. G., Woodman, S. E., Park, D. S. & Lisanti, M. P. Caveolin, caveolae, and endothelial cell function. *Arterioscler. Thromb. Vasc. Biol.* **23,** 1161–1168 (2003).
10. Minshall, R. D., Tiruppathi, C., Vogel, S. M. & Malik, A. B. Vesicle formation and trafficking in endothelial cells and regulation of endothelial barrier function. *Histochem. Cell Biol.* **117,** 105–112 (2002).

11. Dejana, E. & Orsenigo, F. Endothelial adherens junctions at a glance. *J. Cell Sci.* **126,** 2545–2549 (2013).

12. Shapiro, L. *et al.* Structural basis of cell-cell adhesion by cadherins. *Nature* **374,** 327–337 (1995).

13. Giannotta, M., Trani, M. & Dejana, E. VE-cadherin and endothelial adherens junctions: active guardians of vascular integrity. *Dev. Cell* **26,** 441–454 (2013).

14. Carmeliet, P. *et al.* Targeted deficiency or cytosolic truncation of the VE-cadherin gene in mice impairs VEGF-mediated endothelial survival and angiogenesis. *Cell* **98,** 147–157 (1999).

15. Gory-Fauré, S. *et al.* Role of vascular endothelial-cadherin in vascular morphogenesis. *Dev. Camb. Engl.* **126,** 2093–2102 (1999).

16. Crosby, C. V. *et al.* VE-cadherin is not required for the formation of nascent blood vessels but acts to prevent their disassembly. *Blood* **105,** 2771–2776 (2005).

17. Corada, M. *et al.* Vascular endothelial-cadherin is an important determinant of microvascular integrity in vivo. *Proc. Natl. Acad. Sci. U. S. A.* **96,** 9815–9820 (1999).

18. Corada, M. *et al.* A monoclonal antibody to vascular endothelial–cadherin inhibits tumor angiogenesis without side effects on endothelial permeability. *Blood* **100,** 905–911 (2002).

19. Breier, G. *et al.* Molecular cloning and expression of murine vascular endothelial-cadherin in early stage development of cardiovascular system. *Blood* **87,** 630–641 (1996).

20. Brasch, J., Harrison, O. J., Honig, B. & Shapiro, L. Thinking outside the cell: how cadherins drive adhesion. *Trends Cell Biol.* **22,** 299–310 (2012).

21. Takeichi, M. Cadherins: a molecular family important in selective cell-cell adhesion. *Annu. Rev. Biochem.* **59,** 237–252 (1990).

22. Iyer, S., Ferreri, D. M., DeCocco, N. C., Minnear, F. L. & Vincent, P. A. VE-cadherin-p120 interaction is required for maintenance of endothelial barrier function. *Am. J. Physiol. - Lung Cell. Mol. Physiol.* **286,** L1143–L1153 (2004).

23. Dejana, E., Orsenigo, F. & Lampugnani, M. G. The role of adherens junctions and VE-cadherin in the control of vascular permeability. *J. Cell Sci.* **121,** 2115–2122 (2008).

24. Nelson, W. J. Regulation of cell-cell adhesion by the cadherin-catenin complex. *Biochem. Soc. Trans.* **36,** 149–155 (2008).

25. Hartsock, A. & Nelson, W. J. Adherens and tight junctions: structure, function and connections to the actin cytoskeleton. *Biochim. Biophys. Acta* **1778,** 660–669 (2008).

26. Weis, W. I. & Nelson, W. J. Re-solving the Cadherin-Catenin-Actin Conundrum. *J. Biol. Chem.* **281,** 35593–35597 (2006).

27. Wilson, C. W. & Ye, W. Regulation of vascular endothelial junction stability and remodeling through Rap1-Rasip1 signaling. *Cell Adhes. Migr.* **8,** 76–83 (2014).

28. Seebach, J. *et al.* Regulation of endothelial barrier function during flow-induced conversion to an arterial phenotype. *Cardiovasc. Res.* **75,** 596–607 (2007).

29. Huveneers, S. *et al.* Vinculin associates with endothelial VE-cadherin junctions to control force-dependent remodeling. *J. Cell Biol.* **196,** 641–652 (2012).

30. Abu Taha, A., Taha, M., Seebach, J. & Schnittler, H.-J. ARP2/3-mediated junction-associated lamellipodia control VE-cadherin-based cell junction dynamics and maintain monolayer integrity. *Mol. Biol. Cell* **25,** 245–256 (2014).

31. Hoelzle, M. K. & Svitkina, T. The cytoskeletal mechanisms of cell-cell junction formation in endothelial cells. *Mol. Biol. Cell* **23,** 310–323 (2012).

32. Dorland, Y. L. & Huveneers, S. Cell–cell junctional mechanotransduction in endothelial remodeling. *Cell. Mol. Life Sci.* **74,** 279–292 (2017).

33. Timmerman, I. *et al.* A local VE-cadherin and Trio-based signaling complex stabilizes endothelial junctions through Rac1. *J. Cell Sci.* **128,** 3041–3054 (2015).

34. Liu, Z. *et al.* Mechanical tugging force regulates the size of cell-cell junctions. *Proc. Natl. Acad. Sci. U. S. A.* **107,** 9944–9949 (2010).

35. Fernández-Martín, L. *et al.* Crosstalk between reticular adherens junctions and platelet endothelial cell adhesion molecule-1 regulates endothelial barrier function. *Arterioscler. Thromb. Vasc. Biol.* **32,** e90-102 (2012).

36. Pokutta, S. & Weis, W. I. Structure and mechanism of cadherins and catenins in cell-cell contacts. *Annu. Rev. Cell Dev. Biol.* **23,** 237–261 (2007).

37. Alemà, S. & Salvatore, A. M. p120 catenin and phosphorylation: Mechanisms and traits of an unresolved issue. *Biochim. Biophys. Acta BBA - Mol. Cell Res.* **1773,** 47–58 (2007).

38. Lilien, J. & Balsamo, J. The regulation of cadherin-mediated adhesion by tyrosine phosphorylation/dephosphorylation of β-catenin. *Curr. Opin. Cell Biol.* **17,** 459–465 (2005).

39. Lampugnani, M. G. *et al.* Cell confluence regulates tyrosine phosphorylation of adherens junction components in endothelial cells. *J. Cell Sci.* **110,** 2065–2077 (1997).

40. Angelini, D. J. *et al.* TNF-alpha increases tyrosine phosphorylation of vascular endothelial cadherin and opens the paracellular pathway through fyn activation in human lung endothelia. *Am. J. Physiol. Lung Cell. Mol. Physiol.* **291,** L1232-1245 (2006).

41. Gong, P. *et al.* TLR4 Signaling Is Coupled to SRC Family Kinase Activation, Tyrosine Phosphorylation of Zonula Adherens Proteins, and Opening of the Paracellular Pathway in Human Lung Microvascular Endothelia. *J. Biol. Chem.* **283,** 13437–13449 (2008).

42. Gong, H. *et al.* Evidence of a common mechanism of disassembly of adherens junctions through Gα13 targeting of VE-cadherin. *J. Exp. Med.* jem.20131190 (2014). doi:10.1084/jem.20131190

43. Orsenigo, F. *et al.* Phosphorylation of VE-cadherin is modulated by haemodynamic forces and contributes to the regulation of vascular permeability in vivo. *Nat. Commun.* **3,** 1208 (2012).

44. Esser, S., Lampugnani, M. G., Corada, M., Dejana, E. & Risau, W. Vascular endothelial growth factor induces VE-cadherin tyrosine phosphorylation in endothelial cells. *J. Cell Sci.* **111,** 1853–1865 (1998).

45. Turowski, P. *et al.* Phosphorylation of vascular endothelial cadherin controls lymphocyte emigration. *J. Cell Sci.* **121,** 29–37 (2008).

46. Monaghan-Benson, E. & Burridge, K. The Regulation of Vascular Endothelial Growth Factor-induced Microvascular Permeability Requires Rac and Reactive Oxygen Species. *J. Biol. Chem.* **284,** 25602–25611 (2009).

47. Adam, A. P., Sharenko, A. L., Pumiglia, K. & Vincent, P. A. Src-induced Tyrosine Phosphorylation of VE-cadherin Is Not Sufficient to Decrease Barrier Function of Endothelial Monolayers. *J. Biol. Chem.* **285,** 7045–7055 (2010).

48. Wessel, F. *et al.* Leukocyte extravasation and vascular permeability are each controlled in vivo by different tyrosine residues of VE-cadherin. *Nat. Immunol.* **15,** 223–230 (2014).

49. Allingham, M. J., Buul, J. D. van & Burridge, K. ICAM-1-Mediated, Src- and Pyk2-Dependent Vascular Endothelial Cadherin Tyrosine Phosphorylation Is Required for Leukocyte Transendothelial Migration. *J. Immunol.* **179,** 4053–4064 (2007).

50. Gavard, J. & Gutkind, J. S. VEGF controls endothelial-cell permeability by promoting the β-arrestin-dependent endocytosis of VE-cadherin. *Nat. Cell Biol.* **8,** 1223–1234 (2006).

51. Nottebaum, A. F. *et al.* VE-PTP maintains the endothelial barrier via plakoglobin and becomes dissociated from VE-cadherin by leukocytes and by VEGF. *J. Exp. Med.* **205,** 2929–2945 (2008).

52. Chen, X. L. *et al.* VEGF-Induced Vascular Permeability Is Mediated by FAK. *Dev. Cell* **22,** 146–157 (2012).

53. Wallez, Y. *et al.* Src kinase phosphorylates vascular endothelial-cadherin in response to vascular endothelial growth factor: identification of tyrosine 685 as the unique target site. *Oncogene* **26,** 1067–1077 (2006).

54. Seebach, J., Mädler, H.-J., Wojciak-Stothard, B. & Schnittler, H.-J. Tyrosine phosphorylation and the small GTPase rac cross-talk in regulation of endothelial barrier function. *Thromb. Haemost.* **94,** 620–629 (2005).

55. Timmerman, I. *et al.* The tyrosine phosphatase SHP2 regulates recovery of endothelial adherens junctions through control of β-catenin phosphorylation. *Mol. Biol. Cell* **23,** 4212–4225 (2012).

56. Ukropec, J. A., Hollinger, M. K., Salva, S. M. & Woolkalis, M. J. SHP2 Association with VE-Cadherin Complexes in Human Endothelial Cells Is Regulated by Thrombin. *J. Biol. Chem.* **275,** 5983–5986 (2000).

57. Nakamura, Y. *et al.* Role of protein tyrosine phosphatase 1B in vascular endothelial growth factor signaling and cell-cell adhesions in endothelial cells. *Circ. Res.* **102,** 1182–1191 (2008).

58. Lampugnani, M. G. *et al.* Contact inhibition of VEGF-induced proliferation requires vascular endothelial cadherin, β-catenin, and the phosphatase DEP-1/CD148. *J. Cell Biol.* **161,** 793–804 (2003).

59. Sui, X. F. *et al.* Receptor protein tyrosine phosphatase micro regulates the paracellular pathway in human lung microvascular endothelia. *Am. J. Pathol.* **166,** 1247–1258 (2005).

60. Thennes, T. & Mehta, D. Heterotrimeric G proteins, focal adhesion kinase, and endothelial barrier function. *Microvasc. Res.* **83,** 31–44 (2012).

61. Wheeler, D. L., Iida, M. & Dunn, E. F. The Role of Src in Solid Tumors. *The Oncologist* **14,** 667–678 (2009).

62. Levinson, N. M., Seeliger, M. A., Cole, P. A. & Kuriyan, J. Structural basis for the recognition of c-Src by its inactivator Csk. *Cell* **134,** 124–134 (2008).

63. Dehm, S. M. & Bonham, K. SRC gene expression in human cancer: the role of transcriptional activation. *Biochem. Cell Biol. Biochim. Biol. Cell.* **82,** 263–274 (2004).

64. Eliceiri, B. P. *et al.* Selective Requirement for Src Kinases during VEGF-Induced Angiogenesis and Vascular Permeability. *Mol. Cell* **4,** 915–924 (1999).

65. Knezevic, N., Tauseef, M., Thennes, T. & Mehta, D. The G protein βγ subunit mediates reannealing of adherens junctions to reverse endothelial permeability increase by thrombin. *J. Exp. Med.* **206,** 2761–2777 (2009).

66. Han, J. *et al.* A critical role for Lyn kinase in strengthening endothelial integrity and barrier function. *Blood* **122,** 4140–4149 (2013).

67. Lum, H. & Malik, A. B. Regulation of vascular endothelial barrier function. *Am. J. Physiol. - Lung Cell. Mol. Physiol.* **267,** L223–L241 (1994).

68. Lambeng, N. *et al.* Vascular Endothelial–Cadherin Tyrosine Phosphorylation in Angiogenic and Quiescent Adult Tissues. *Circ. Res.* **96,** 384–391 (2005).

69. Komarova, Y. A., Mehta, D. & Malik, A. B. Dual Regulation of Endothelial Junctional Permeability. *Sci. Signal.* **2007,** re8 (2007).

70. Birukova, A. A., Tian, X., Tian, Y., Higginbotham, K. & Birukov, K. G. Rap-afadin axis in control of Rho signaling and endothelial barrier recovery. *Mol. Biol. Cell* **24,** 2678–2688 (2013).

71. Bergeron, A. *et al.* Lung Abnormalities after Dasatinib Treatment for Chronic Myeloid Leukemia. *Am. J. Respir. Crit. Care Med.* **176,** 814–818 (2007).

72. Corey, S. J. & Day, R. M. Shockingly: the loss of Lyn leads to leakiness. *Blood* **122,** 4009–4010 (2013).

73. Vouret-Craviari, V., Bourcier, C., Boulter, E. & Obberghen-Schilling, E. V. Distinct signals via Rho GTPases and Src drive shape changes by thrombin and sphingosine-1-phosphate in endothelial cells. *J. Cell Sci.* **115,** 2475–2484 (2002).

74. Birukova, A. A. *et al.* Microtubule disassembly induces cytoskeletal remodeling and lung vascular barrier dysfunction: role of Rho-dependent mechanisms. *J. Cell. Physiol.* **201,** 55–70 (2004).

75. Birukova, A. A. *et al.* Role of Rho GTPases in thrombin-induced lung vascular endothelial cells barrier dysfunction. *Microvasc. Res.* **67,** 64–77 (2004).

76. Spindler, V., Schlegel, N. & Waschke, J. Role of GTPases in control of microvascular permeability. *Cardiovasc. Res.* **87,** 243–253 (2010).

77. Takai, Y., Sasaki, T. & Matozaki, T. Small GTP-Binding Proteins. *Physiol. Rev.* **81,** 153–208 (2001).

78. Aelst, L. V. & D'Souza-Schorey, C. Rho GTPases and signaling networks. *Genes Dev.* **11,** 2295–2322 (1997).

79. Schmidt, A. & Hall, A. Guanine nucleotide exchange factors for Rho GTPases: turning on the switch. *Genes Dev.* **16,** 1587–1609 (2002).

80. Gavard, J. & Gutkind, J. S. VEGF controls endothelial-cell permeability by promoting the β-arrestin-dependent endocytosis of VE-cadherin. *Nat. Cell Biol.* **8,** 1223–1234 (2006).

81. Woodcock, S. A. *et al.* Src-Induced Disassembly of Adherens Junctions Requires Localized Phosphorylation and Degradation of the Rac Activator Tiam1. *Mol. Cell* **33,** 639–653 (2009).

82. Feng, H. *et al.* Activation of Rac1 by Src-dependent phosphorylation of Dock180Y1811 mediates PDGFRα-stimulated glioma tumorigenesis in mice and humans. *J. Clin. Invest.* **121,** 4670–4684 (2011).

83. Miyamoto, Y., Yamauchi, J. & Itoh, H. Src Kinase Regulates the Activation of a Novel FGD-1-related Cdc42 Guanine Nucleotide Exchange Factor in the Signaling Pathway from the Endothelin A Receptor to JNK. *J. Biol. Chem.* **278,** 29890–29900 (2003).

84. Fincham, V. J., Chudleigh, A. & Frame, M. C. Regulation of p190 Rho-GAP by v-Src is linked to cytoskeletal disruption during transformation. *J. Cell Sci.* **112,** 947–956 (1999).

85. Kouklis, P., Konstantoulaki, M. & Malik, A. B. VE-cadherin-induced Cdc42 Signaling Regulates Formation of Membrane Protrusions in Endothelial Cells. *J. Biol. Chem.* **278,** 16230–16236 (2003).

86. Duluc, L. & Wojciak-Stothard, B. Rho GTPases in the regulation of pulmonary vascular barrier function. *Cell Tissue Res.* **355,** 675–685 (2014).

87. Nelson, C. M., Pirone, D. M., Tan, J. L. & Chen, C. S. Vascular Endothelial-Cadherin Regulates Cytoskeletal Tension, Cell Spreading, and Focal Adhesions by Stimulating RhoA. *Mol. Biol. Cell* **15,** 2943–2953 (2004).

88. Hordijk, P. L. Regulation of NADPH Oxidases The Role of Rac Proteins. *Circ. Res.* **98,** 453–462 (2006).

89. Birukov, K. G. *et al.* Differential regulation of alternatively spliced endothelial cell myosin light chain kinase isoforms by p60(Src). *J. Biol. Chem.* **276,** 8567–8573 (2001).

90. Karginov, A. V. *et al.* Dissecting motility signaling through activation of specific Src-effector complexes. *Nat. Chem. Biol.* **10,** 286–290 (2014).

91. Chen, C. S., Alonso, J. L., Ostuni, E., Whitesides, G. M. & Ingber, D. E. Cell shape provides global control of focal adhesion assembly. *Biochem. Biophys. Res. Commun.* **307,** 355–361 (2003).

92. Geiger, B., Bershadsky, A., Pankov, R. & Yamada, K. M. Transmembrane crosstalk between the extracellular matrix--cytoskeleton crosstalk. *Nat. Rev. Mol. Cell Biol.* **2,** 793–805 (2001).

93. Rankin, S. & Rozengurt, E. Platelet-derived growth factor modulation of focal adhesion kinase (p125FAK) and paxillin tyrosine phosphorylation in Swiss 3T3 cells. Bell-shaped dose response and cross-talk with bombesin. *J. Biol. Chem.* **269,** 704–710 (1994).

94. Thomas, S. M. & Brugge, J. S. Cellular functions regulated by Src family kinases. *Annu. Rev. Cell Dev. Biol.* **13,** 513–609 (1997).

95. Eliceiri, B. P. *et al.* Src-mediated coupling of focal adhesion kinase to integrin αvβ5 in vascular endothelial growth factor signaling. *J. Cell Biol.* **157,** 149–160 (2002).

96. Yuan, S. Y. Protein kinase signaling in the modulation of microvascular permeability. *Vascul. Pharmacol.* **39,** 213–223 (2002).

97. Miyamoto, S. *et al.* Integrin function: molecular hierarchies of cytoskeletal and signaling molecules. *J. Cell Biol.* **131,** 791–805 (1995).

98. Pang, J.-H., Kraemer, A., Stehbens, S. J., Frame, M. C. & Yap, A. S. Recruitment of Phosphoinositide 3-Kinase Defines a Positive Contribution of Tyrosine Kinase Signaling to E-cadherin Function. *J. Biol. Chem.* **280,** 3043–3050 (2005).

99. Vanhaesebroeck, B., Guillermet-Guibert, J., Graupera, M. & Bilanges, B. The emerging mechanisms of isoform-specific PI3K signalling. *Nat. Rev. Mol. Cell Biol.* **11,** 329–341 (2010).

100. Cantrell, D. A. Phosphoinositide 3-kinase signalling pathways. *J. Cell Sci.* **114,** 1439–1445 (2001).

101. Coelho, C. M. & Leevers, S. J. Do growth and cell division rates determine cell size in multicellular organisms? *J. Cell Sci.* **113 (Pt 17),** 2927–2934 (2000).

102. Hawkins, P. T., Jackson, T. R. & Stephens, L. R. Platelet-derived growth factor stimulates synthesis of PtdIns(3,4,5)P3 by activating a PtdIns(4,5)P2 3-OH kinase. *Nature* **358,** 157–159 (1992).

103. Rameh, L. E. *et al.* A Comparative Analysis of the Phosphoinositide Binding Specificity of Pleckstrin Homology Domains. *J. Biol. Chem.* **272,** 22059–22066 (1997).

104. Jean, S. & Kiger, A. A. Classes of phosphoinositide 3-kinases at a glance. *J. Cell Sci.* **127,** 923–928 (2014).

105. Pawson, T. Protein modules and signalling networks. *Nature* **373,** 573–580 (1995).

106. Rei, K., Nobes, C. D., Thomas, G., Hall, A. & Cantrell, D. A. Phosphatidylinositol 3-kinase signals activate a selective subset of Rac/Rho-dependent effector pathways. *Curr. Biol.* **6,** 1445–1455 (1996).

107. Alessi, D. R. & Cohen, P. Mechanism of activation and function of protein kinase B. *Curr. Opin. Genet. Dev.* **8,** 55–62 (1998).

108. Bellacosa, A. *et al.* Akt activation by growth factors is a multiple-step process: the role of the PH domain. *Oncogene* **17,** 313–325 (1998).

109. Alessi, D. R. *et al.* Characterization of a 3-phosphoinositide-dependent protein kinase which phosphorylates and activates protein kinase Bα. *Curr. Biol.* **7,** 261–269 (1997).

110. Alessi, D. R., Kozlowski, M. T., Weng, Q. P., Morrice, N. & Avruch, J. 3-Phosphoinositide-dependent protein kinase 1 (PDK1) phosphorylates and activates the p70 S6 kinase in vivo and in vitro. *Curr. Biol. CB* **8,** 69–81 (1998).

111. Williams, M. R. *et al.* The role of 3-phosphoinositide-dependent protein kinase 1 in activating AGC kinases defined in embryonic stem cells. *Curr. Biol. CB* **10,** 439–448 (2000).

112. Vanhaesebroeck, B. & Alessi, D. R. The PI3K-PDK1 connection: more than just a road to PKB. *Biochem. J.* **346,** 561–576 (2000).

113. Hemmings, B. A. & Restuccia, D. F. PI3K-PKB/Akt Pathway. *Cold Spring Harb. Perspect. Biol.* **4,** (2012).

114. Nicholson, K. M. & Anderson, N. G. The protein kinase B/Akt signalling pathway in human malignancy. *Cell. Signal.* **14,** 381–395 (2002).

115. Cantley, L. C. *et al.* Oncogenes and signal transduction. *Cell* **64,** 281–302 (1991).

116. Kraynov, V. S. *et al.* Localized Rac Activation Dynamics Visualized in Living Cells. *Science* **290,** 333–337 (2000).

117. Rotty, J. D., Wu, C. & Bear, J. E. New insights into the regulation and cellular functions of the ARP2/3 complex. *Nat. Rev. Mol. Cell Biol.* **14,** 7–12 (2013).

118. Lebensohn, A. M. & Kirschner, M. W. Activation of the WAVE complex by coincident signals controls actin assembly. *Mol. Cell* **36,** 512–524 (2009).

119. Weiger, M. C. *et al.* Spontaneous phosphoinositide 3-kinase signaling dynamics drive spreading and random migration of fibroblasts. *J. Cell Sci.* **122,** 313–323 (2009).

120. Cohen, P. The origins of protein phosphorylation. *Nat. Cell Biol.* **4,** E127–E130 (2002).

121. Gautier, A., Deiters, A. & Chin, J. W. Light-Activated Kinases Enable Temporal Dissection of Signaling Networks in Living Cells. *J. Am. Chem. Soc.* **133,** 2124–2127 (2011).

122. Bishop, A. C. *et al.* Design of allele-specific inhibitors to probe protein kinase signaling. *Curr. Biol. CB* **8,** 257–266 (1998).

123. Bishop, A. C. *et al.* Generation of Monospecific Nanomolar Tyrosine Kinase Inhibitors via a Chemical Genetic Approach. *J. Am. Chem. Soc.* **121,** 627–631 (1999).

124. Bishop, A. C. *et al.* A chemical switch for inhibitor-sensitive alleles of any protein kinase. *Nature* **407,** 395–401 (2000).

125. Zhang, C. *et al.* Structure-guided Inhibitor Design Expands the Scope of Analog-Sensitive Kinase Technology. *ACS Chem. Biol.* **8,** 1931–1938 (2013).

126. Weiss, E. L., Bishop, A. C., Shokat, K. M. & Drubin, D. G. Chemical genetic analysis of the budding-yeast p21-activated kinase Cla4p. *Nat. Cell Biol.* **2,** 677–685 (2000).

127. Fan, Q.-W., Zhang, C., Shokat, K. M. & Weiss, W. A. Chemical Genetic Blockade of Transformation Reveals Dependence on Aberrant Oncogenic Signaling. *Curr. Biol.* **12,** 1386–1394 (2002).

128. Benjamin, K. R., Zhang, C., Shokat, K. M. & Herskowitz, I. Control of landmark events in meiosis by the CDK Cdc28 and the meiosis-specific kinase Ime2. *Genes Dev.* **17,** 1524–1539 (2003).

129. Okuzumi, T. *et al.* Inhibitor hijacking of Akt activation. *Nat. Chem. Biol.* **5,** 484–493 (2009).

130. Au-Yeung, B. B. *et al.* A genetically selective inhibitor demonstrates a function for the kinase Zap70 in regulatory T cells independent of its catalytic activity. *Nat. Immunol.* **11,** 1085–1092 (2010).

131. Karginov, A. V. & Hahn, K. M. Allosteric activation of kinases: design and application of RapR kinases. *Curr. Protoc. Cell Biol. Editor. Board Juan Bonifacino Al* **Chapter 14,** Unit 14.13. (2011).

132. Bazzoni, G. & Dejana, E. Endothelial Cell-to-Cell Junctions: Molecular Organization and Role in Vascular Homeostasis. *Physiol. Rev.* **84,** 869–901 (2004).

133. Vestweber, D. VE-Cadherin The Major Endothelial Adhesion Molecule Controlling Cellular Junctions and Blood Vessel Formation. *Arterioscler. Thromb. Vasc. Biol.* **28,** 223–232 (2008).

134. Xu, G. *et al.* Continuous association of cadherin with beta-catenin requires the non-receptor tyrosine-kinase Fer. *J. Cell Sci.* **117,** 3207–3219 (2004).

135. Piedra, J. *et al.* p120 Catenin-Associated Fer and Fyn Tyrosine Kinases Regulate β-Catenin Tyr-142 Phosphorylation and β-Catenin-α-Catenin Interaction. *Mol. Cell. Biol.* **23,** 2287–2297 (2003).

136. Kim, L. & Wong, T. W. The cytoplasmic tyrosine kinase FER is associated with the catenin-like substrate pp120 and is activated by growth factors. *Mol. Cell. Biol.* **15,** 4553–4561 (1995).

137. Karginov, A. V., Ding, F., Kota, P., Dokholyan, N. V. & Hahn, K. M. Engineered allosteric activation of kinases in living cells. *Nat. Biotechnol.* **28,** 743–747 (2010).

138. Klomp, J. E. *et al.* Mimicking transient activation of protein kinases in living cells. *Proc. Natl. Acad. Sci.* **113,** 14976–14981 (2016).

139. Chu, P.-H. *et al.* Engineered kinase activation reveals unique morphodynamic phenotypes and associated trafficking for Src family isoforms. *Proc. Natl. Acad. Sci.* **111,** 12420–12425 (2014).

140. Ray, A.-M., Klomp, J. E., Collins, K. B. & Karginov, A. V. Dissecting Kinase Effector Signaling Using the RapRTAP Methodology. *Methods Mol. Biol. Clifton NJ* **1636,** 21–33 (2017).

141. Dubrovskyi, O., Birukova, A. A. & Birukov, K. G. Measurement of local permeability at subcellular level in cell models of agonist- and ventilator-induced lung injury. *Lab. Investig. J. Tech. Methods Pathol.* **93,** 254–263 (2013).

142. Shao, L., Kner, P., Rego, E. H. & Gustafsson, M. G. L. Super-resolution 3D microscopy of live whole cells using structured illumination. *Nat. Methods* **8,** 1044–1046 (2011).

143. Gustafsson, M. G. L. *et al.* Three-dimensional resolution doubling in wide-field fluorescence microscopy by structured illumination. *Biophys. J.* **94,** 4957–4970 (2008).

144. Tsygankov, D. *et al.* CellGeo: A computational platform for the analysis of shape changes in cells with complex geometries. *J. Cell Biol.* **204,** 443–460 (2014).

145. Huang, Y.-T., Chen, S.-U., Chou, C.-H. & Lee, H. Sphingosine 1-phosphate induces platelet/endothelial cell adhesion molecule-1 phosphorylation in human endothelial cells through cSrc and Fyn. *Cell. Signal.* **20,** 1521–1527 (2008).

146. Seebach, J. *et al.* The CellBorderTracker, a novel tool to quantitatively analyze spatiotemporal endothelial junction dynamics at the subcellular level. *Histochem. Cell Biol.* (2015). doi:10.1007/s00418-015-1357-8

147. Cain, R. J., Vanhaesebroeck, B. & Ridley, A. J. The PI3K p110α isoform regulates endothelial adherens junctions via Pyk2 and Rac1. *J. Cell Biol.* **188,** 863–876 (2010).

148. Bryce, N. S. *et al.* Cortactin Promotes Cell Motility by Enhancing Lamellipodial Persistence. *Curr. Biol.* **15,** 1276–1285 (2005).

149. Lapetina, S., Mader, C. C., Machida, K., Mayer, B. J. & Koleske, A. J. Arg interacts with cortactin to promote adhesion-dependent cell edge protrusion. *J. Cell Biol.* **185,** 503–519 (2009).

150. Potter, M. D., Barbero, S. & Cheresh, D. A. Tyrosine phosphorylation of VE-cadherin prevents binding of p120- and beta-catenin and maintains the cellular mesenchymal state. *J. Biol. Chem.* **280,** 31906–31912 (2005).

151. van Nieuw Amerongen, G. P. & van Hinsbergh, V. W. M. Targets for pharmacological intervention of endothelial hyperpermeability and barrier function. *Vascul. Pharmacol.* **39,** 257–272 (2002).

152. Paul, R. *et al.* Src deficiency or blockade of Src activity in mice provides cerebral protection following stroke. *Nat. Med.* **7,** 222–227 (2001).

153. Lowell, C. A. & Berton, G. Resistance to endotoxic shock and reduced neutrophil migration in mice deficient for the Src-family kinases Hck and Fgr. *Proc. Natl. Acad. Sci.* **95,** 7580–7584 (1998).

154. Scheppke, L. *et al.* Retinal vascular permeability suppression by topical application of a novel VEGFR2/Src kinase inhibitor in mice and rabbits. *J. Clin. Invest.* **118,** 2337–2346 (2008).

155. Olsson, A.-K., Dimberg, A., Kreuger, J. & Claesson-Welsh, L. VEGF receptor signalling - in control of vascular function. *Nat. Rev. Mol. Cell Biol.* **7,** 359–371 (2006).

156. Hu, G., Place, A. T. & Minshall, R. D. Regulation of endothelial permeability by Src kinase signaling: vascular leakage versus transcellular transport of drugs and macromolecules. *Chem. Biol. Interact.* **171,** 177–189 (2008).

157. Etienne, S. *et al.* ICAM-1 signaling pathways associated with Rho activation in microvascular brain endothelial cells. *J. Immunol. Baltim. Md 1950* **161,** 5755–5761 (1998).

158. Tilghman, R. W. & Hoover, R. L. The Src-cortactin pathway is required for clustering of E-selectin and ICAM-1 in endothelial cells. *FASEB J. Off. Publ. Fed. Am. Soc. Exp. Biol.* **16,** 1257–1259 (2002).

159. Yang, L., Kowalski, J. R., Zhan, X., Thomas, S. M. & Luscinskas, F. W. Endothelial cell cortactin phosphorylation by Src contributes to polymorphonuclear leukocyte transmigration in vitro. *Circ. Res.* **98,** 394–402 (2006).

160. Liu, G. *et al.* ICAM-1-activated Src and eNOS signaling increase endothelial cell surface PECAM-1 adhesivity and neutrophil transmigration. *Blood* **120,** 1942–1952 (2012).

161. Hanks, S. K. Genomic analysis of the eukaryotic protein kinase superfamily: a perspective. *Genome Biol.* **4,** 111 (2003).

162. Manning, G., Whyte, D. B., Martinez, R., Hunter, T. & Sudarsanam, S. The protein kinase complement of the human genome. *Science* **298,** 1912–1934 (2002).

163. Davies, S. P., Reddy, H., Caivano, M. & Cohen, P. Specificity and mechanism of action of some commonly used protein kinase inhibitors. *Biochem. J.* **351,** 95–105 (2000).

164. Garske, A. L., Peters, U., Cortesi, A. T., Perez, J. L. & Shokat, K. M. Chemical genetic strategy for targeting protein kinases based on covalent complementarity. *Proc. Natl. Acad. Sci.* **108,** 15046–15052 (2011).

165. Lampson, M. A. & Kapoor, T. M. Unraveling cell division mechanisms with small-molecule inhibitors. *Nat. Chem. Biol.* **2,** 19–27 (2006).

166. Perona, R. Cell signalling: growth factors and tyrosine kinase receptors. *Clin. Transl. Oncol. Off. Publ. Fed. Span. Oncol. Soc. Natl. Cancer Inst. Mex.* **8,** 77–82 (2006).

167. Hunter, T. Protein kinases and phosphatases: The Yin and Yang of protein phosphorylation and signaling. *Cell* **80,** 225–236 (1995).

168. Marshall, C. J. Specificity of receptor tyrosine kinase signaling: transient versus sustained extracellular signal-regulated kinase activation. *Cell* **80,** 179–185 (1995).

169. Wend, S. *et al.* Optogenetic control of protein kinase activity in mammalian cells. *ACS Synth. Biol.* **3,** 280–285 (2014).

170. MacNevin, C. J. *et al.* Ratiometric Imaging Using a Single Dye Enables Simultaneous Visualization of Rac1 and Cdc42 Activation. *J. Am. Chem. Soc.* **138,** 2571–2575 (2016).

171. Bravo-Cordero, J. J., Moshfegh, Y., Condeelis, J. & Hodgson, L. Live cell imaging of RhoGTPase biosensors in tumor cells. *Methods Mol. Biol. Clifton NJ* **1046,** 359–370 (2013).

172. Cai, X. *et al.* Spatial and Temporal Regulation of Focal Adhesion Kinase Activity in Living Cells. *Mol. Cell. Biol.* **28,** 201–214 (2008).

173. Gerwins, P., Blank, J. L. & Johnson, G. L. Cloning of a novel mitogen-activated protein kinase kinase kinase, MEKK4, that selectively regulates the c-Jun amino terminal kinase pathway. *J. Biol. Chem.* **272,** 8288–8295 (1997).

174. Hodgson, L., Pertz, O. & Hahn, K. M. Design and optimization of genetically encoded fluorescent biosensors: GTPase biosensors. *Methods Cell Biol.* **85,** 63–81 (2008).

175. Kmiecik, T. E. & Shalloway, D. Activation and suppression of pp60c-src transforming ability by mutation of its primary sites of tyrosine phosphorylation. *Cell* **49,** 65–73 (1987).

176. Kraybill, B. C., Elkin, L. L., Blethrow, J. D., Morgan, D. O. & Shokat, K. M. Inhibitor scaffolds as new allele specific kinase substrates. *J. Am. Chem. Soc.* **124,** 12118–12128 (2002).

177. Cooper, J. A. & Howell, B. The when and how of Src regulation. *Cell* **73,** 1051–1054 (1993).

178. Ridley, A. J., Paterson, H. F., Johnston, C. L., Diekmann, D. & Hall, A. The small GTP-binding protein rac regulates growth factor-induced membrane ruffling. *Cell* **70,** 401–410 (1992).

179. Ridley, A. J. Rho GTPases and cell migration. *J. Cell Sci.* **114,** 2713–2722 (2001).

180. Machacek, M. *et al.* Coordination of Rho GTPase activities during cell protrusion. *Nature* **461,** 99–103 (2009).

181. Dwivedi, S., Pandey, D., Khandoga, A. L., Brandl, R. & Siess, W. Rac1-mediated signaling plays a central role in secretion-dependent platelet aggregation in human blood stimulated by atherosclerotic plaque. *J. Transl. Med.* **8,** 128 (2010).

182. Zeller, K. S. *et al.* PI3-kinase p110α mediates β1 integrin-induced Akt activation and membrane protrusion during cell attachment and initial spreading. *Cell. Signal.* **22,** 1838–1848 (2010).

183. Hawkins, P. T. *et al.* PDGF stimulates an increase in GTP-Rac via activation of phosphoinositide 3-kinase. *Curr. Biol. CB* **5,** 393–403 (1995).

184. Ma, A. D., Metjian, A., Bagrodia, S., Taylor, S. & Abrams, C. S. Cytoskeletal reorganization by G protein-coupled receptors is dependent on phosphoinositide 3-kinase gamma, a Rac guanosine exchange factor, and Rac. *Mol. Cell. Biol.* **18,** 4744–4751 (1998).

185. Welch, H. C. E., Coadwell, W. J., Stephens, L. R. & Hawkins, P. T. Phosphoinositide 3-kinase-dependent activation of Rac. *FEBS Lett.* **546,** 93–97 (2003).

186. Alessi, D. R. *et al.* Characterization of a 3-phosphoinositide-dependent protein kinase which phosphorylates and activates protein kinase Balpha. *Curr. Biol. CB* **7,** 261–269 (1997).

187. Feng, J., Park, J., Cron, P., Hess, D. & Hemmings, B. A. Identification of a PKB/Akt Hydrophobic Motif Ser-473 Kinase as DNA-dependent Protein Kinase. *J. Biol. Chem.* **279,** 41189–41196 (2004).

188. Hemmings, B. A. & Restuccia, D. F. PI3K-PKB/Akt Pathway. *Cold Spring Harb. Perspect. Biol.* **4,** a011189 (2012).

189. Gao, X. *et al.* PI3K/Akt signaling requires spatial compartmentalization in plasma membrane microdomains. *Proc. Natl. Acad. Sci. U. S. A.* **108,** 14509–14514 (2011).

190. Vlahos, C. J., Matter, W. F., Hui, K. Y. & Brown, R. F. A specific inhibitor of phosphatidylinositol 3-kinase, 2-(4-morpholinyl)-8-phenyl-4H-1-benzopyran-4-one (LY294002). *J. Biol. Chem.* **269,** 5241–5248 (1994).

191. Wymann, M. P. *et al.* Wortmannin inactivates phosphoinositide 3-kinase by covalent modification of Lys-802, a residue involved in the phosphate transfer reaction. *Mol. Cell. Biol.* **16,** 1722–1733 (1996).

192. Yip, S.-C. *et al.* The distinct roles of Ras and Rac in PI 3-kinase-dependent protrusion during EGF-stimulated cell migration. *J. Cell Sci.* **120,** 3138–3146 (2007).

193. El-Sibai, M. *et al.* RhoA/ROCK-mediated switching between Cdc42- and Rac1-dependent protrusion in MTLn3 carcinoma cells. *Exp. Cell Res.* **314,** 1540–1552 (2008).

194. Li, A. & Machesky, L. M. Melanoblasts on the move. *Small GTPases* **3,** 115–119 (2012).

195. Penuel, E. & Martin, G. S. Transformation by v-Src: Ras-MAPK and PI3K-mTOR Mediate Parallel Pathways. *Mol. Biol. Cell* **10,** 1693–1703 (1999).

196. Servitja, J.-M., Marinissen, M. J., Sodhi, A., Bustelo, X. R. & Gutkind, J. S. Rac1 Function Is Required for Src-induced Transformation EVIDENCE OF A ROLE FOR TIAM1 AND VAV2 IN RAC ACTIVATION BY SRC. *J. Biol. Chem.* **278,** 34339–34346 (2003).

197. Dejana, E. Endothelial cell–cell junctions: happy together. *Nat. Rev. Mol. Cell Biol.* **5,** 261–270 (2004).

198. Cain, R. J., Vanhaesebroeck, B. & Ridley, A. J. Different PI 3-kinase inhibitors have distinct effects on endothelial permeability and leukocyte transmigration. *Int. J. Biochem. Cell Biol.* **44,** 1929–1936 (2012).

199. Resh, M. D. Myristylation and palmitylation of Src family members: the fats of the matter. *Cell* **76,** 411–413 (1994).

200. Kasahara, K. *et al.* Trafficking of Lyn through the Golgi caveolin involves the charged residues on αE and αI helices in the kinase domain. *J. Cell Biol.* **165,** 641–652 (2004).

201. Kasahara, K. *et al.* Rapid trafficking of c-Src, a non-palmitoylated Src-family kinase, between the plasma membrane and late endosomes/lysosomes. *Exp. Cell Res.* **313,** 2651–2666 (2007).

202. Kamps, M. P., Buss, J. E. & Sefton, B. M. Mutation of NH2-terminal glycine of p60src prevents both myristoylation and morphological transformation. *Proc. Natl. Acad. Sci. U. S. A.* **82,** 4625–4628 (1985).

203. Vogel, S. M. & Malik, A. B. Cytoskeletal Dynamics and Lung Fluid Balance. in *Comprehensive Physiology* (John Wiley & Sons, Inc., 2011).

204. Nalbant, P., Hodgson, L., Kraynov, V., Toutchkine, A. & Hahn, K. M. Activation of Endogenous Cdc42 Visualized in Living Cells. *Science* **305,** 1615–1619 (2004).

205. Pertz, O., Hodgson, L., Klemke, R. L. & Hahn, K. M. Spatiotemporal dynamics of RhoA activity in migrating cells. *Nature* **440,** 1069–1072 (2006).

206. García-Mata, R. *et al.* Analysis of Activated GAPs and GEFs in Cell Lysates. in *Methods in Enzymology* (ed. William E. Balch, C. J. D., and Alan Hall) **Volume 406,** 425–437 (Academic Press, 2006).

207. Wend, S. *et al.* Optogenetic control of protein kinase activity in mammalian cells. *ACS Synth. Biol.* **3,** 280–285 (2014).

208. Levskaya, A., Weiner, O. D., Lim, W. A. & Voigt, C. A. Spatiotemporal Control of Cell Signalling Using A Light-Switchable Protein Interaction. *Nature* **461,** 997–1001 (2009).

209. Krishnamurthy, V. V. *et al.* Reversible optogenetic control of kinase activity during differentiation and embryonic development. *Dev. Camb. Engl.* **143,** 4085–4094 (2016).

210. O'Neill, P. R., Kalyanaraman, V. & Gautam, N. Subcellular optogenetic activation of Cdc42 controls local and distal signaling to drive immune cell migration. *Mol. Biol. Cell* **27,** 1442–1450 (2016).

211. Zhou, X. X., Fan, L. Z., Li, P., Shen, K. & Lin, M. Z. Optical control of cell signaling by single-chain photoswitchable kinases. *Science* **355,** 836–842 (2017).

212. Dagliyan, O. *et al.* Engineering extrinsic disorder to control protein activity in living cells. *Science* **354,** 1441–1444 (2016).

CHAPTER 6: VITAE

Jennifer E. Klomp

Education:

University of Illinois at Chicago, Chicago, IL — December 2017
PhD. Cellular and Molecular Pharmacology

Central Michigan University, Mount Pleasant, MI — December 2007
M.Sc. Biology

Grand Valley State University, Allendale, MI — June 2004
B.Sc. Biology and Chemistry

Positions/Employment:

1. PhD Candidate /Graduate Research Assistant: Department of Pharmacology, University of Illinois in Chicago (Chicago, Illinois), 2012-2017.
   Supervisor: Dr. Andrei Karginov
   Description: 1.) Design and application of inducible and reversible kinases via protein engineering. 2.) The role of c-Src in the regulation of adherens junctions and implications for endothelial barrier function.

2. Graduate Teaching Assistant – Receptor Pharmacology: Department of Pharmacology, University of Illinois in Chicago (Chicago, Illinois), 2017.
   Description: Responsible for course set-up, proctoring exams, and the running of review sessions through-out the semester.

3. Senior Research Technician: Laboratory of Transcriptional Regulation, Van Andel Research Institute (Grand Rapids, Michigan), Dr. Steven J. Triezenberg (Principal Investigator), 2007-2012.
   Description: Post-translation modifications of VP16 and gene regulation of herpes simplex virus type 1

4. M.S. Candidate/Graduate Research Assistant: Biology Department, Central Michigan University (Mount Pleasant, Michigan), 2006-2007.
   Supervisor: Dr. Greg Colores
   Description: 1.) Optimizing multiplex PCR for detecting a variety of polyaromatic hydrocarbon-degrading bacteria; 2.) Examination microbial composition and diversity in nestling Tree Swallows (*Tachycineta bicolor*).

5. Graduate Teaching Assistant – General Microbiology: Biology Department, Central Michigan University (Mount Pleasant, Michigan), 2006-2007.
   Description: Instructor of laboratory classes; responsible for lectures, homework, and quizzes given during the laboratory portion of the class.

6. M.S. Candidate/Graduate Research Assistant: Biology Department, Portland State University (Portland, Oregon), 2004-2005. Supervisors: Dr. Michael Murphy and Dr. Anna-Louise Reysenbach
   Description: Evaluating the microbial composition of Spotted Towhees (*Pipilo maculatus*) using molecular techniques.

7. Graduate Teaching Assistant – Introductory Biology: Biology Department, Portland State University Biology Department (Portland, Oregon), 2004-2005.
   Description: Instructor of laboratory classes; responsible for lectures, homework, and quizzes given during the laboratory portion of the class.

8. Undergraduate Student Researcher: Biology Department, Grand Valley State University (Allendale, Michigan), 2002-2204.
   Supervisors: Dr. Michael Lombardo and Dr. Patrick Thorpe
   Description: Evaluating the establishment of *Lactobacillus* sp. & *Vibrio* sp. in Tree Swallows (*Tachycineta bicolor*) using culture techniques.

Publications:

- **Klomp, J.E**., V. Huyot, A-M Ray, K.B. Collins, and A.V. Karginov. Mimicking transient activation of a protein kinase in living cells. PNAS. vol. 113 no. 52 14976–14981

- Zimnicka, A.M., Husain, Y.S., Shajahan, A.N., Sverdlov, M., Chaga, O., Chen, Z., Toth, P.T., **Klomp, J.,** Karginov, A.V., Tiruppathi, C., et al. (2016). Src-dependent phosphorylation of caveolin-1 Tyr14 promotes swelling and release of caveolae. Mol. Biol. Cell. E15–11 – 0756.

- Ray, A.-M., **J.E. Klomp,** K.B. Collins, and A.V. Karginov. Dissecting kinase effector signaling using the RapRTAP methodology. Kinase Signaling Networks, Methods in Molecular Biology, vol. 1636,

- Kutluay, S.B., S.L. DeVos, **J.E. Klomp**, and S.J. Triezenberg. 2009. Transcriptional coactivators are not required for herpes simplex virus type 1 immediate-early gene expression in vitro. Journal of Virology 83, 3436-49.

- **Klomp, J.E.,** M.T. Murphy, S. Bartos Smith, J.E. McKay, I. Ferrera, and A.L. Reysenbach, 2008. Cloacal microbial communities of female spotted towhees Pipilo maculatus: microgeographic variation and individual sources of variability. Journal of Avian Biology 3 (5): 530-538.

Presentations:

Oral Presentations:

- "Mimicking transient activation of protein kinases in living cells" FASEB SRC: Protein Kinase Signaling Network (July 18, 2016)

- "Mimicking transient activation of protein kinases in living cells" Chicago Cancer Biology Retreat (November 19, 2016)

- "Mimicking transient activation of protein kinases in living cells" ASCB (December 7, 2016)

Poster Presentations:

First Author Poster Presentations were given at the meetings listed below -

2004: AFO/Wilson Annual Meeting
2006: American Society of Microbiology – Michigan Chapter Spring meeting
2007: American Society of Microbiology – Annual Meeting
2008: Manipulation of Nuclear Processes by DNA Viruses
2009: International Herpesvirus Workshop
2010: International Herpesvirus Workshop
2011: Manipulation of Nuclear Processes by DNA Viruses
2014: University of Illinois Cancer Research Forum
2014: Chicago Biomedical Consortium
2014: American Society of Cell Biology General Meeting (2 posters)
2015: Chicago Symposium of Cell Signaling
2015: FASEB Protein Kinases and Protein Phosphorylation (3 posters)
2015: University of Illinois Cancer Research Forum
2015: University of Illinois College of Medicine Research Forum
2015: American Society of Cell Biology General Meeting (2 posters)
2016: FASEB SRC: Protein Kinase Signaling Network
2016: American Society of Cell Biology General Meeting

Honors and Awards:

- FASEB SRC Travel Award, 2016
- Chicago Cytoskeleton Outstanding Poster – Honorable Mention, 2016
- CCTS/COM Pre-doctoral Education in Clinical and Translational Science (PECTS) Fellowship program, 2015-2016
- Provost Deiss Award, University of Illinois – Chicago, 2014
- T32: Training program in lung biology and pathobiology, 2013-2015
- Research Award, The American Ornithological Union, 2005
- Summer Undergraduate Research Program Award, Grand Valley State University, 2003

Committees and Leadership Roles:

- Student Faculty Representative for the Department of Pharmacology, 2014-2015
- GEMSSA (Graduate Education in Medical Science Student Association) Officer, Director of Communications, 2015-2016
- GEMSSA Symposium Research Forum Committee, Board Member, 2016

CHAPTER 7: APPENDIX

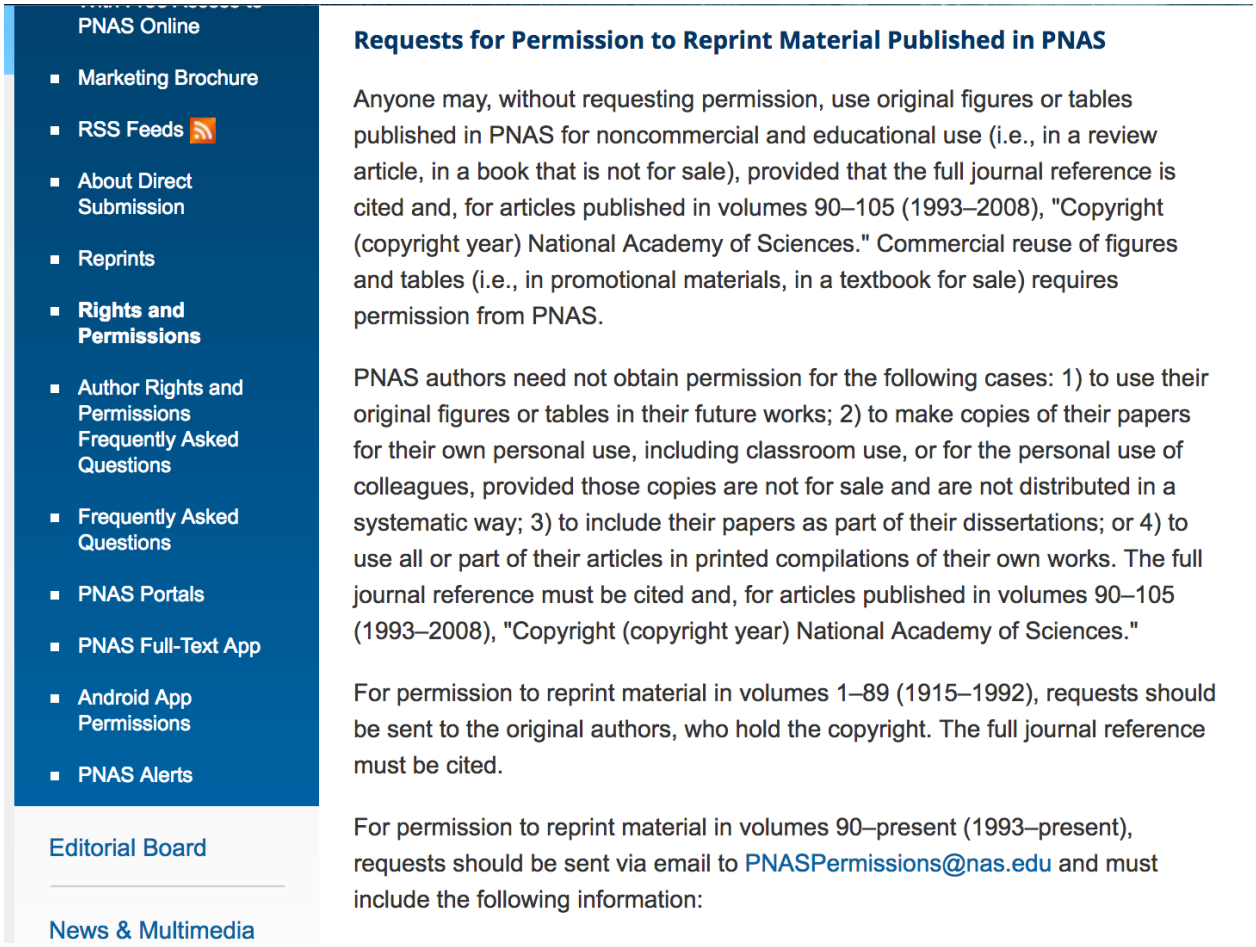

PNAS Online

- Marketing Brochure
- RSS Feeds
- About Direct Submission
- Reprints
- **Rights and Permissions**
- Author Rights and Permissions Frequently Asked Questions
- Frequently Asked Questions
- PNAS Portals
- PNAS Full-Text App
- Android App Permissions
- PNAS Alerts

Editorial Board

News & Multimedia

Requests for Permission to Reprint Material Published in PNAS

Anyone may, without requesting permission, use original figures or tables published in PNAS for noncommercial and educational use (i.e., in a review article, in a book that is not for sale), provided that the full journal reference is cited and, for articles published in volumes 90–105 (1993–2008), "Copyright (copyright year) National Academy of Sciences." Commercial reuse of figures and tables (i.e., in promotional materials, in a textbook for sale) requires permission from PNAS.

PNAS authors need not obtain permission for the following cases: 1) to use their original figures or tables in their future works; 2) to make copies of their papers for their own personal use, including classroom use, or for the personal use of colleagues, provided those copies are not for sale and are not distributed in a systematic way; 3) to include their papers as part of their dissertations; or 4) to use all or part of their articles in printed compilations of their own works. The full journal reference must be cited and, for articles published in volumes 90–105 (1993–2008), "Copyright (copyright year) National Academy of Sciences."

For permission to reprint material in volumes 1–89 (1915–1992), requests should be sent to the original authors, who hold the copyright. The full journal reference must be cited.

For permission to reprint material in volumes 90–present (1993–present), requests should be sent via email to PNASPermissions@nas.edu and must include the following information: